Introduction to Magnetic Imaging

Rudolf Schäfer
IFW-Dresden

Domain Observation Techniques

An ideal imaging technique:

- should image magnetic microstructure with lateral resolution in the range from nanometer up to millimeter
- should image depth sensitive, with option to pure surface sensitivity
- should be able to image magnetization in working devices that may be buried under non-magnetic overlayers
- should be able to image magnetization while applying an arbitrary magnetic field
- should allow sample manipulation (like heating, cooling, stressing etc.)
- should be fast enough to follow dynamics on a time scale comparable to that of spin precession
- should not disturb magnetic structure

Domain Observation Techniques

Sensitivity of domain observation methods

Main goal of domain observation: Determination of magnetization vector *M*(*r*)

$\boldsymbol{B} = \mu_0 (\boldsymbol{H} + \boldsymbol{M}) \qquad (\boldsymbol{H} = \boldsymbol{H}_{ext} + \boldsymbol{H}_{stray})$

$\text{div } \boldsymbol{B} = 0$

↓

$\text{div } \boldsymbol{H}_{stray} = - \text{div } \boldsymbol{M}$

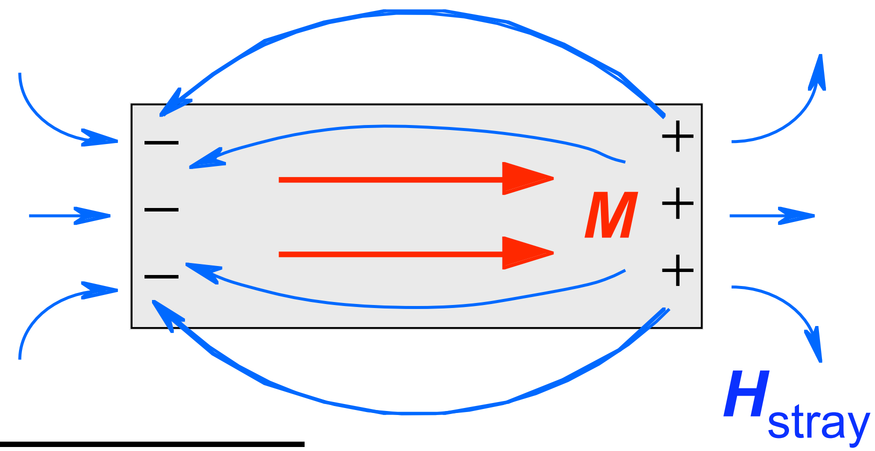

- sensitive to $\boldsymbol{H}_{stray}$
  - Bitter technique
  - magnetotactic bacteria
  - magnetic force microscopy
- sensitive to $\boldsymbol{M}$
  - magneto-optical microscopy
  - X-ray spectroscopy
  - polarized electrons
- sensitive to $\boldsymbol{B}$
  - transmission electron microscopy
- sensitive to lattice distortions
  - X-ray, neutron scattering

Domain Observation Techniques

History: first imaging of domains (*F. Bitter*, 1931)

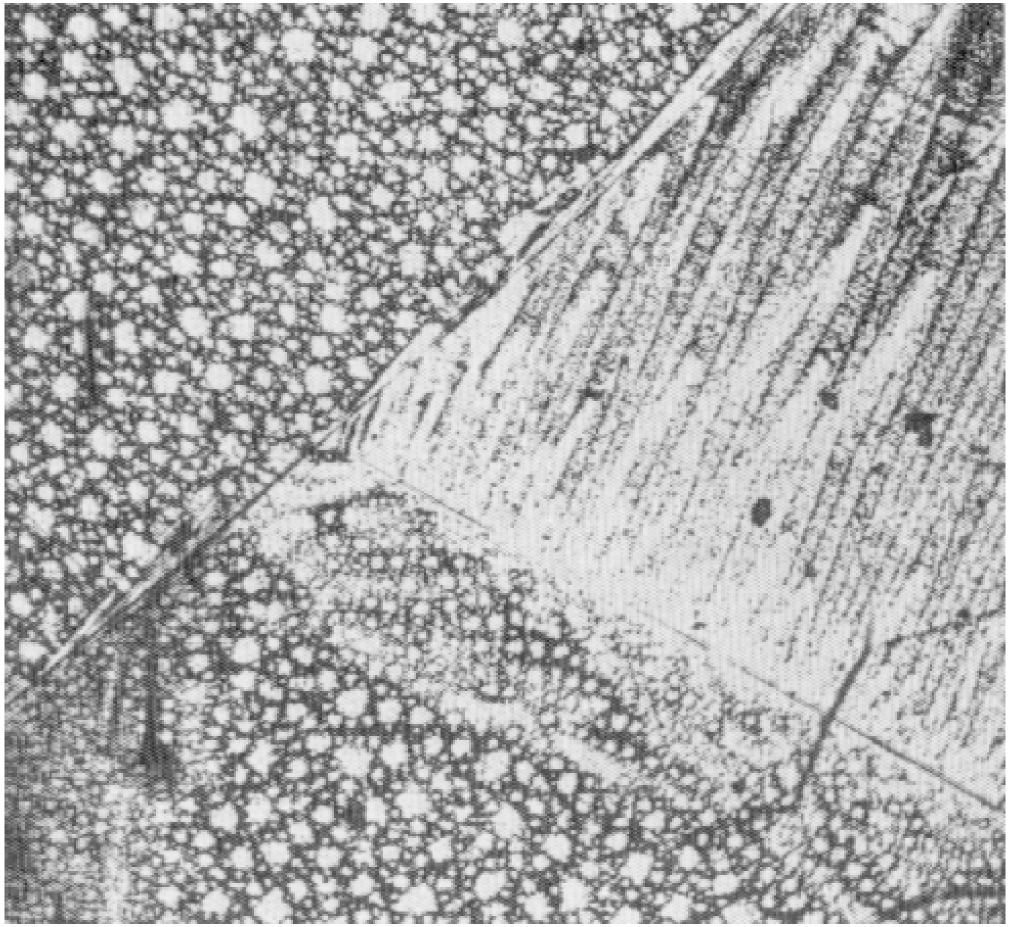

cobalt

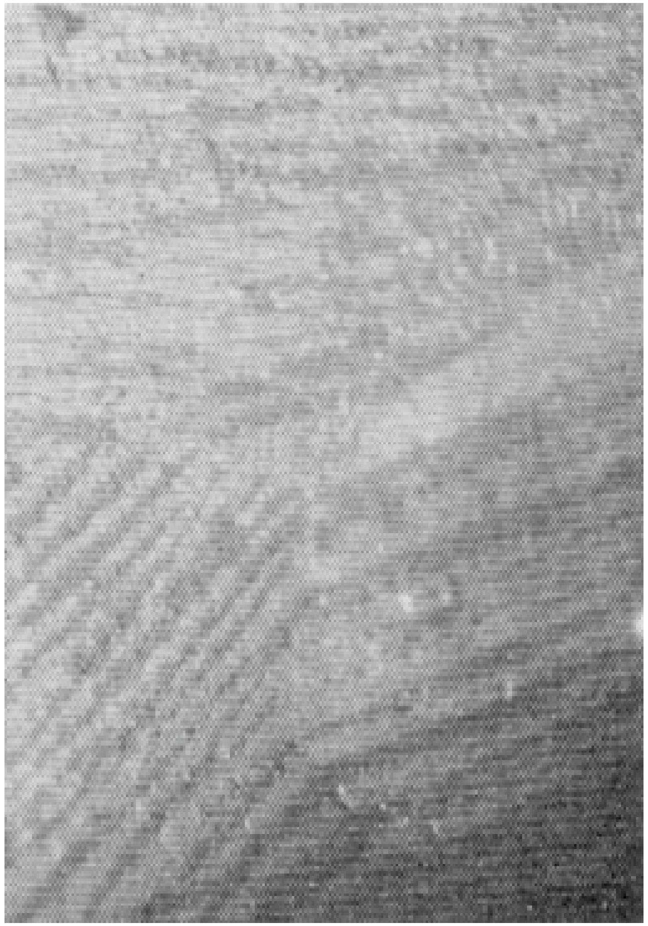

FeSi

1. Bitter technique

1. Bitter technique

Principle

• Magnetic colloid: Magnetite particles (diameter about 10 nm) in water

• accumulation in stray field at sample surface

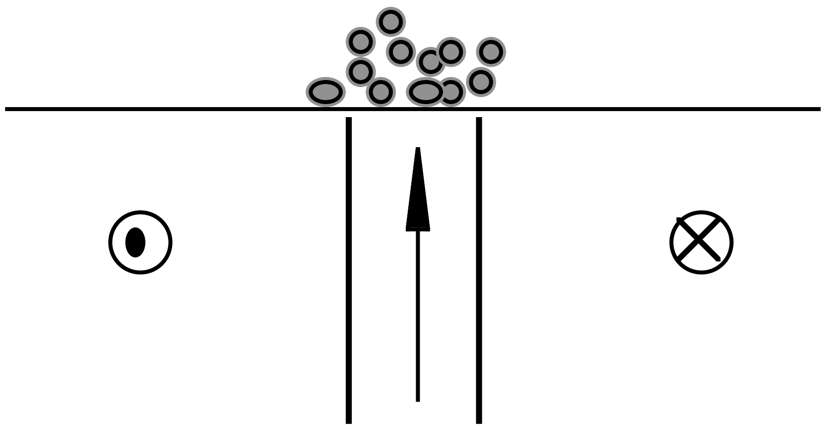

Sensitivity

• reversible agglomeration in weak magnetic field

→ increase of volume, elongated shape

→ large susceptibility

→ large sensitivity to stray fields

in order of a few 100 A/m

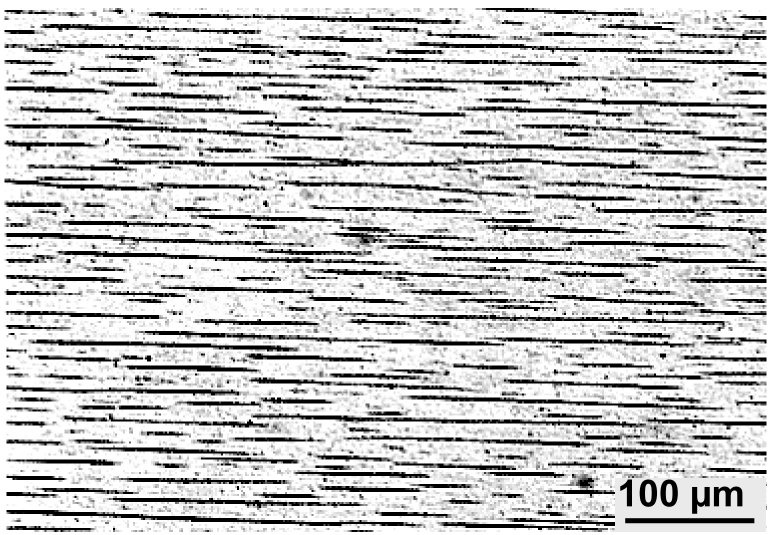

agglomeration in magnetic field (560 A/m)

1. Bitter technique

Sensitivity

Increase of sensitivity in weak perpendicular field

→ domain imaging in soft magnetic materials

NiFe sheet

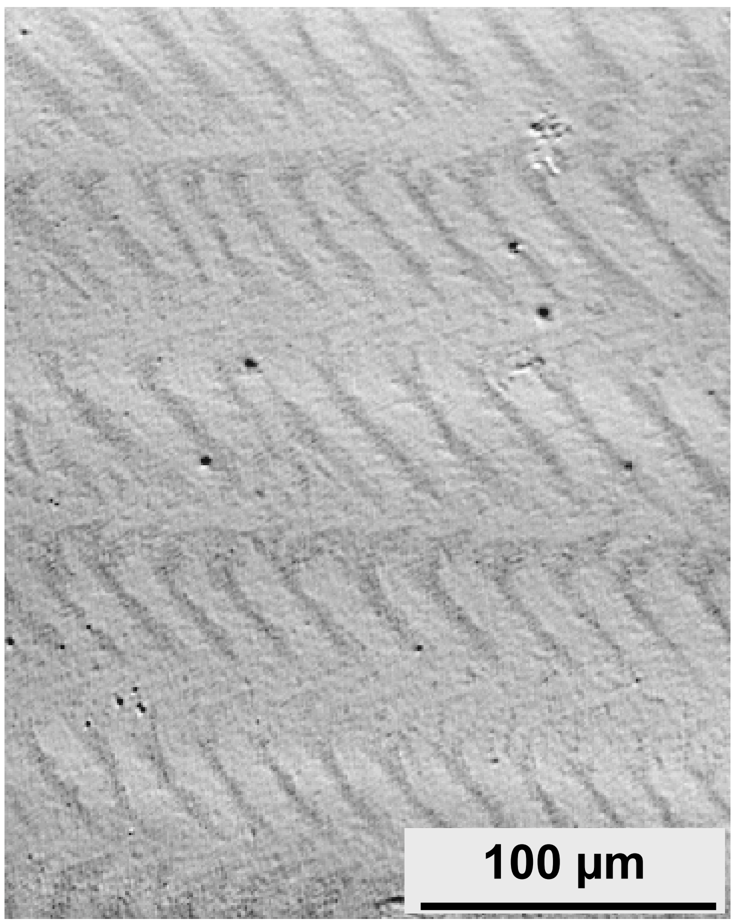

without auxiliary field

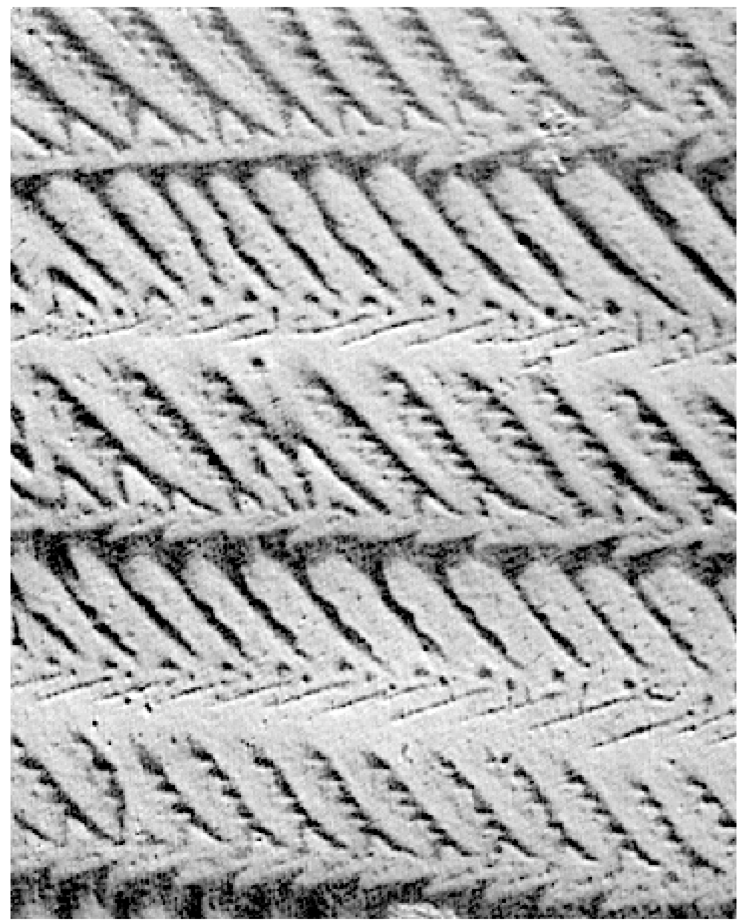

with perpendicular field

⊙ **1.5 kA/m**

1. Bitter technique

Dry colloid technique

allowing colloid to dry on surface
adding agent
→ strippable film
→ imaging in electron microscope

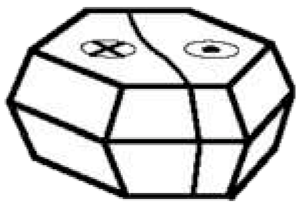

Ba-Ferrite particles (courtesy K. Goto, Sendai)

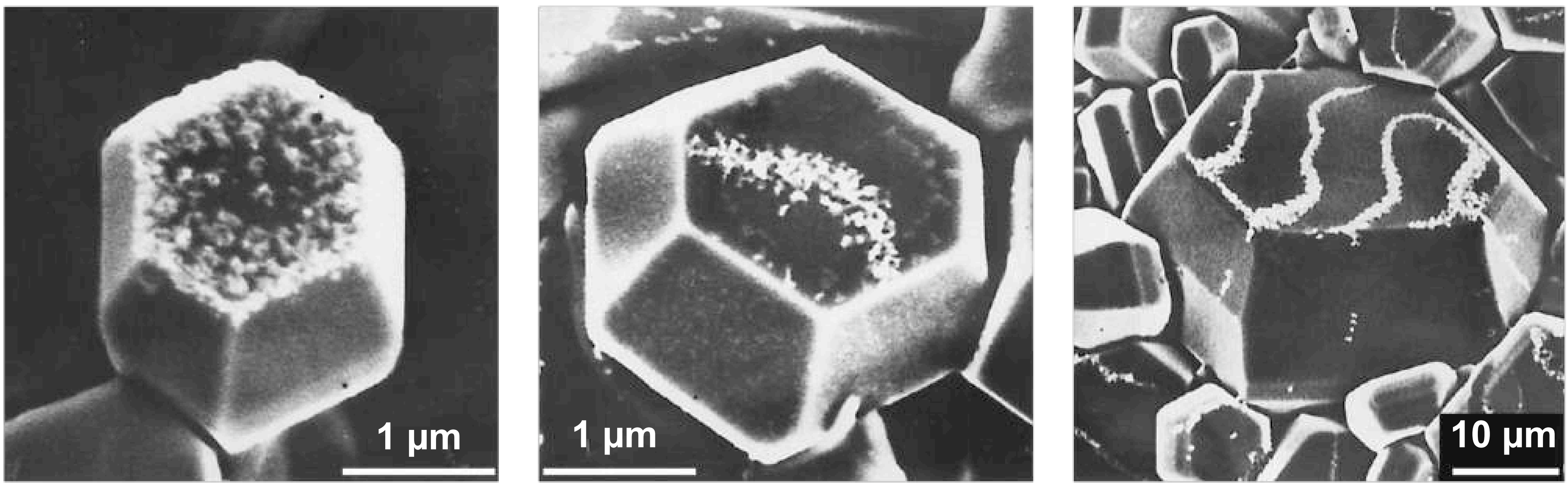

Dry colloid technique:	**Static domain observation on rough, 3-dimensional surfaces at high resolution of some 10 nm**

1. Bitter technique

Dry colloid technique

CoCr recording medium (courtesy J. Simsová, Prague)

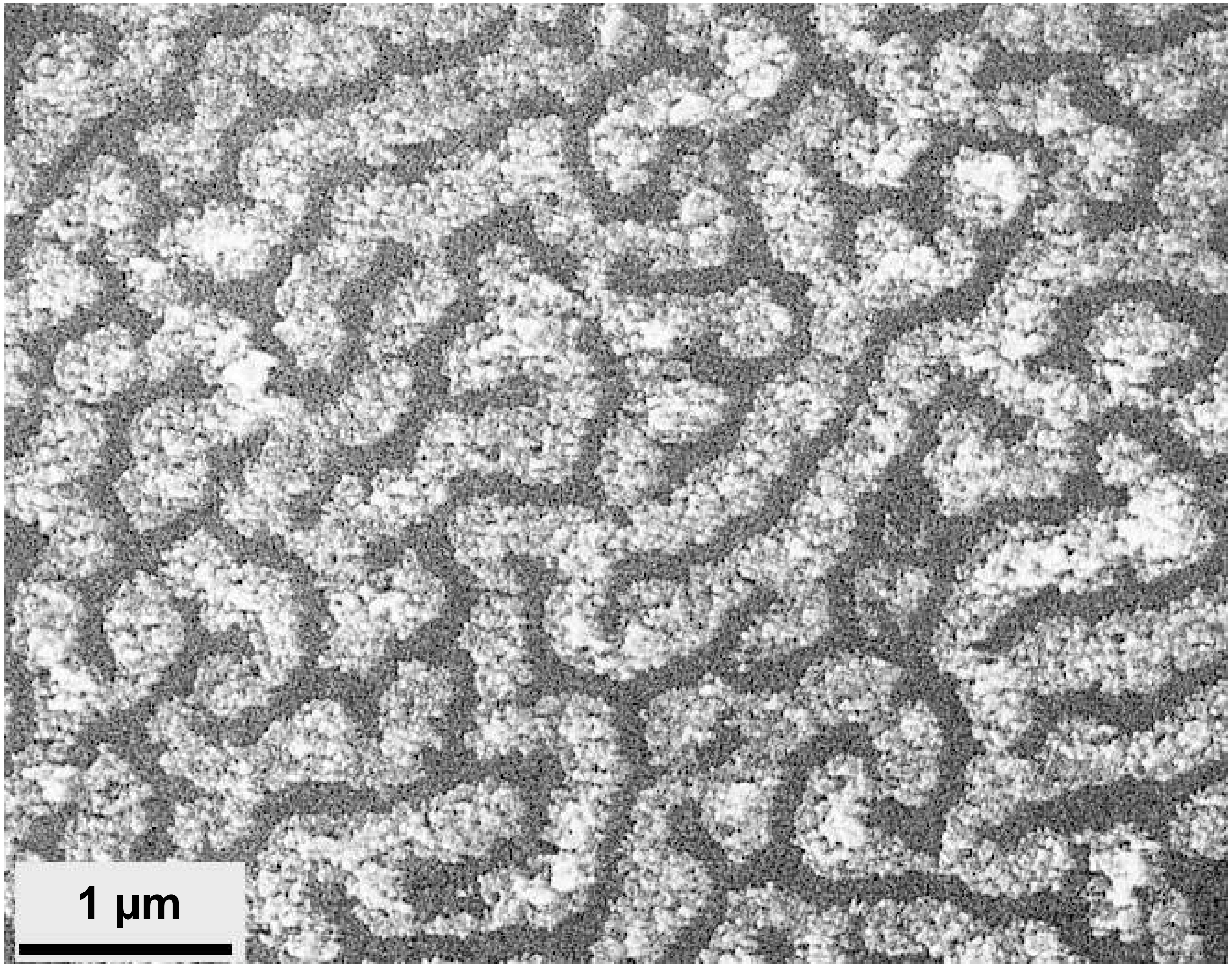

1. Bitter technique

Visible and invisible features

V-lines

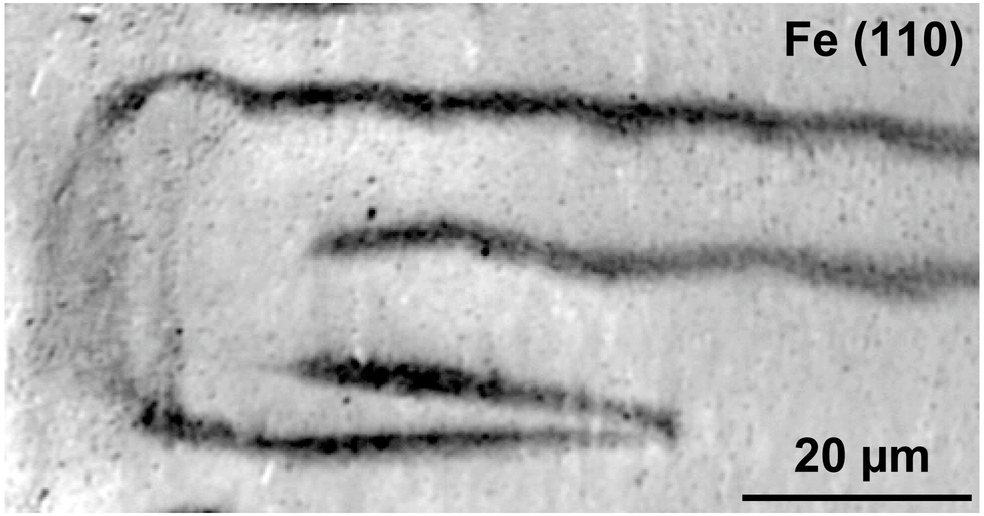

Bitter image

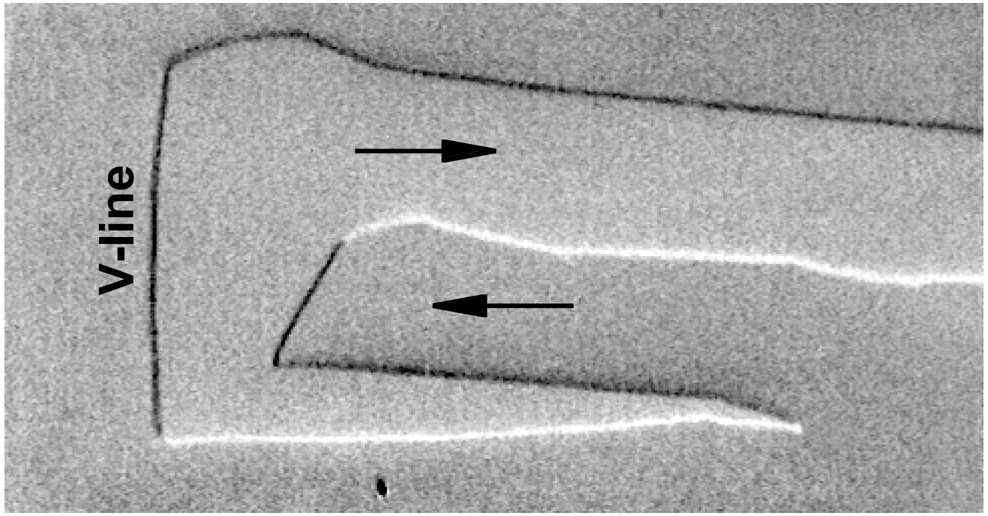

Kerr image

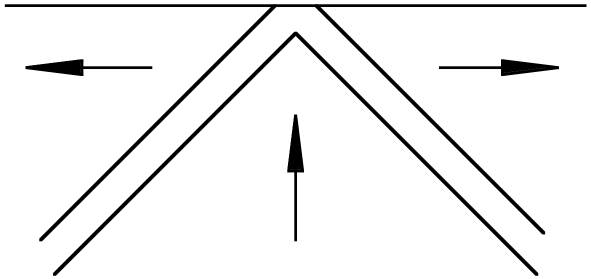

V-line

1. Bitter technique

Visible and invisible features

□-lines

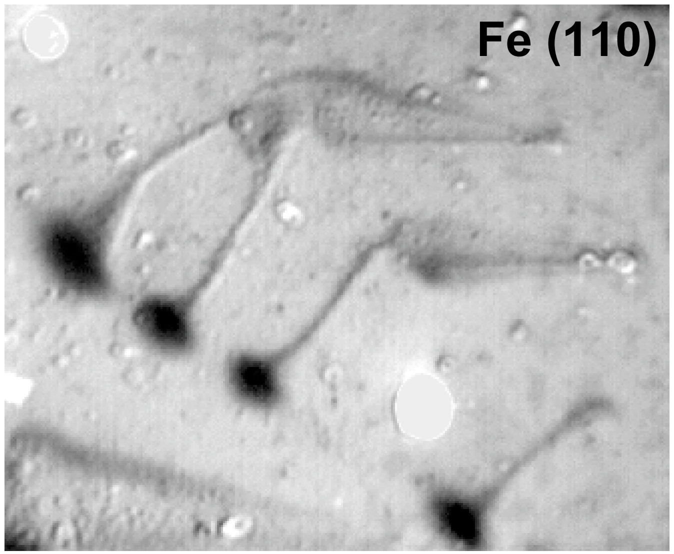

Bitter image

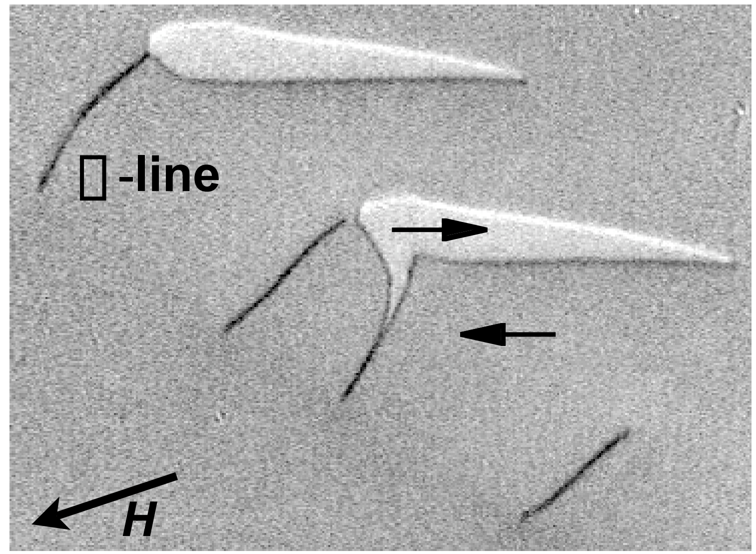

Kerr image

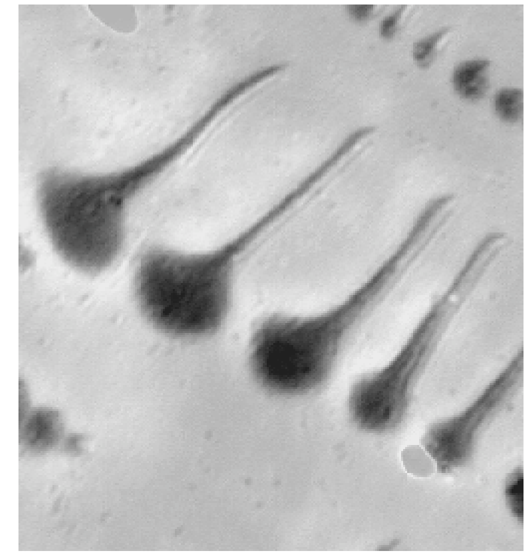

Bitter image

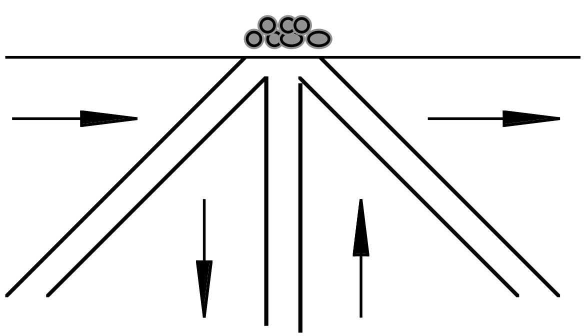

□-line

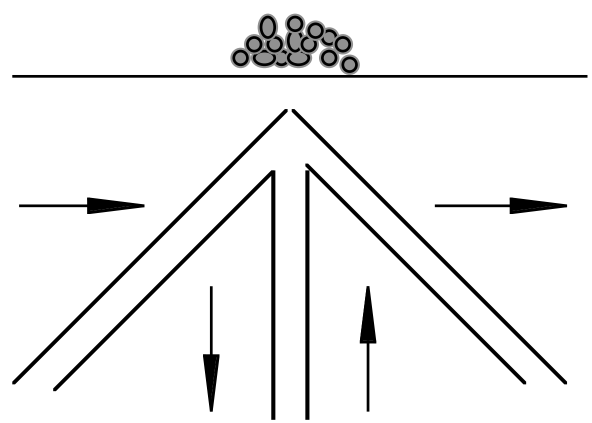

1. Bitter technique

Toner powder emulsion

Laser printer toner + water + household detergent

transformer steel *(courtesy S. Arai, Nippon steel)*

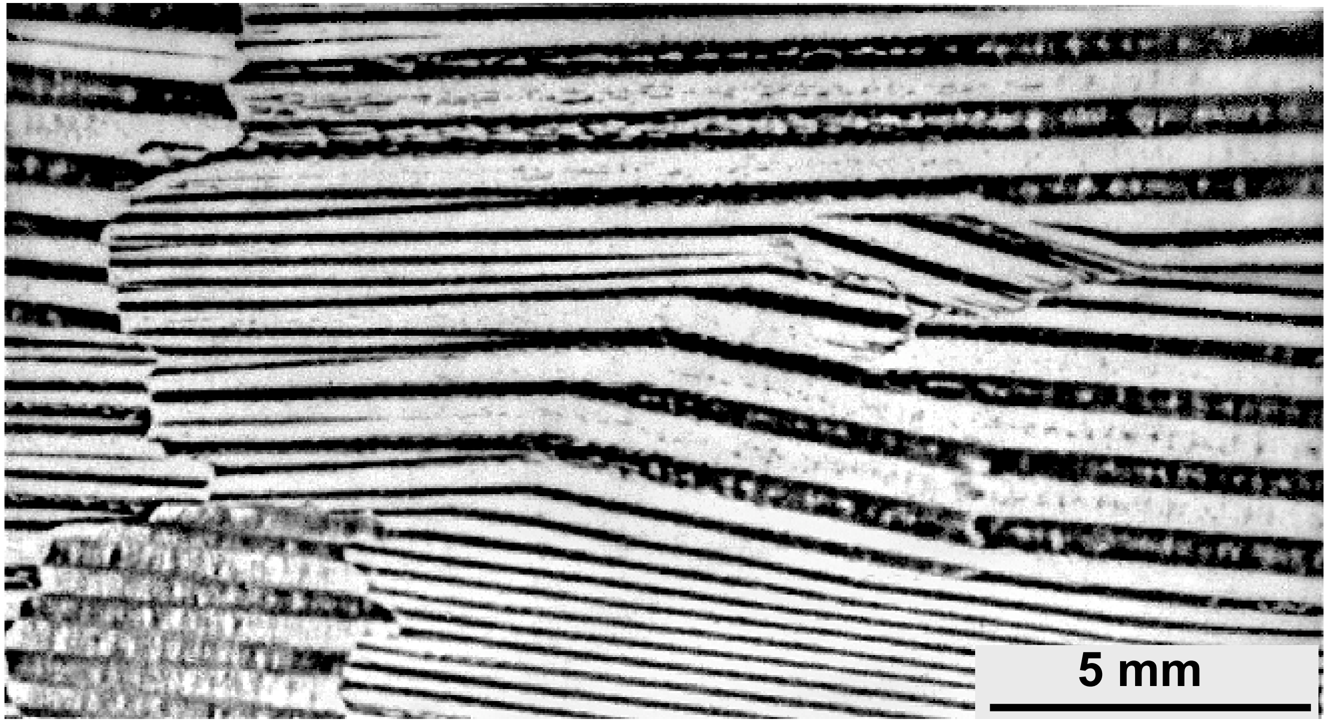

2. Kerr microscopy

Basics

Kerr effect

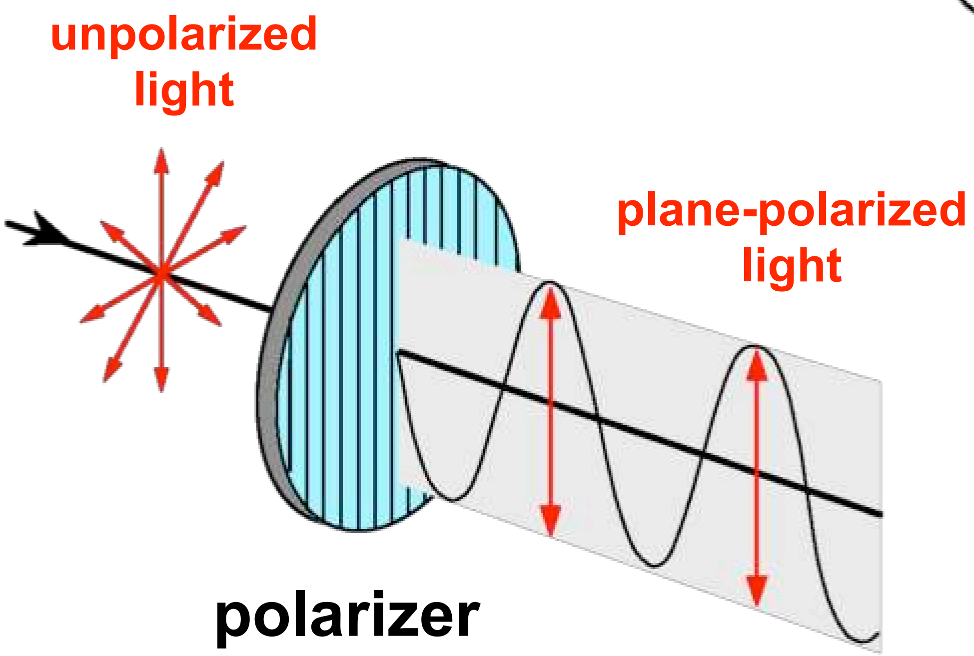
unpolarized
light
plane-polarized
light
polarizer

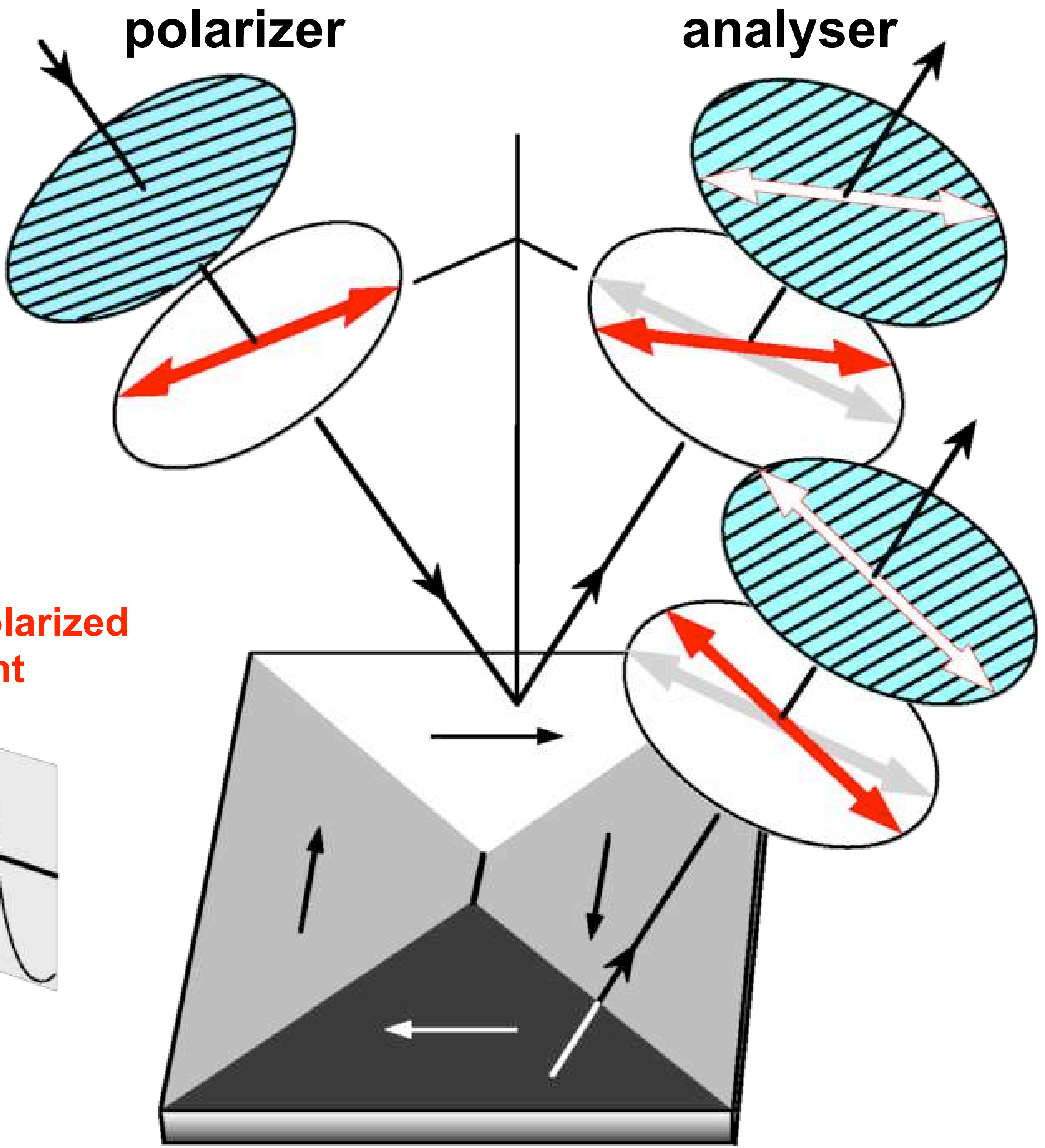
polarizer
analyser

Kerr and Faraday effects

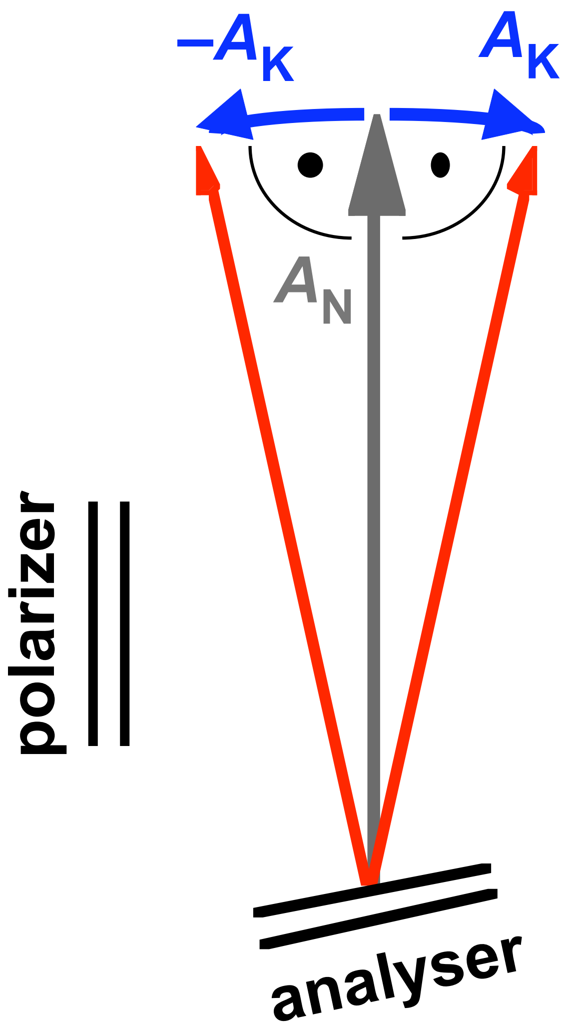

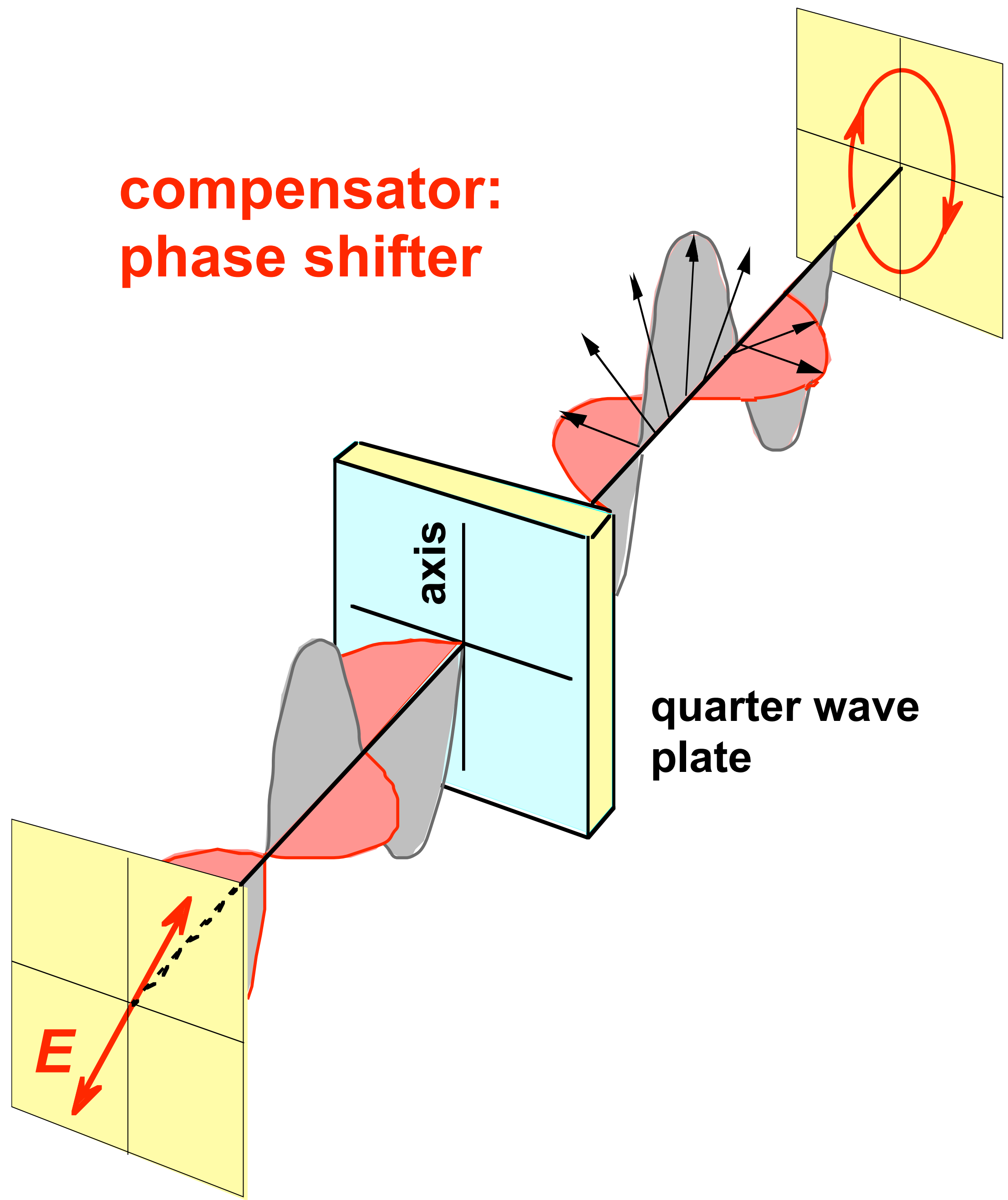

Kerr microscope

maximum resolution:
about 300 nm (with oil immersion)

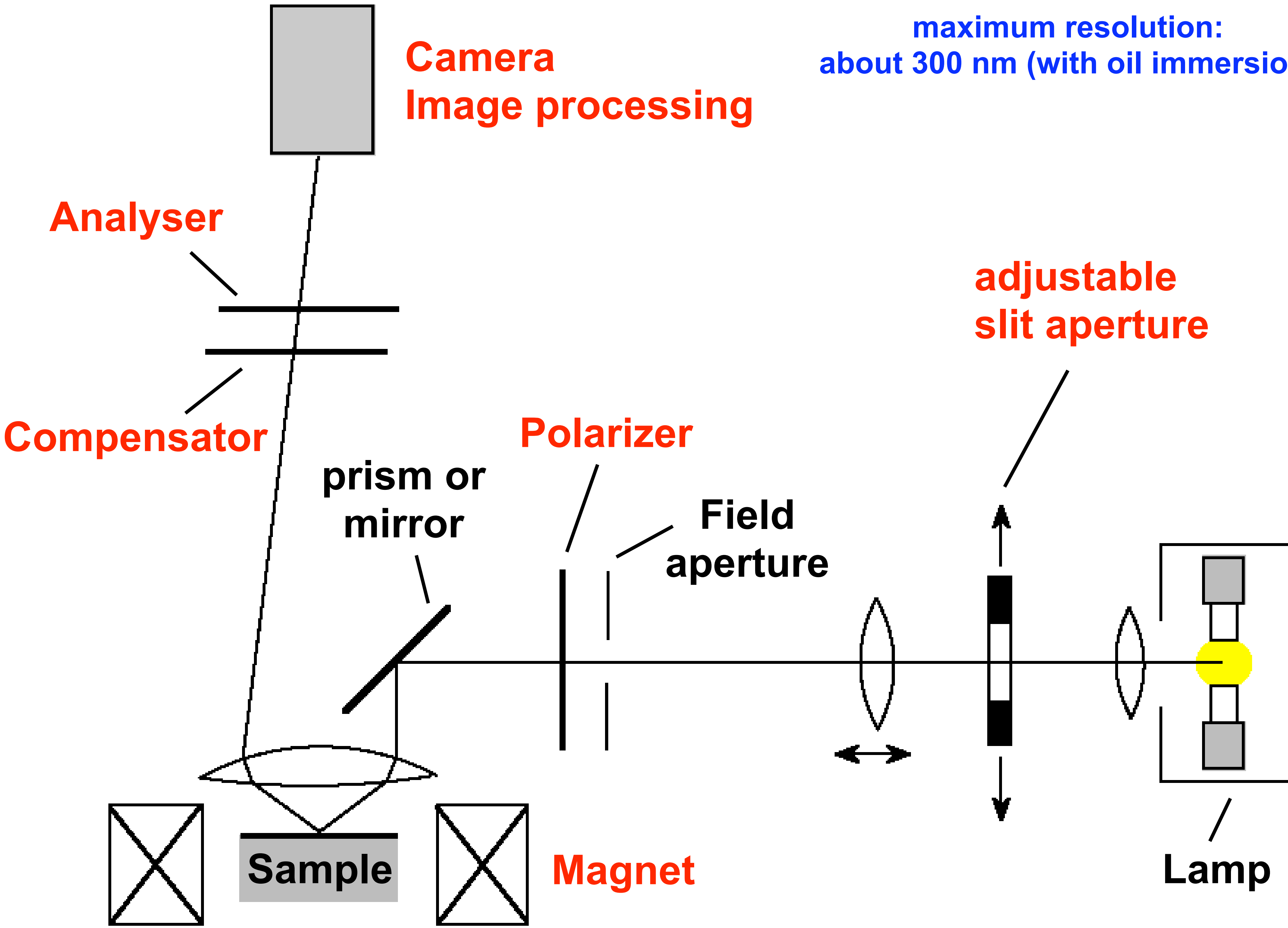

Wide-field Kerr microscope

Kerr microscope at IFW-Dresden

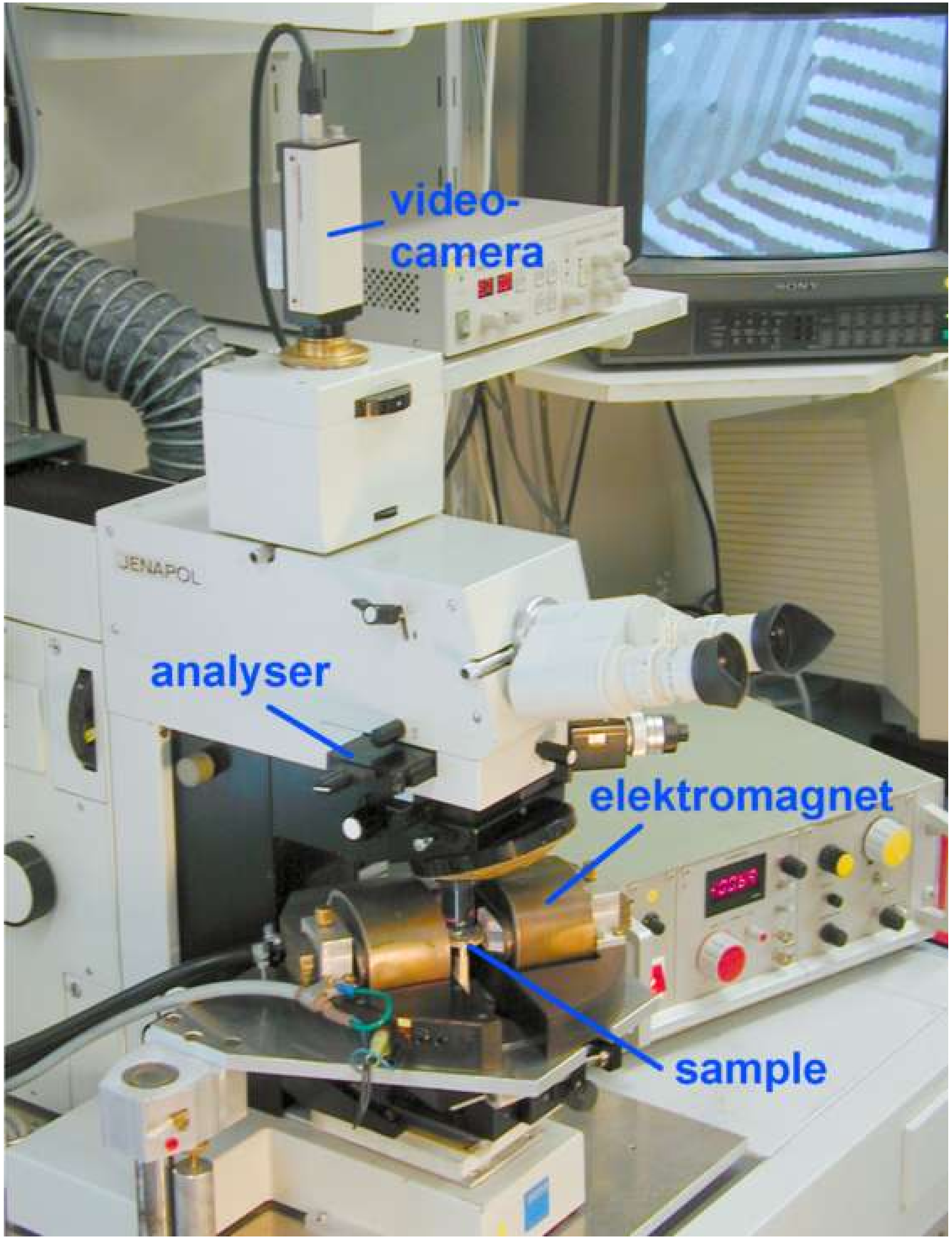

Contrast enhancement in Kerr microscopy

Antireflection coating

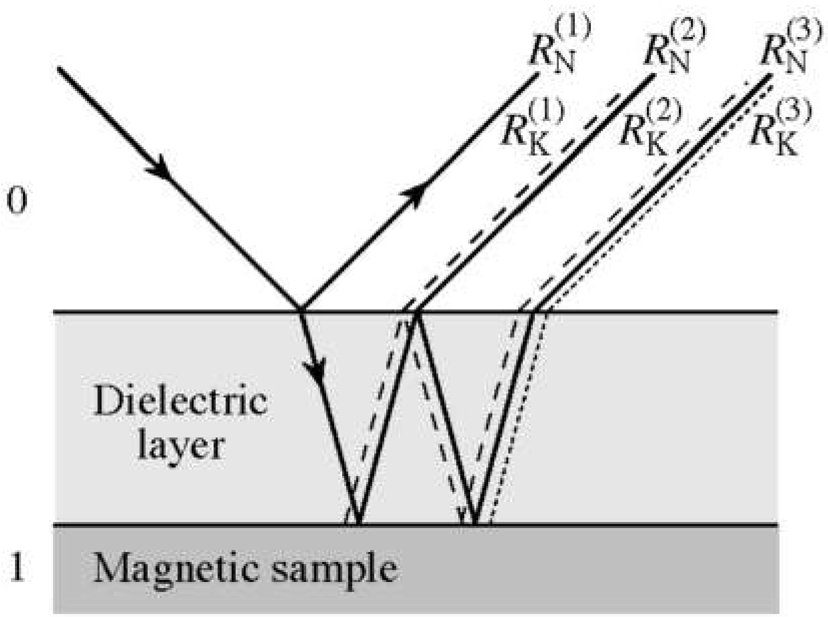

phase shift $R_N^{(1)} / R_N^{(2)}$: 180°

phase shift $R_N^{(2)} / R_N^{(3)}$: 360°

$$R_N^{(1)} = R_N^{(2)} + R_N^{(3)} + \dots$$

 regular amplitude zero
Kerr amplitude enhanced

amorphous ribbon

without interference layer

with ZnS interference layer

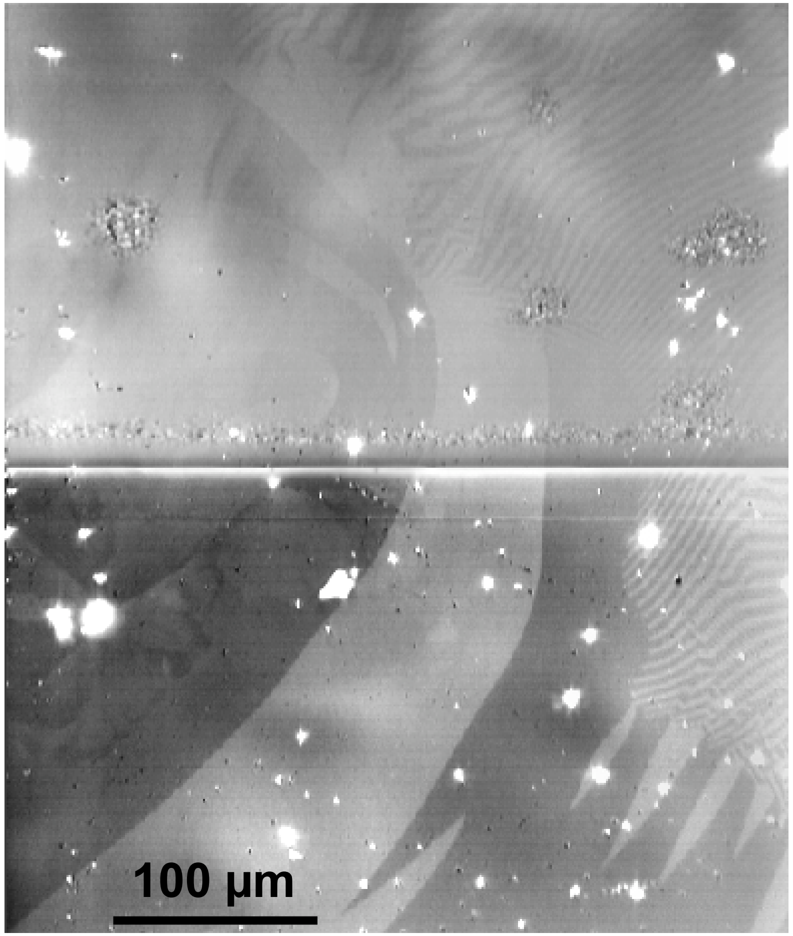

Contrast enhancement in Kerr microscopy

Digitally enhanced Kerr microscopy (difference image technique)

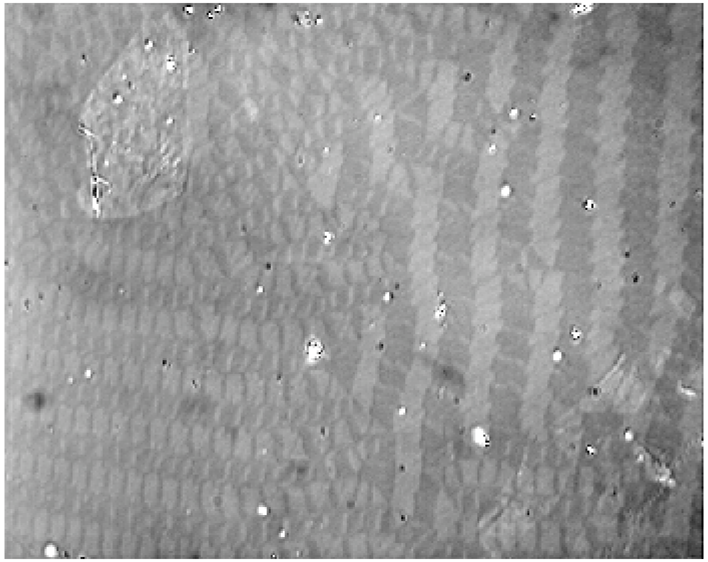

Original image

–

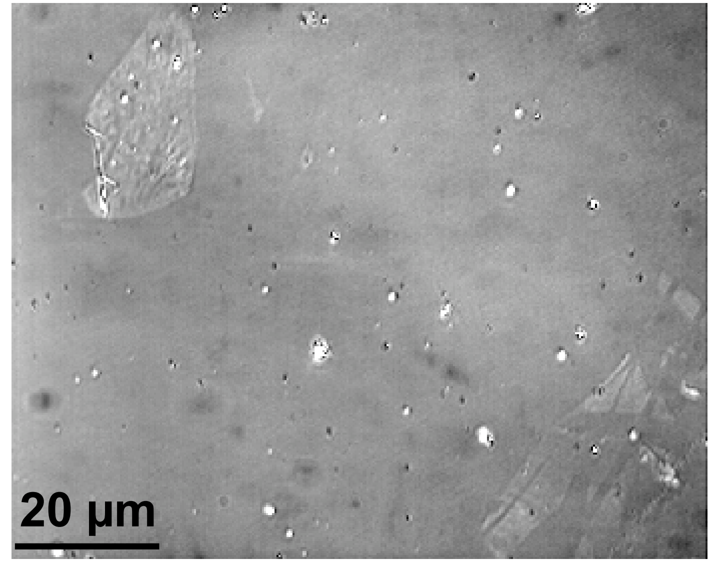

Reference image

amorphous
ribbon

↓

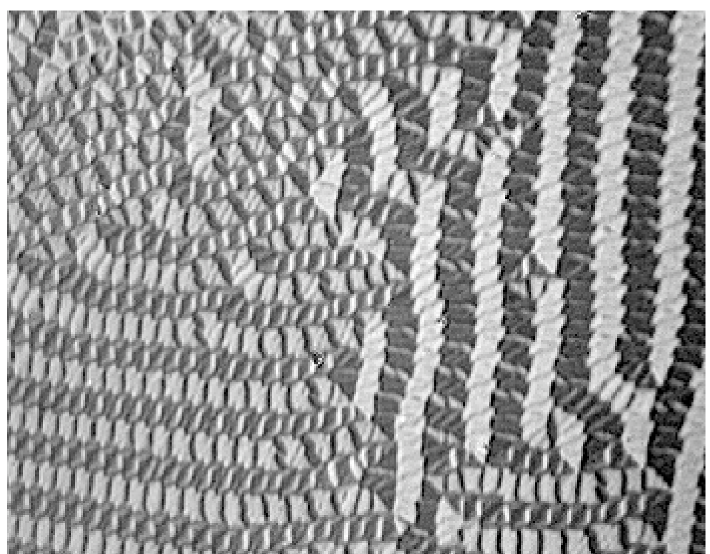

Difference image

Advantages and Drawbacks

Sample manipulation: mechanical stress

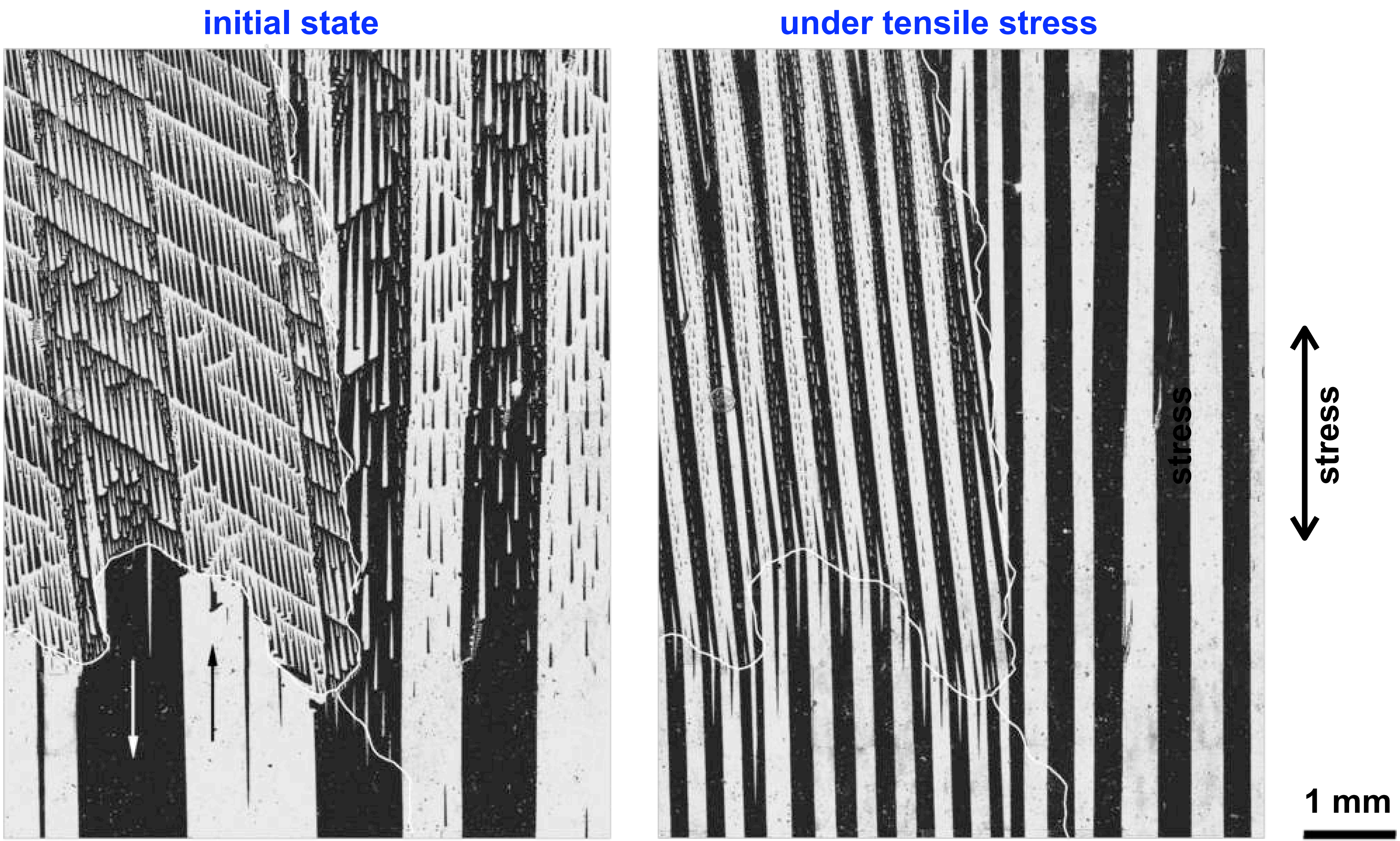

transformer steel

Kerr microscopy: change of magnification

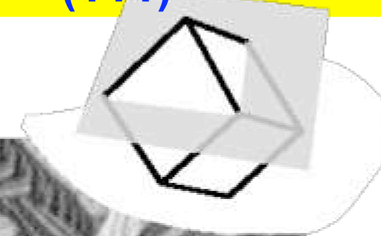

Branched domains on Fe (111) surface

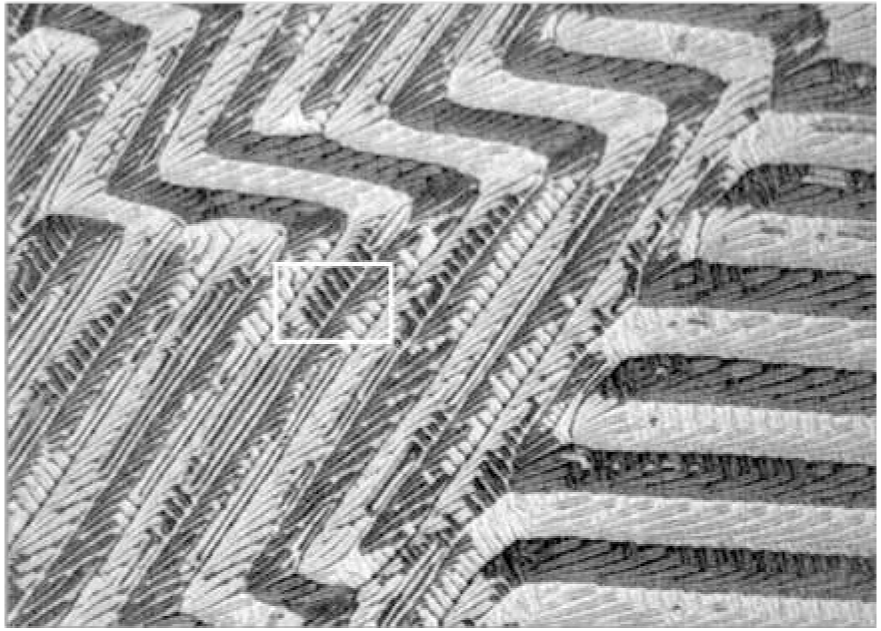

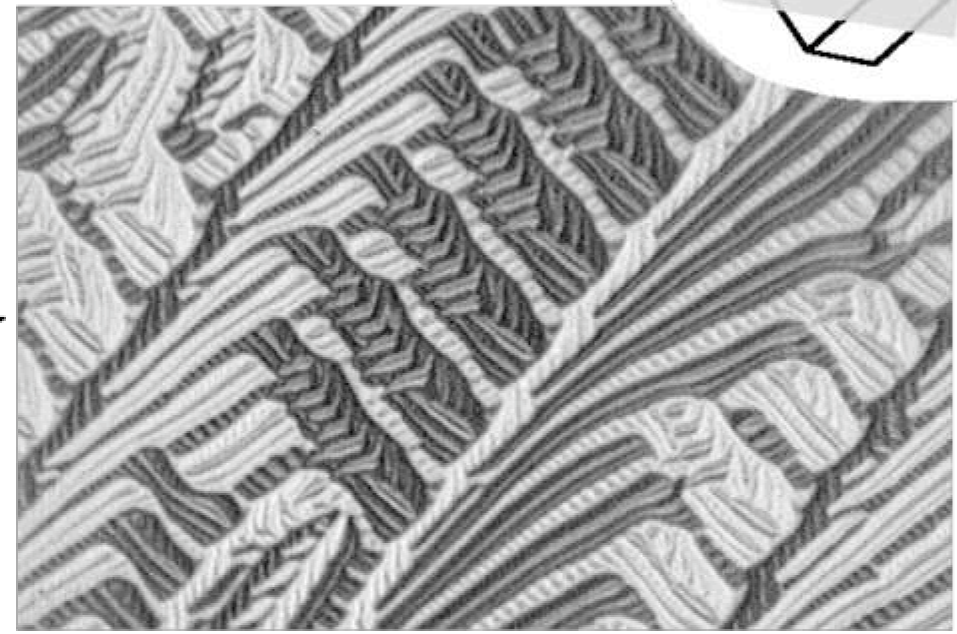

50 µm

50 µm

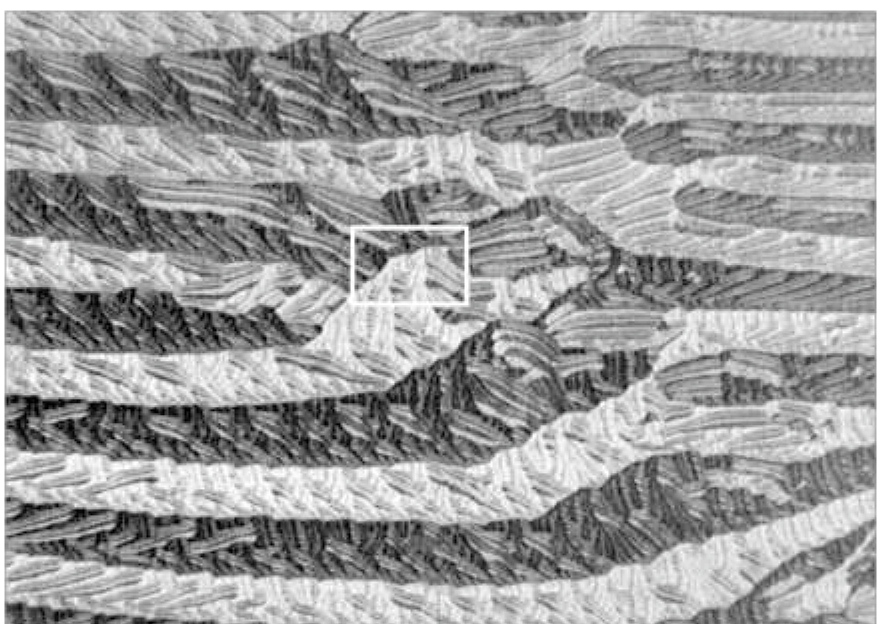

Kerr microscopy: about resolution

Co basal plane

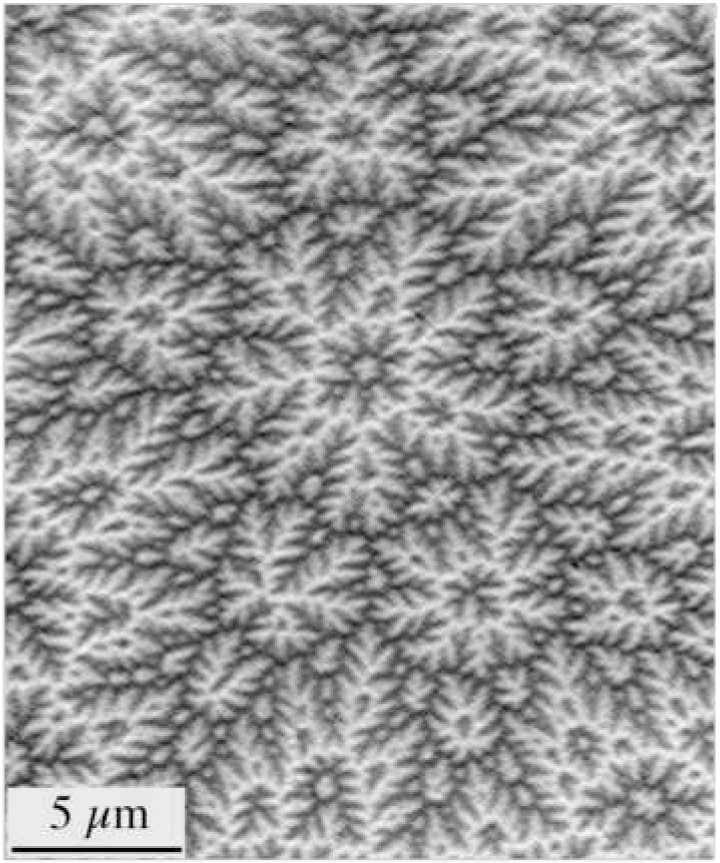

asymmetric Bloch wall (met. Glass)

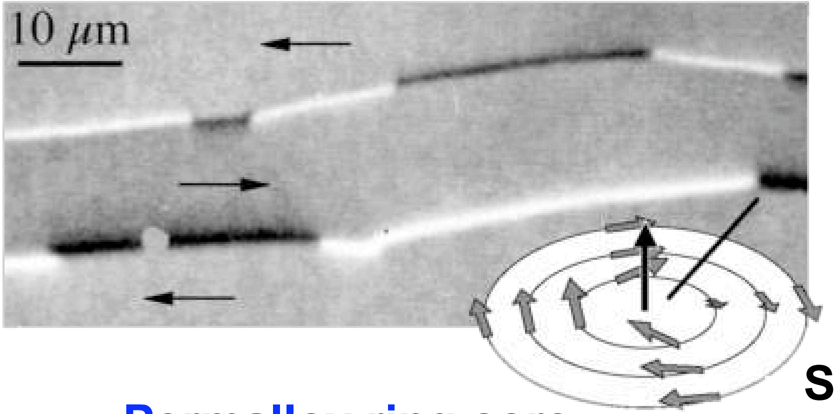

Surface swirl

Permalloy ring core

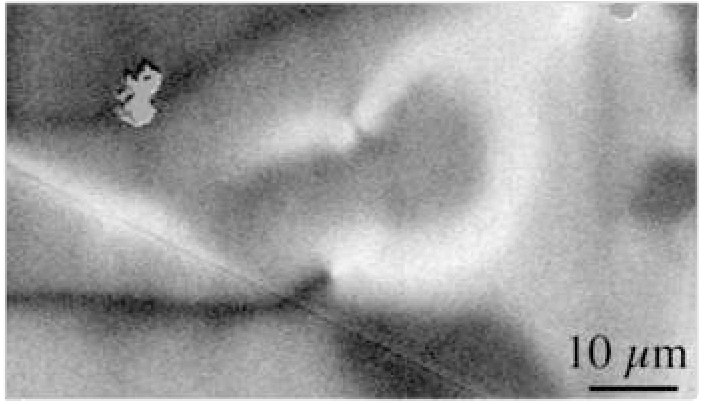

amorphous layer (1 μm thick)

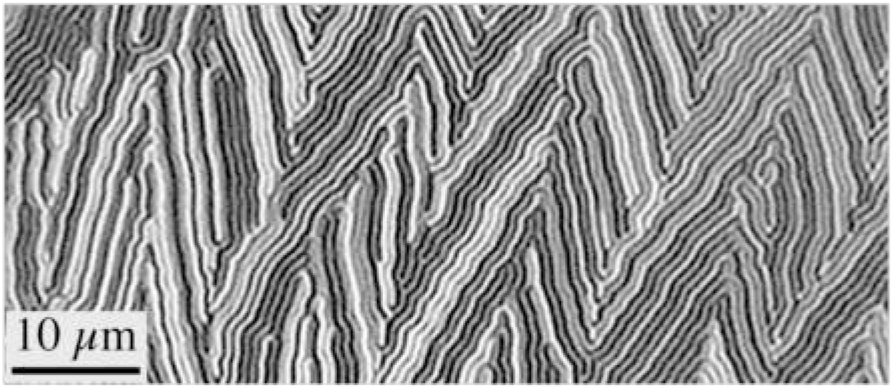

Crosstie wall (Permalloy)

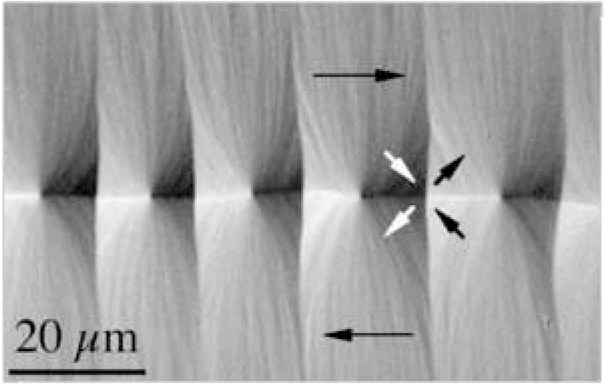

Kerr microscopy: about resolution

Co elements (courtesy Axel Carl)

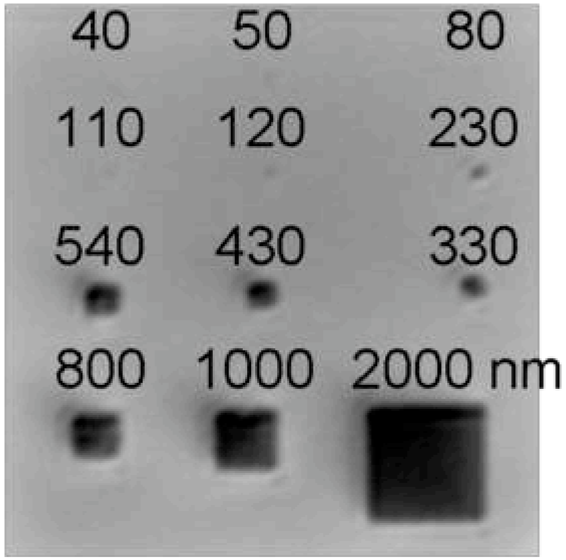

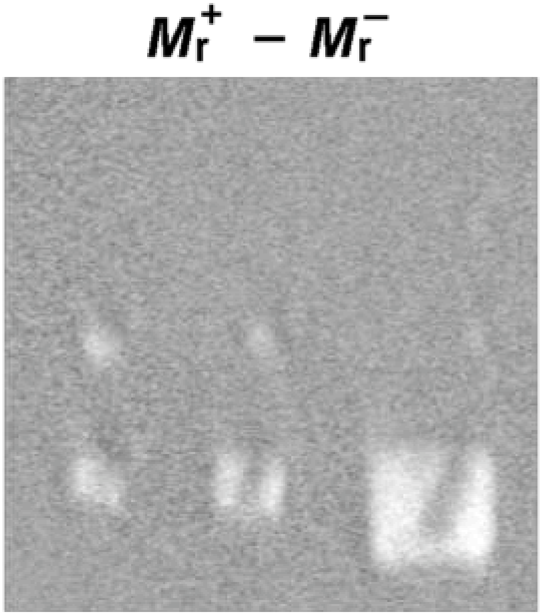

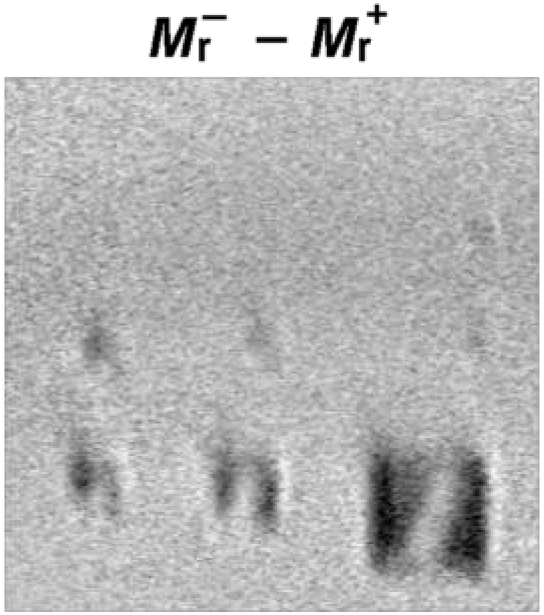

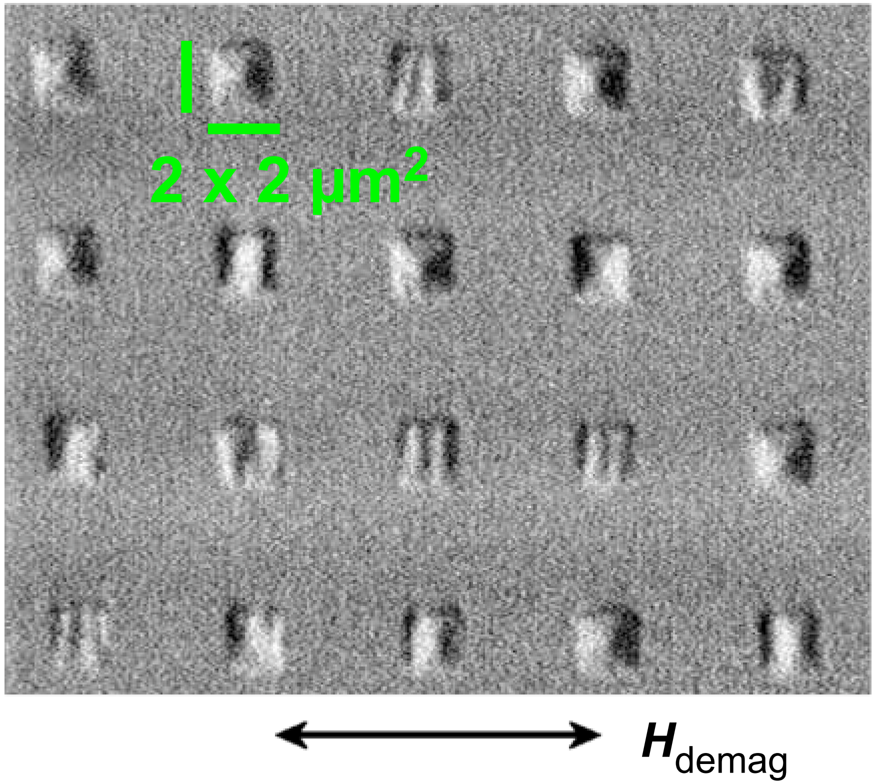

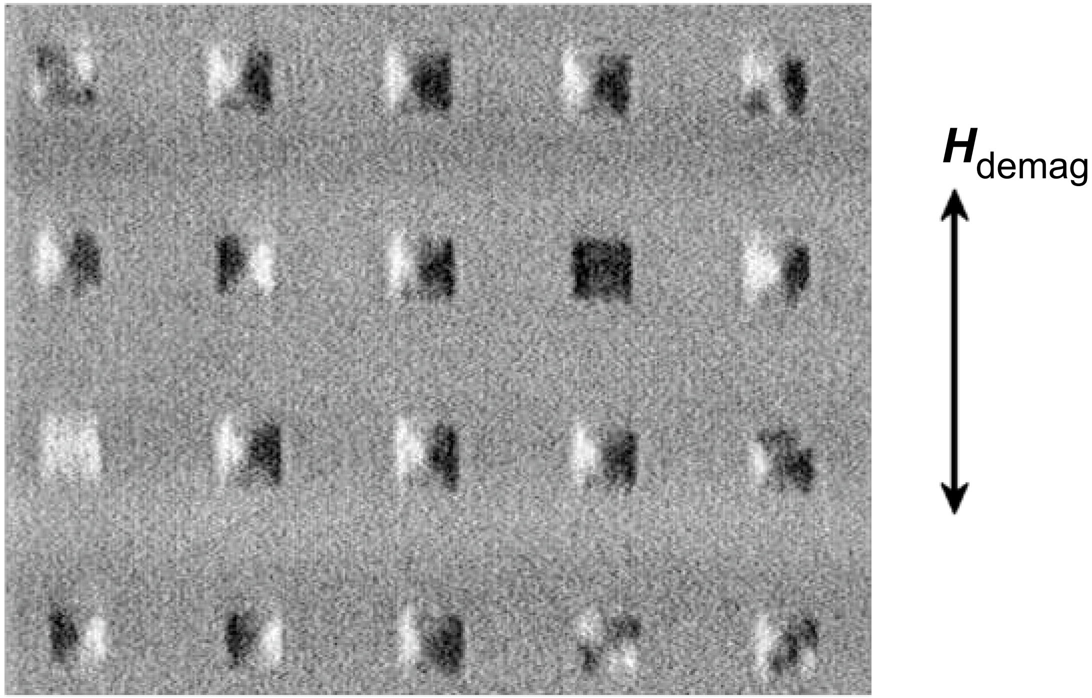

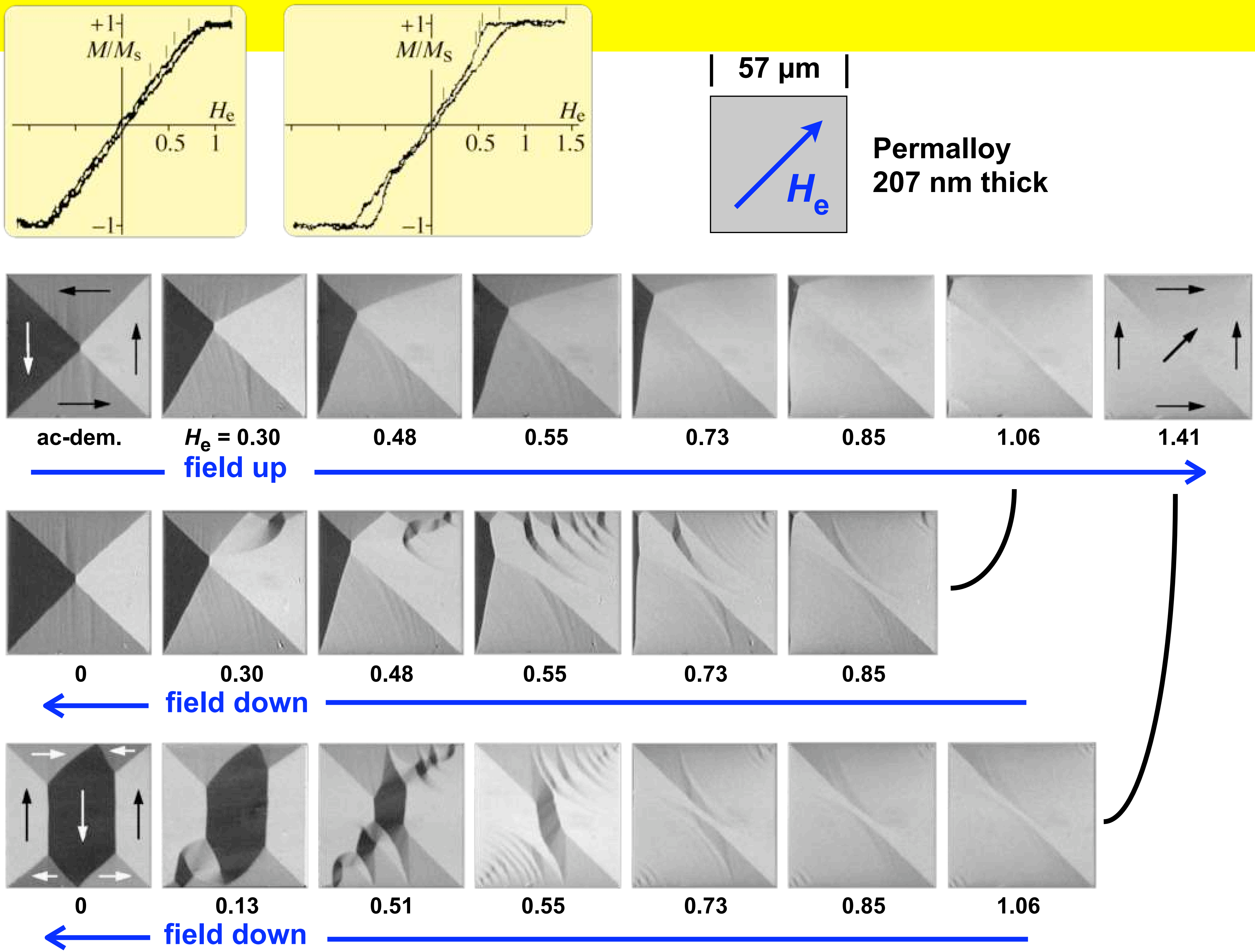

+1
M/Ms
He
0.5
1
-1
+1
M/Ms
He
0.5
1
1.5
-1
57 µm
He
Permalloy
207 nm thick
ac-dem.
He = 0.30
0.48
0.55
0.73
0.85
1.06
1.41
field up
0
0.30
0.48
0.55
0.73
0.85
field down
0
0.13
0.51
0.55
0.73
0.85
1.06
field down

Kerr microscopy: high / low temperature observation

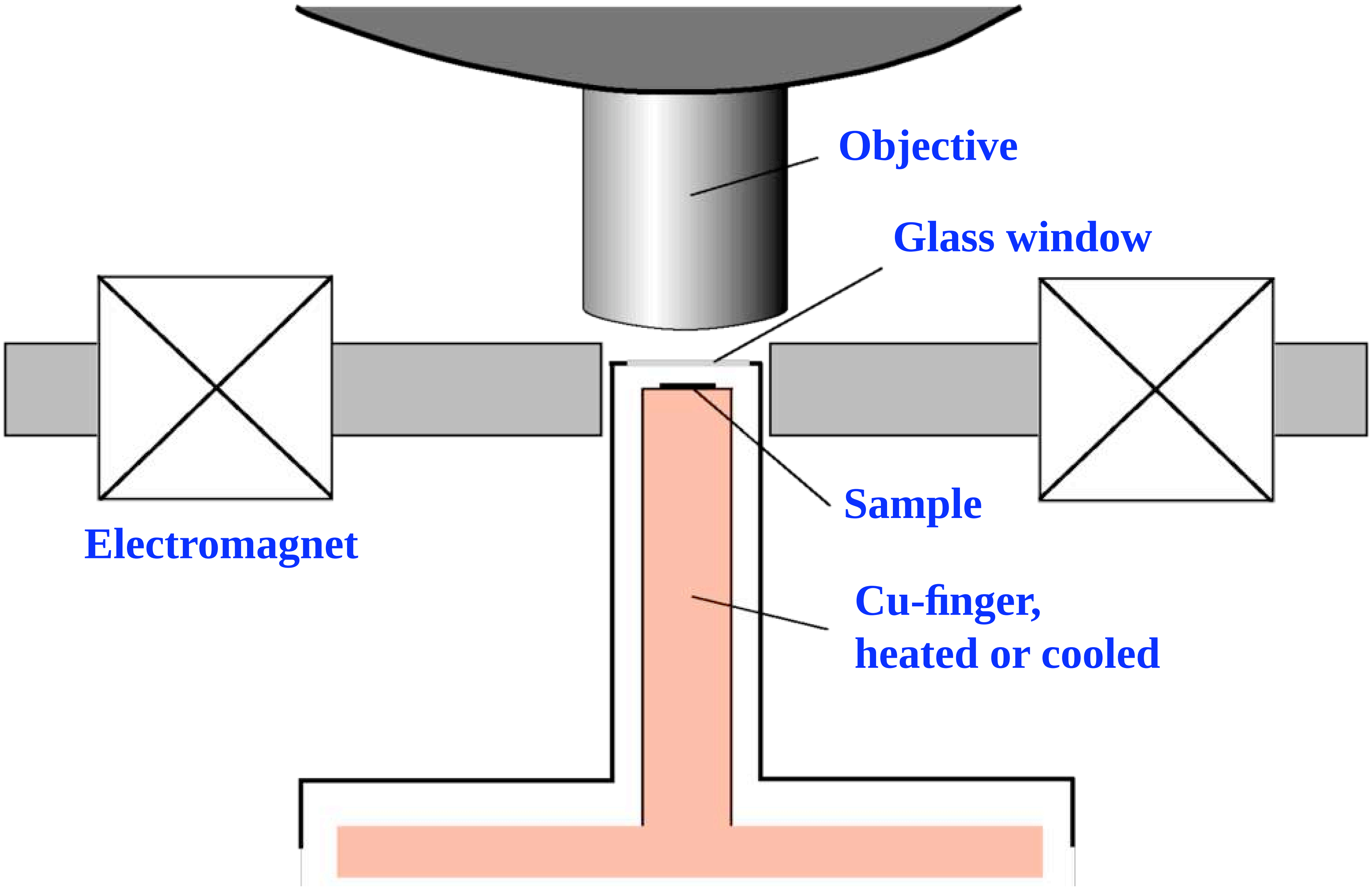

Kerr microscopy: high / low temperature observation

Heating of soft magnetic nanocrystalline ribbon, $Fe_{73}Si_{16}B_7Cu_1Nb_3$

- rapid quenching → amorphous ribbon $\xrightarrow{550°C}$ nanocrystalline ribbon
- random anisotropy model: exchange interaction averages over anisotropic grains

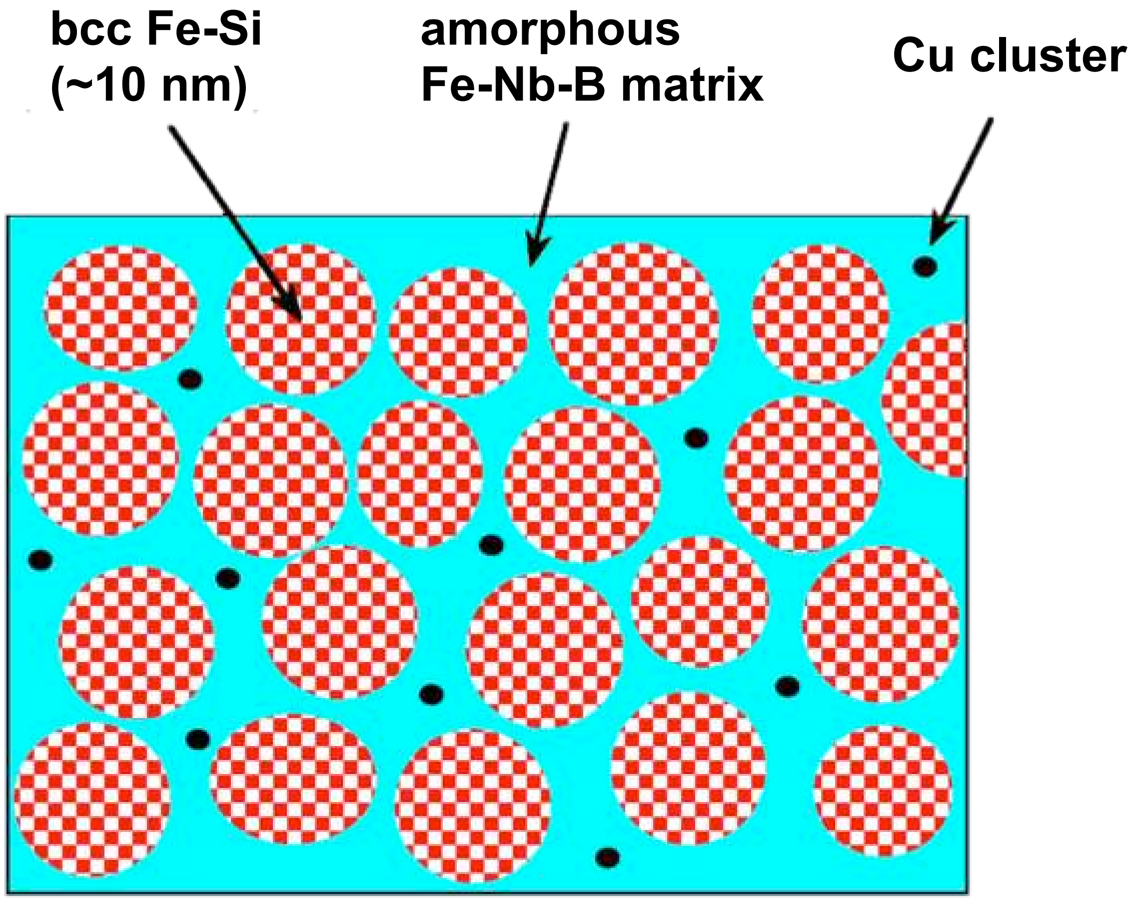

Kerr microscopy: high / low temperature observation

Heating of nanocrystalline ribbon above T_c (amorphous)

annealed in rotating field

annealed under tensile stress

annealed in dc field

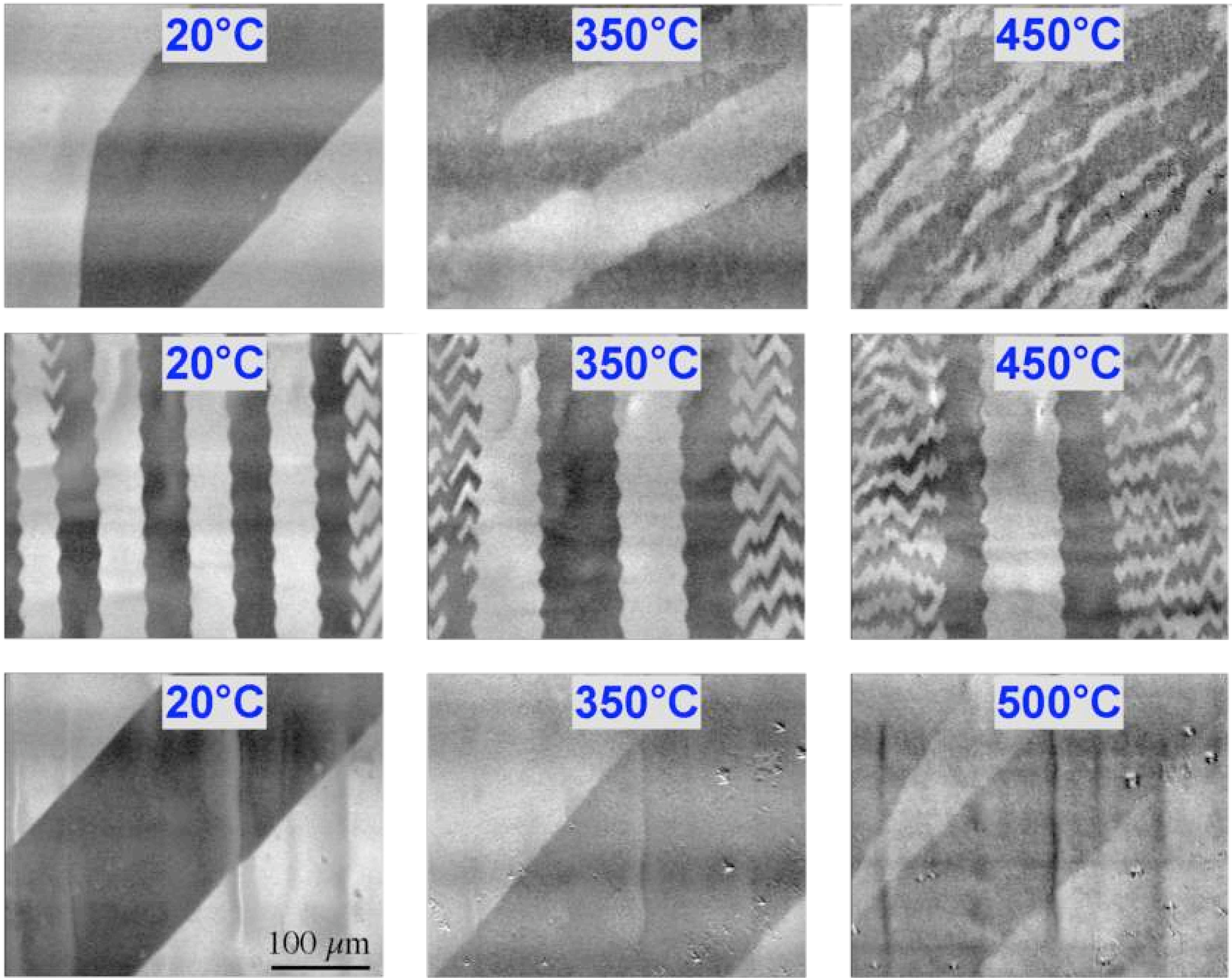

Quantitative Kerr microscopy

Quantitative Kerr microscopy

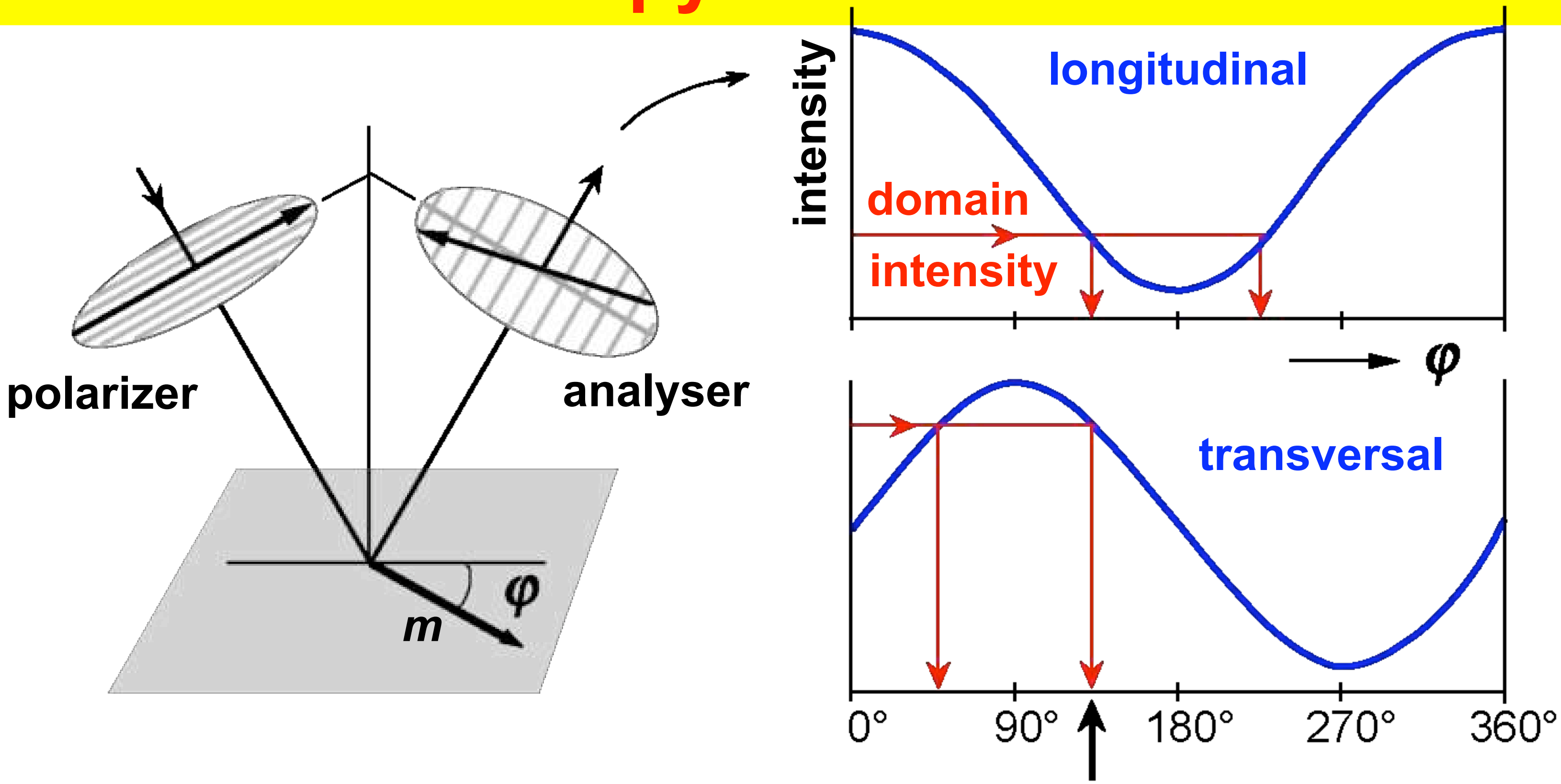

domains on (100)-FeSi sheet

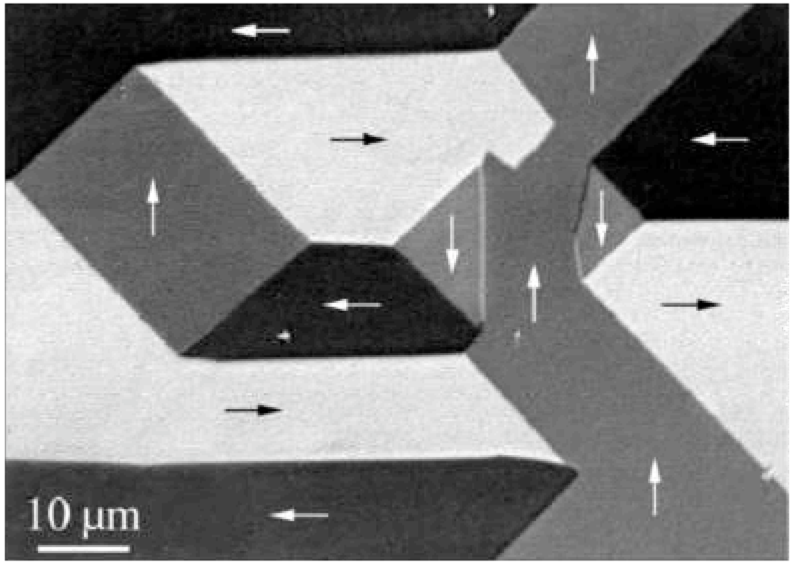

transversal

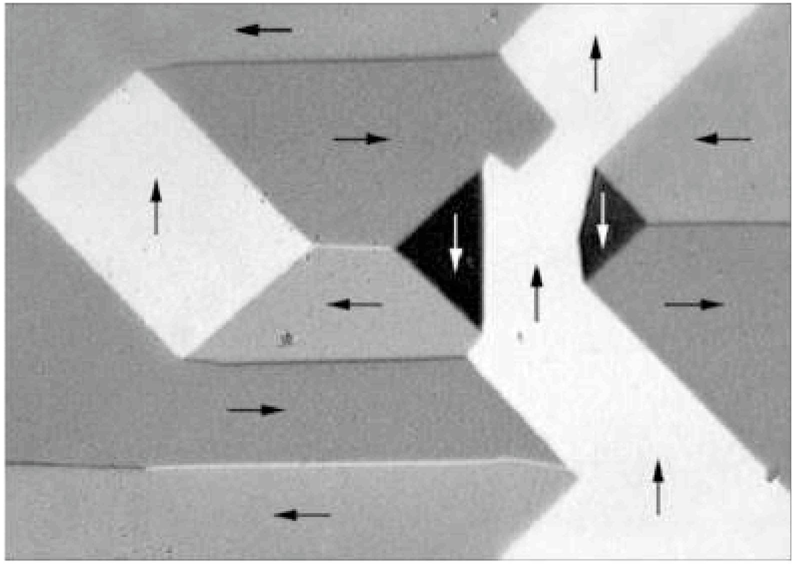

longitudinal

Quantitative Kerr microscopy

Domains in magnetostriction-free amorphous ribbon

as-quenched state

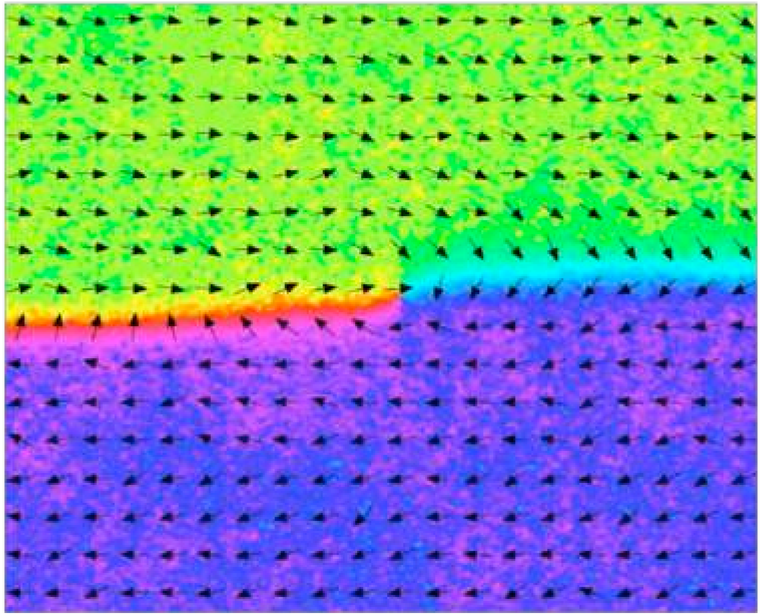

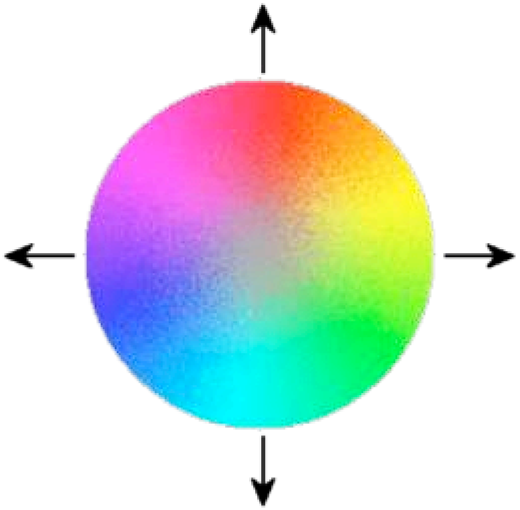

after annealing in rotating field

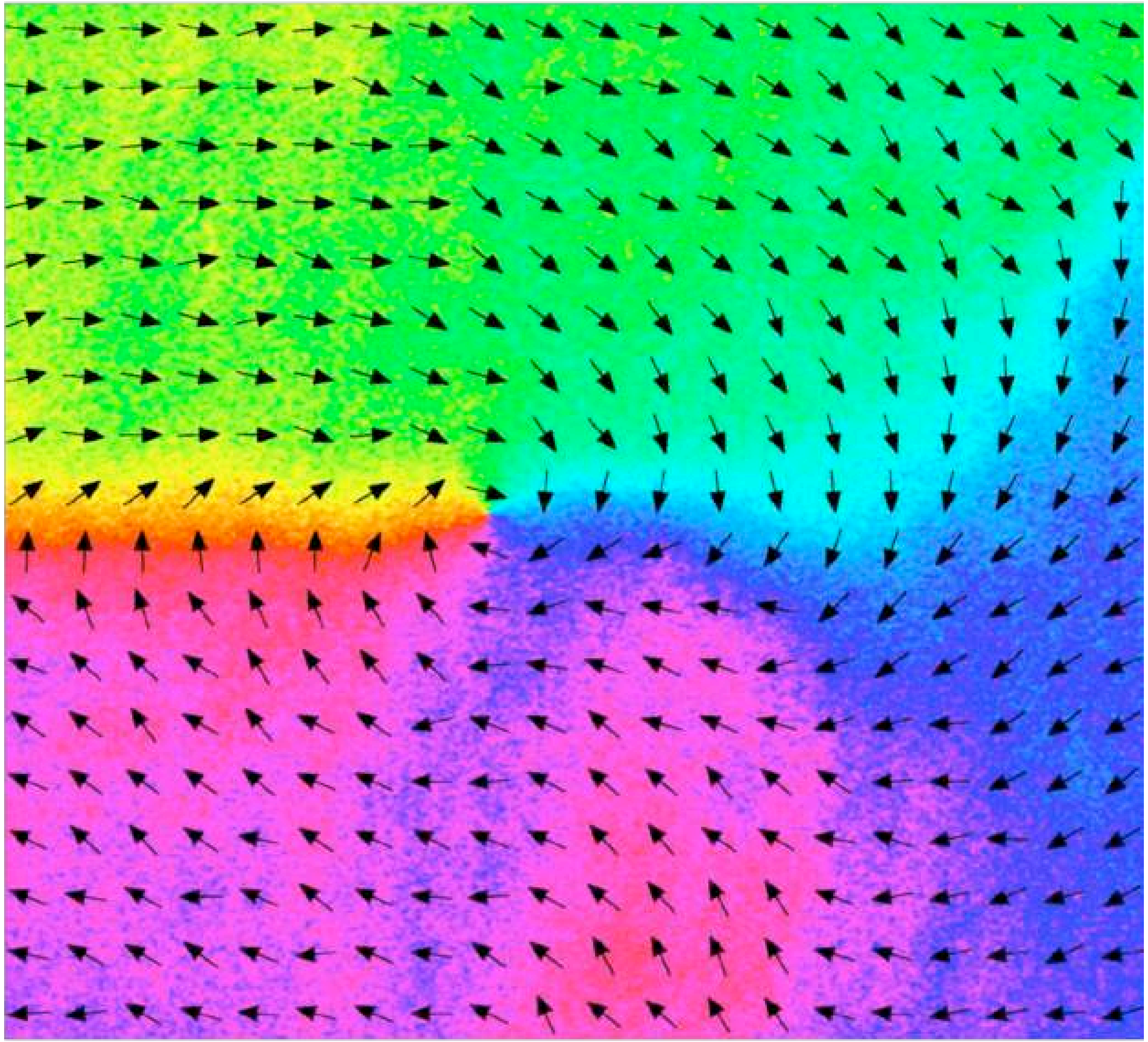

5 µm

Quantitative Kerr microscopy

Separation of polar and planar magnetization components by difference imaging

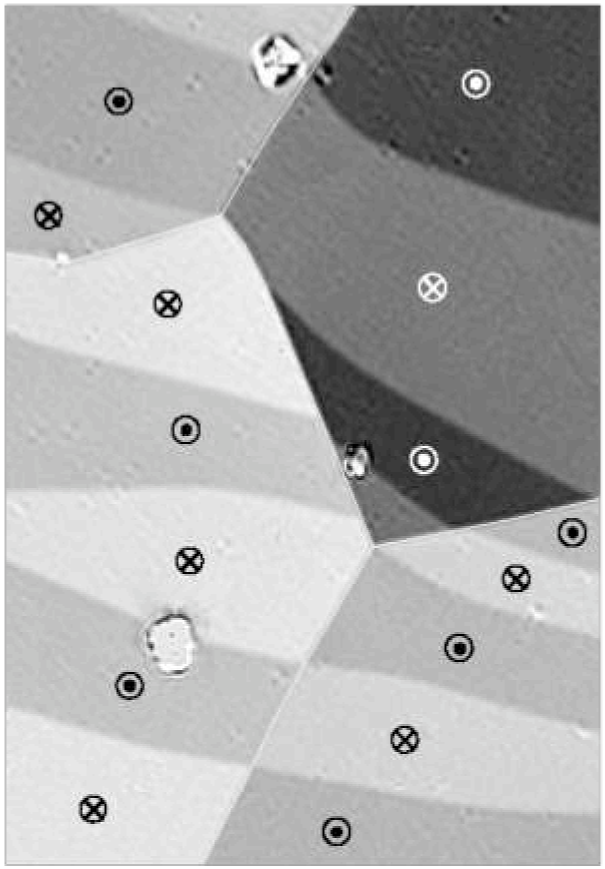

perpendicular incidence:
only polar component

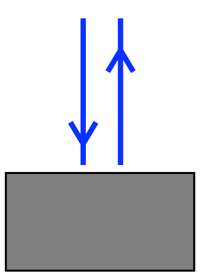

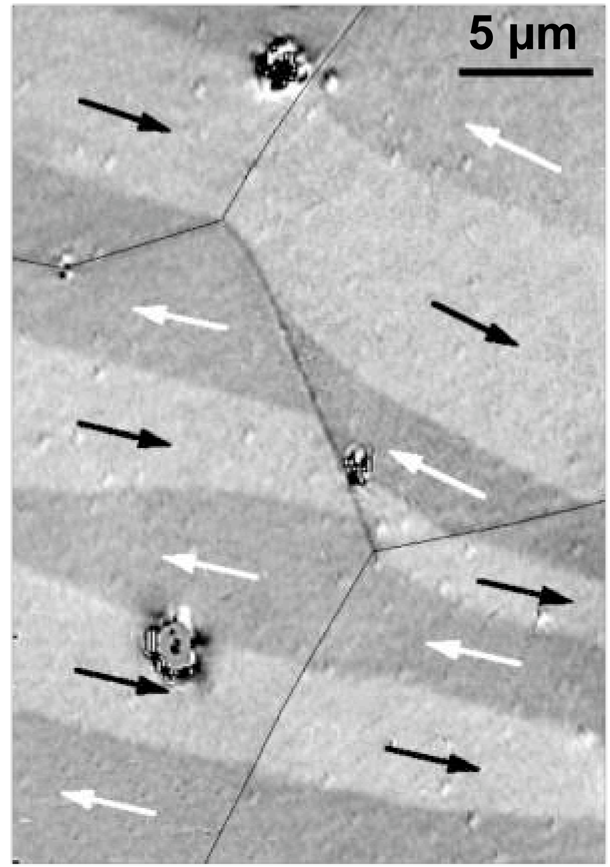

oblique incidence:
("aperture" difference image)
only planar component

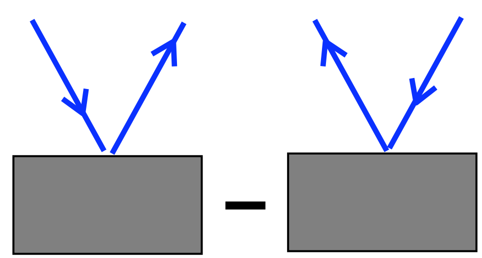

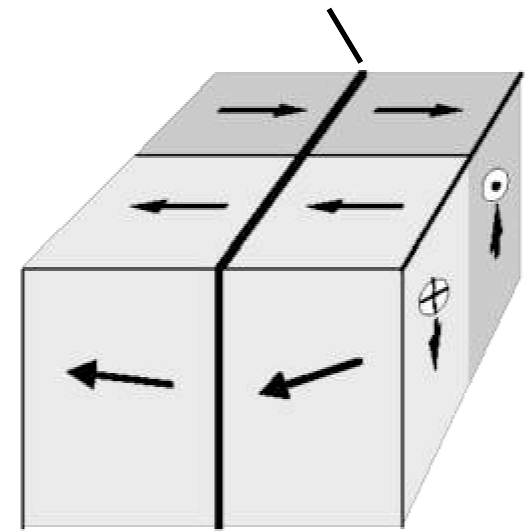

NdFeB

Quantitative Kerr microscopy

surface ⊥ texture axis

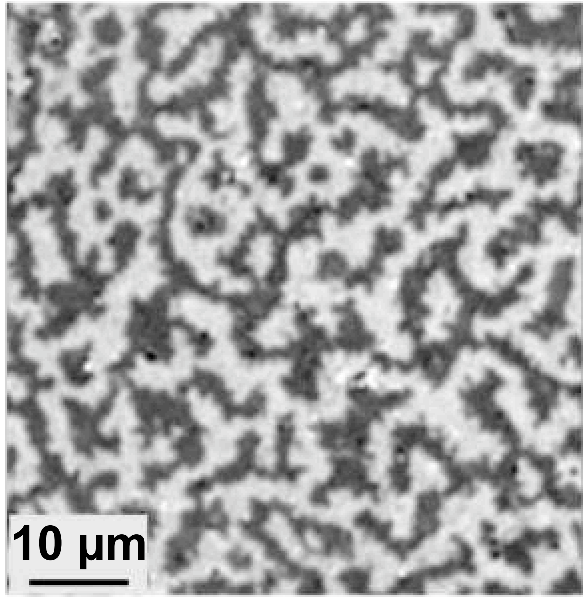

surface || texture axis

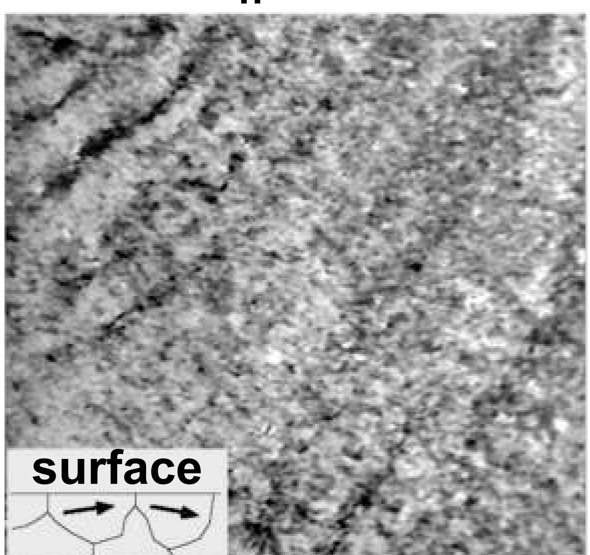

regular Kerr image

Interaction domains in fine-grained NdFeB material

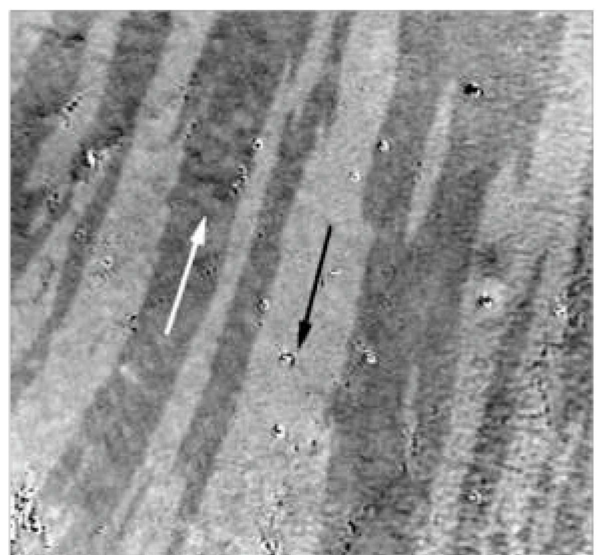

“aperture-difference image” shows pure planar components

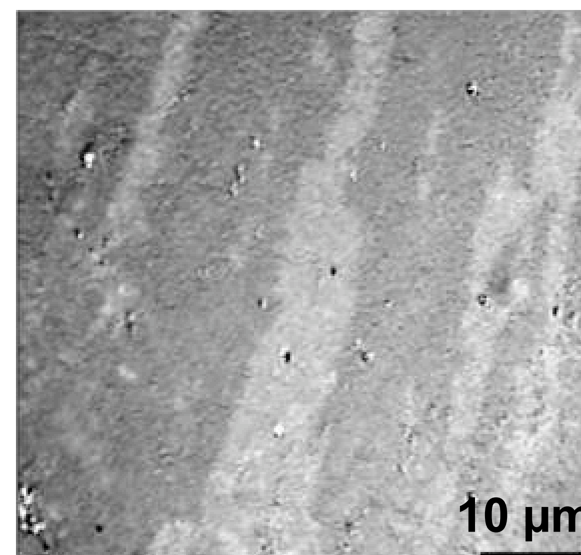

in magnetic field

Depth sensitivity

Depth sensitivity of Kerr microscopy

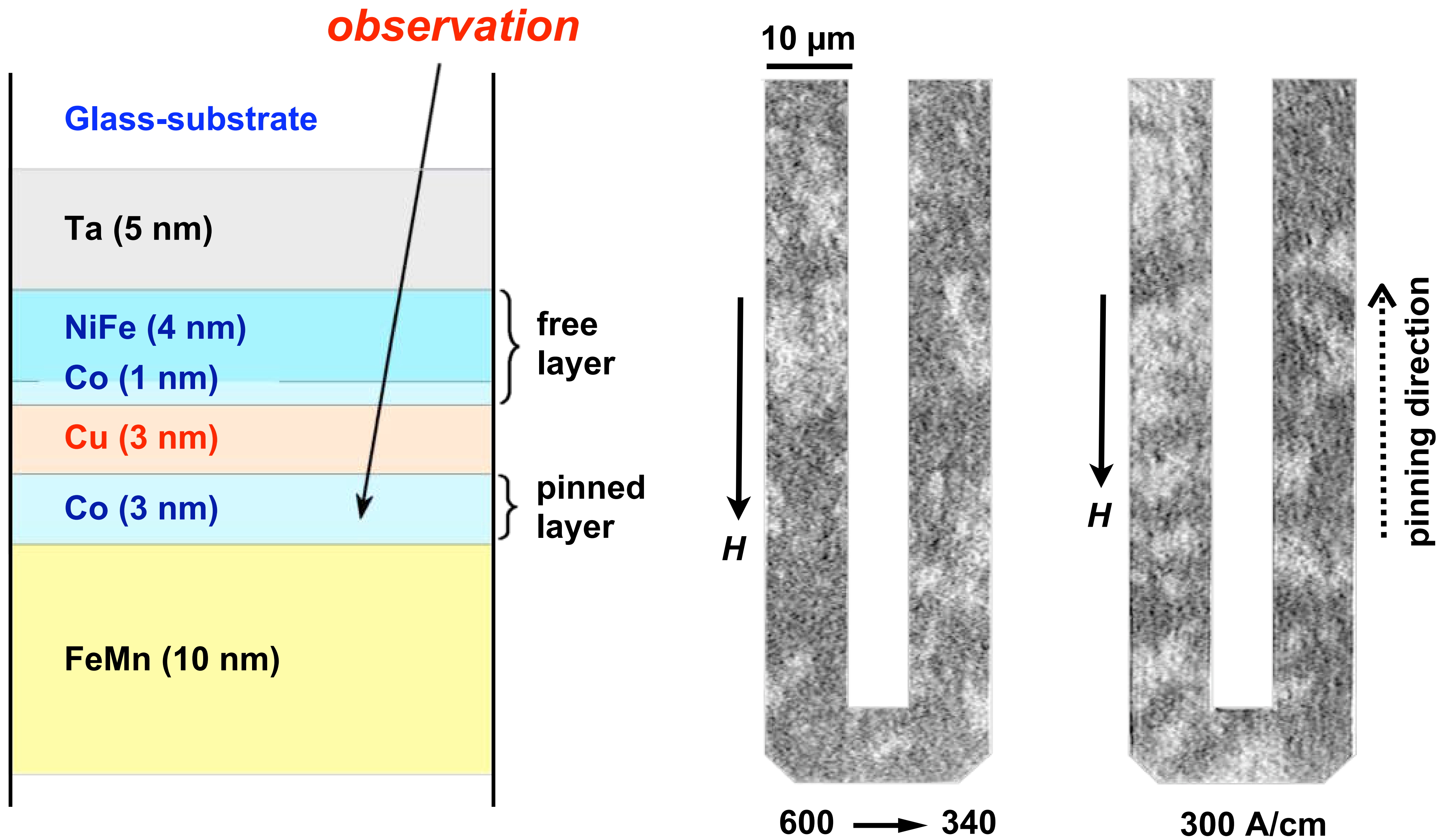

Depth sensitivity of Kerr microscopy

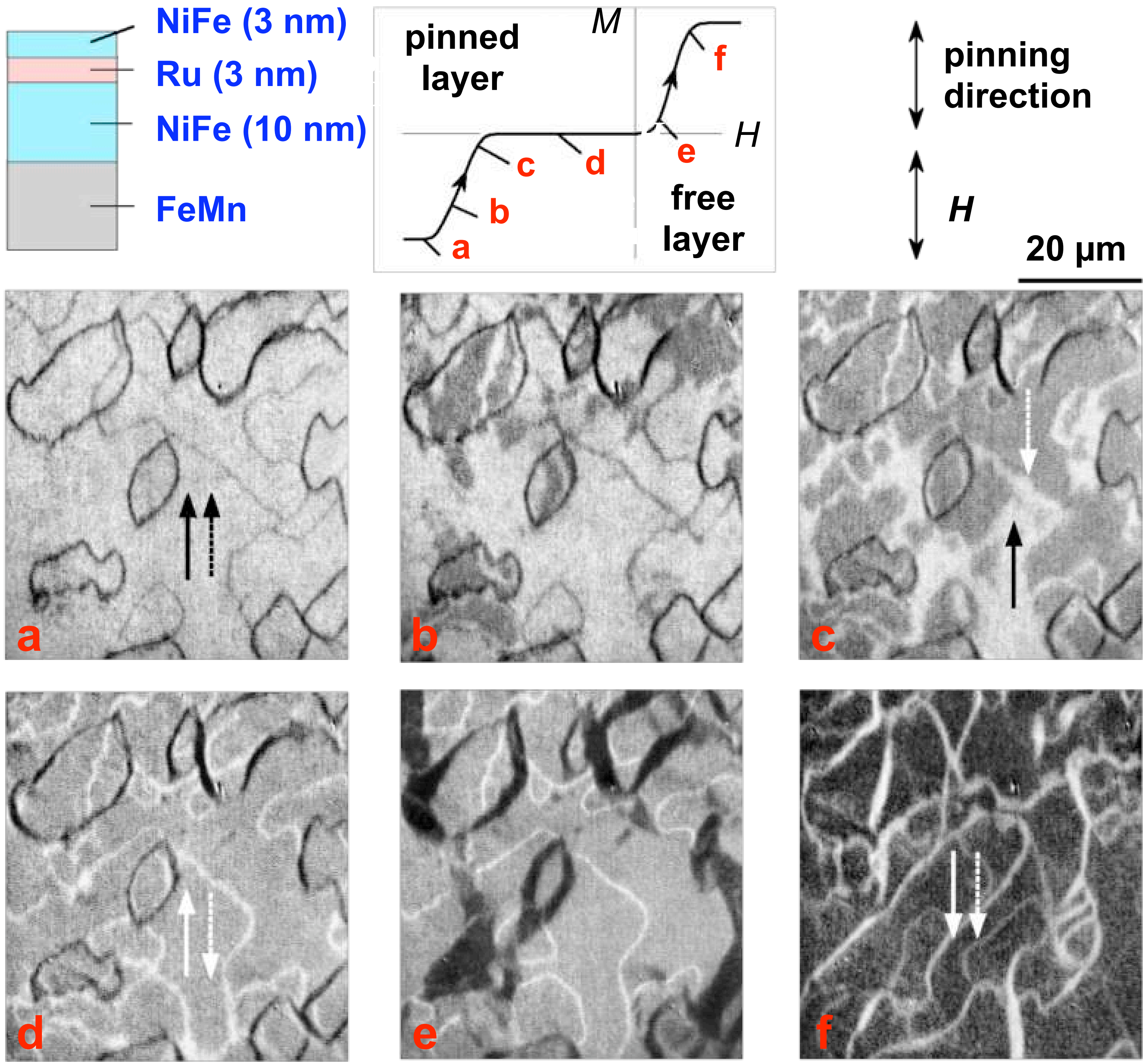

Sample: S. Parkin, IBM

Depth selective Kerr microscopy

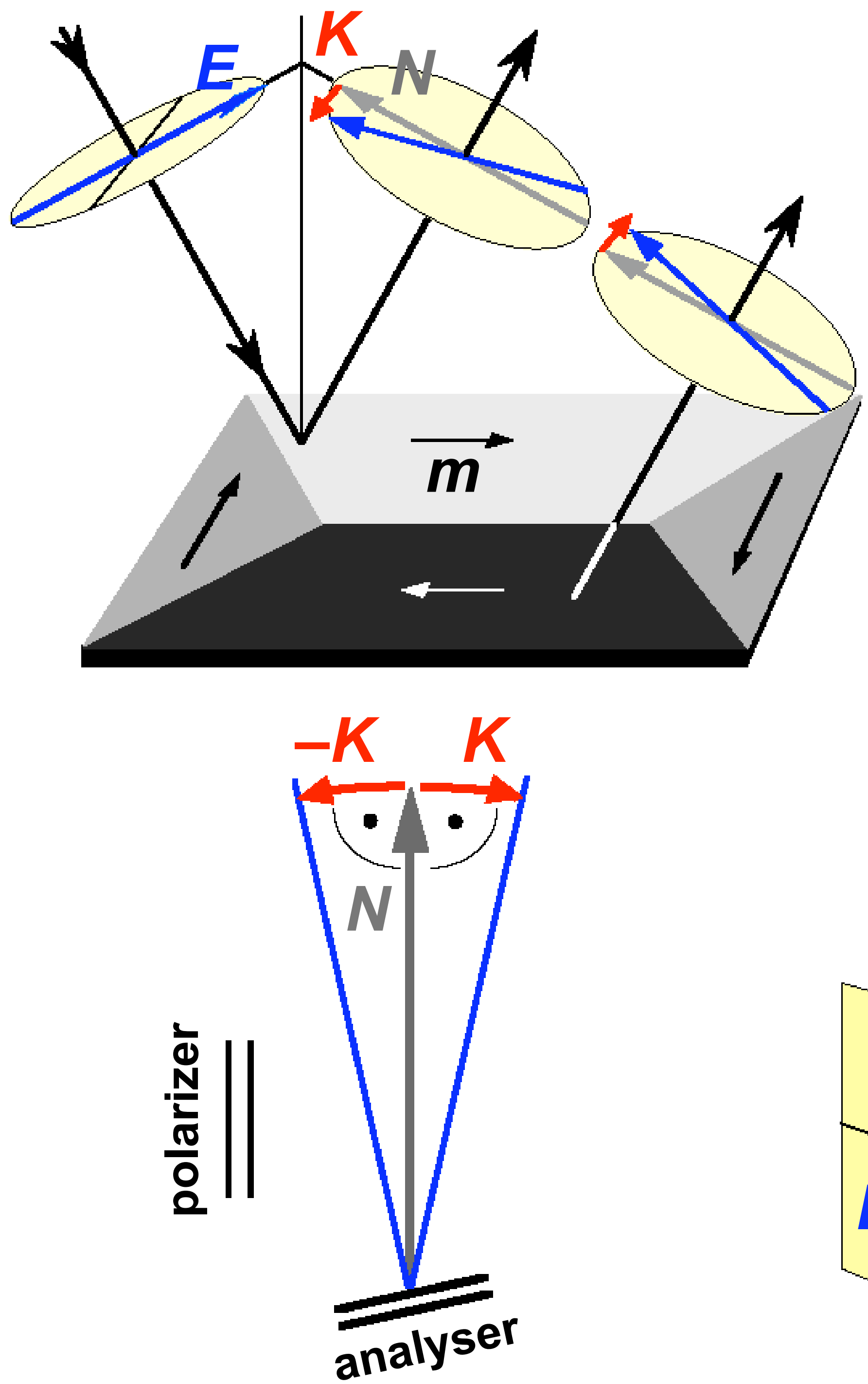

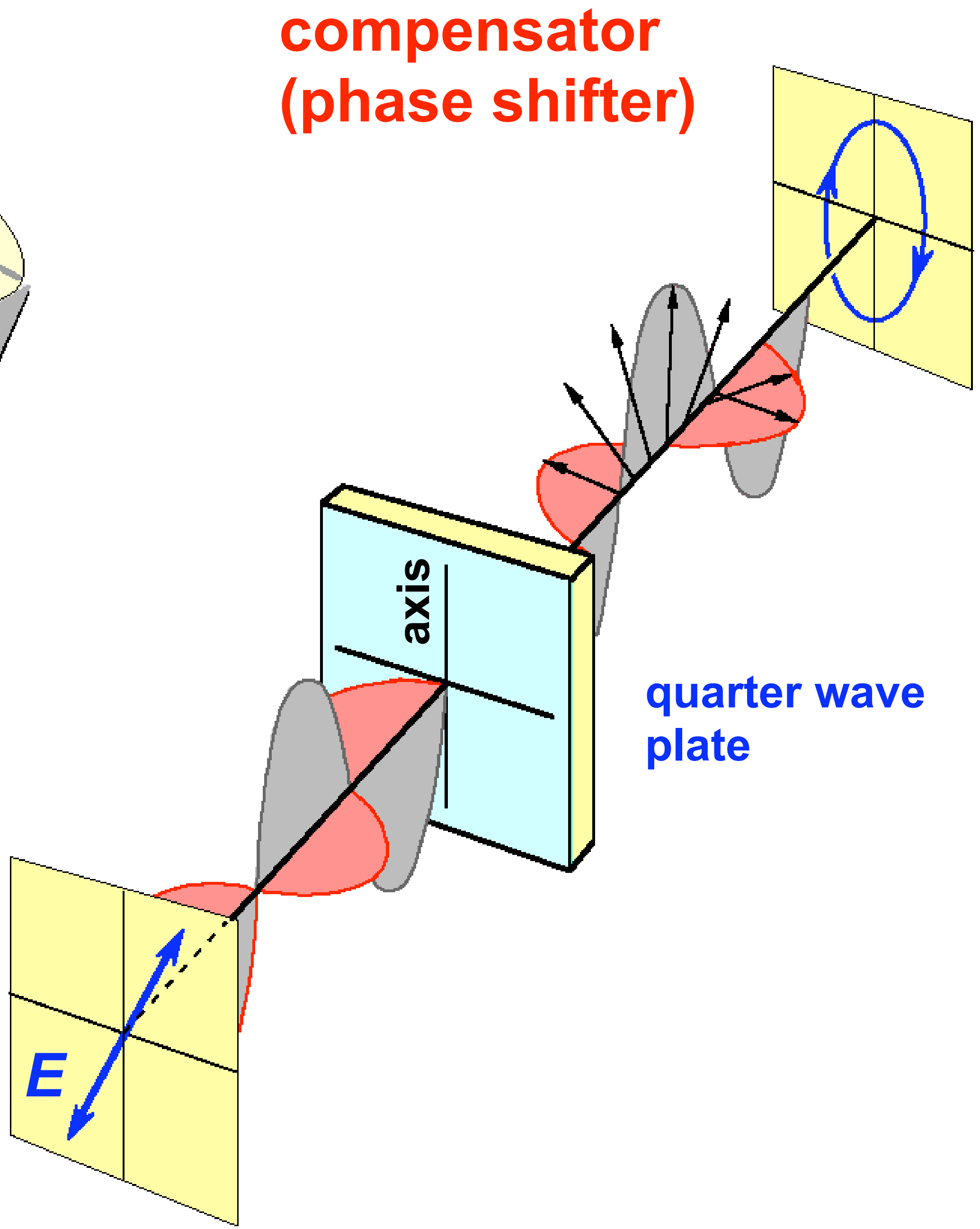

Depth selective Kerr microscopy

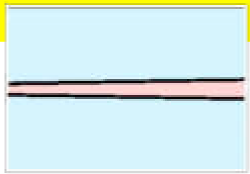

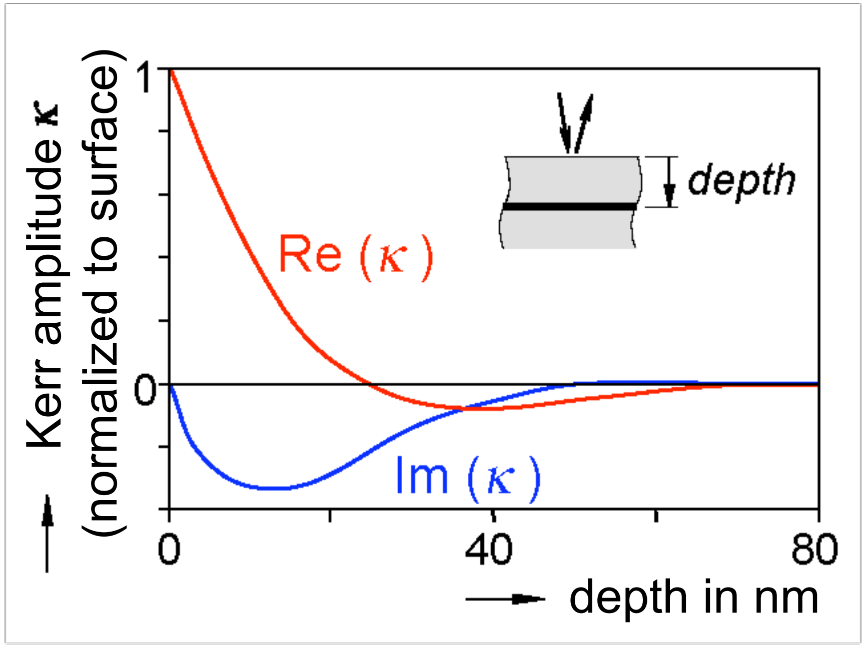

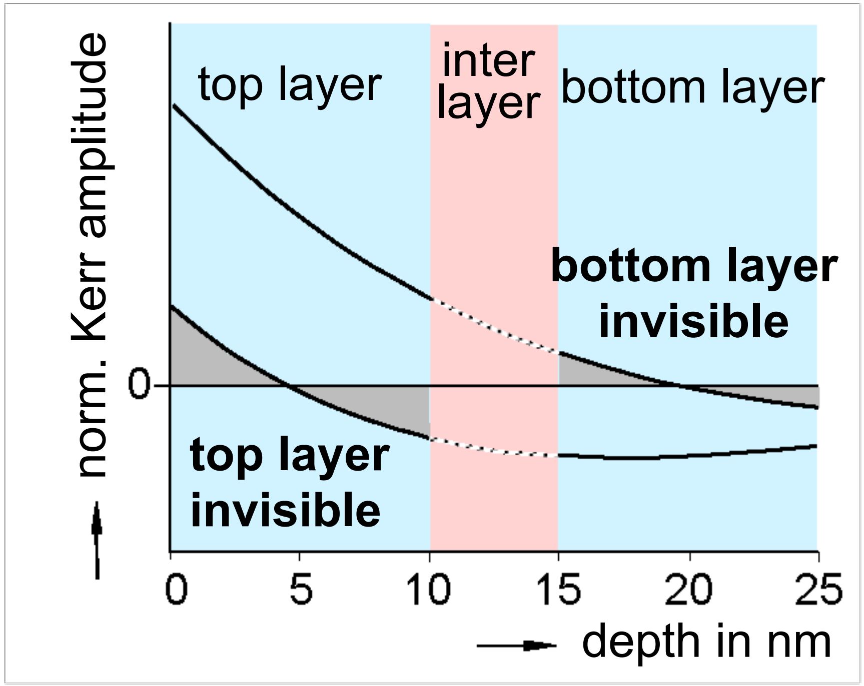

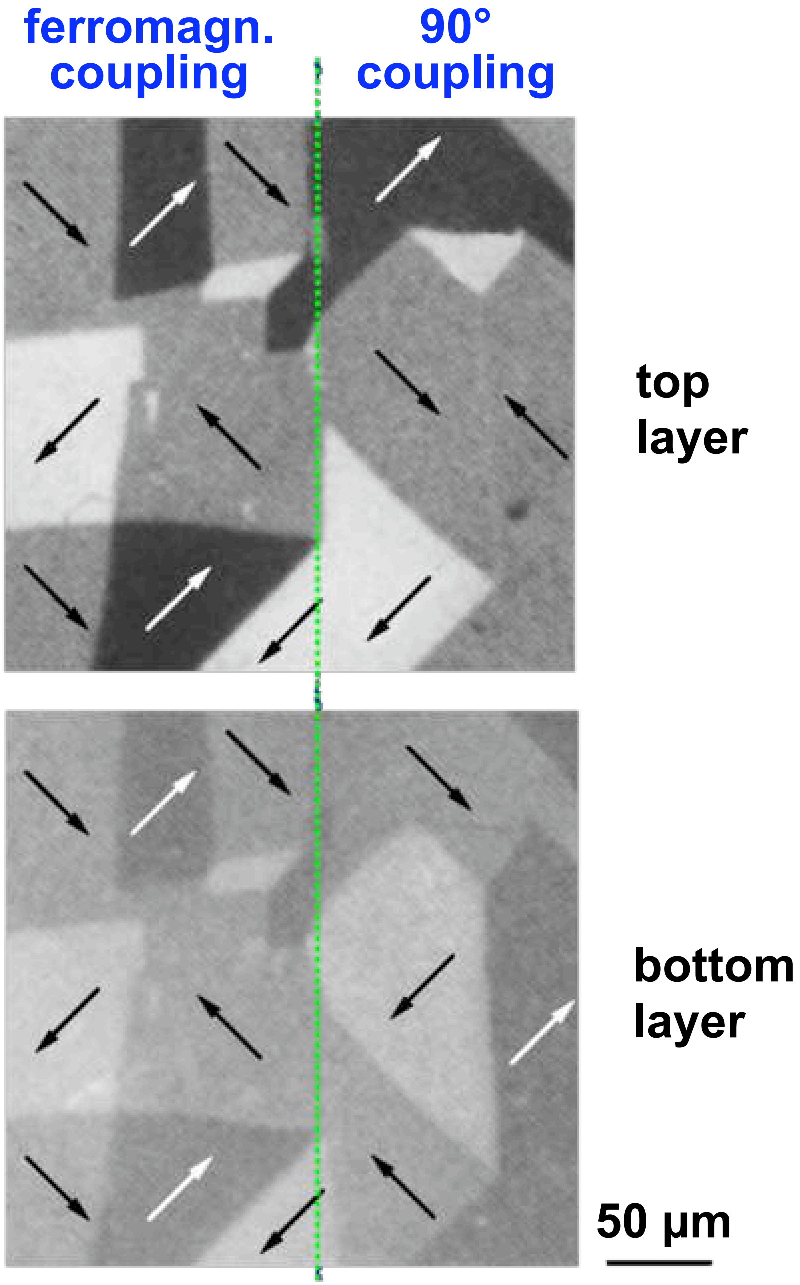

Depth selective Kerr microscopy

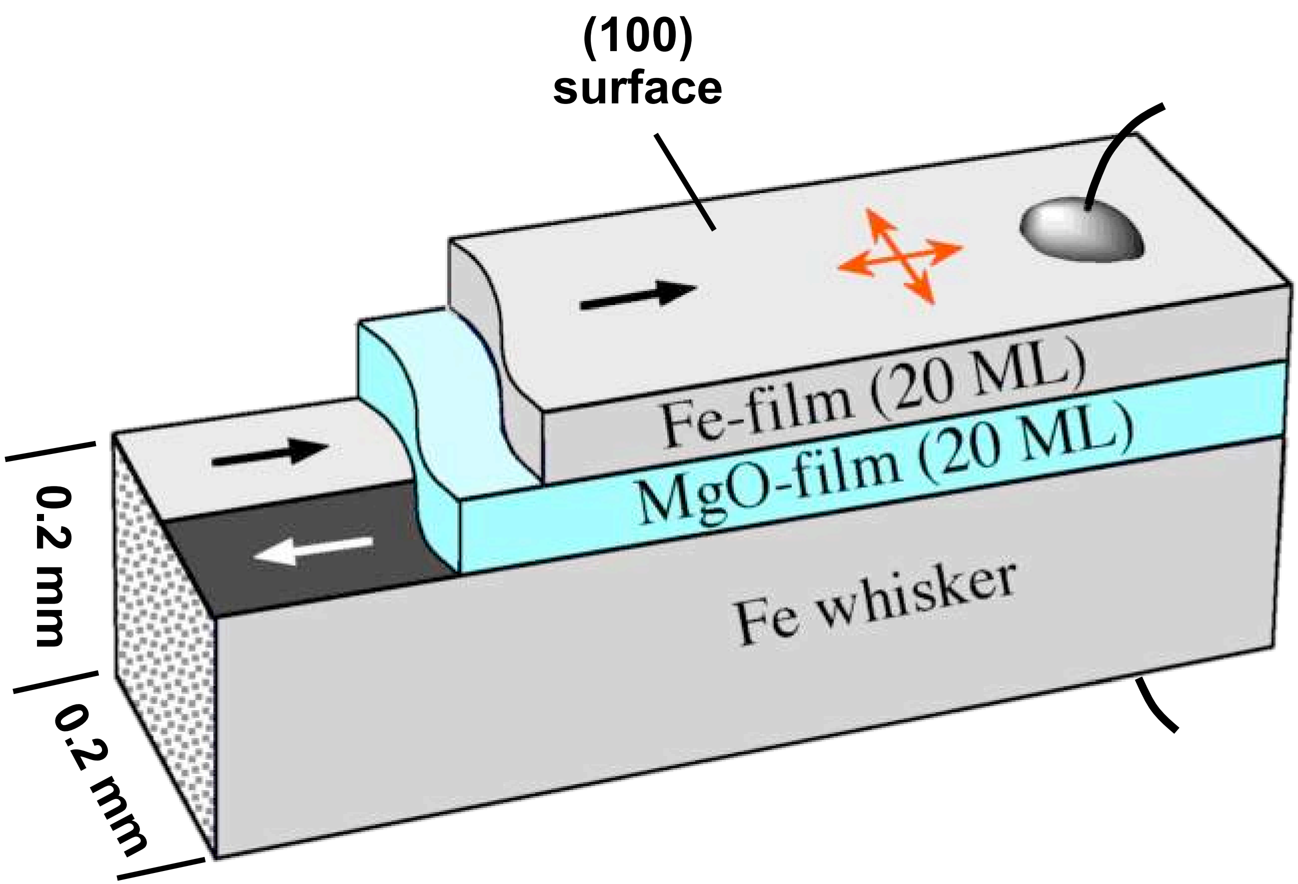

Epitaxial growth of films on whisker

Selective imaging of whisker and film domains

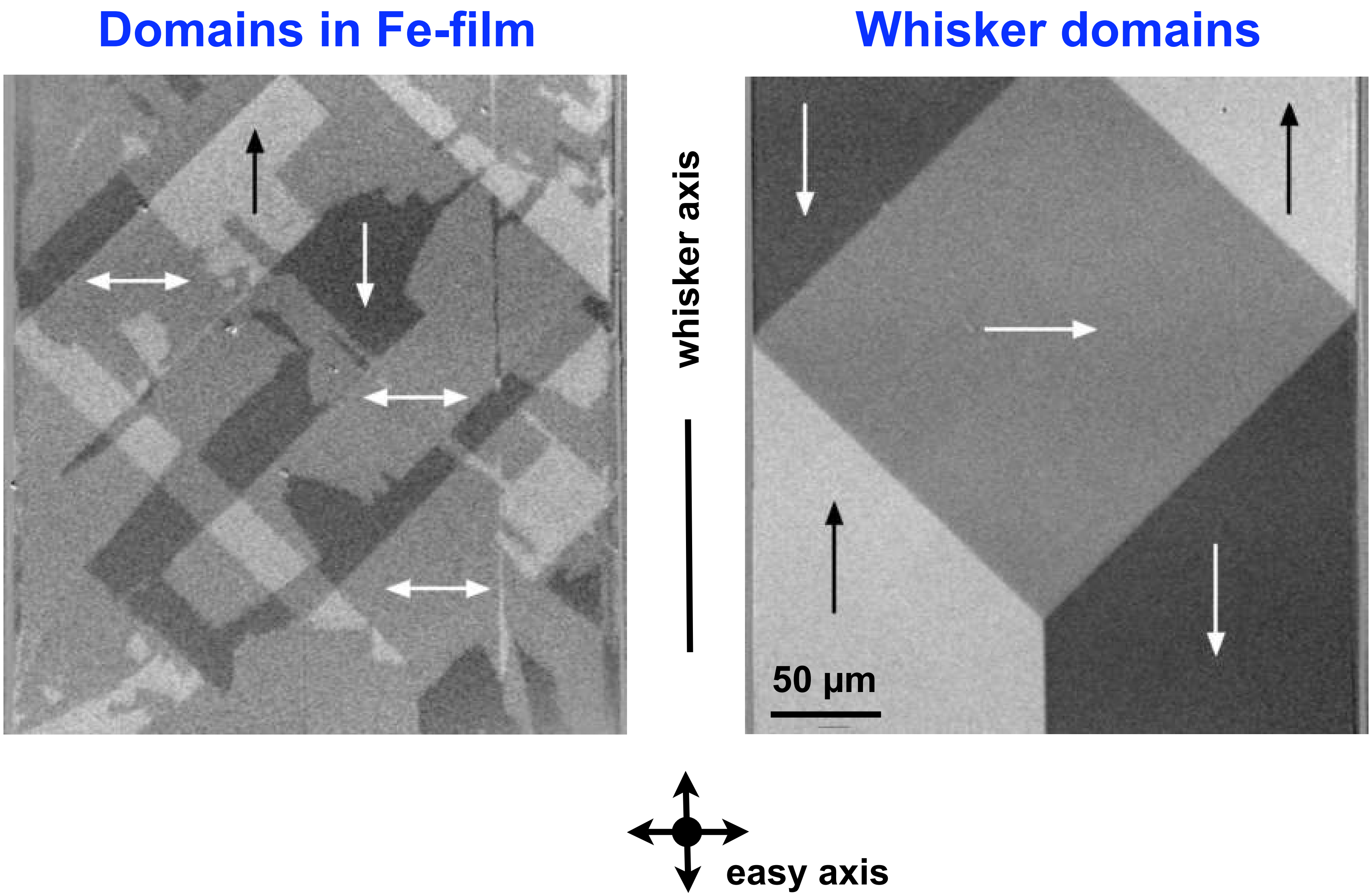

Selective imaging of whisker and film domains

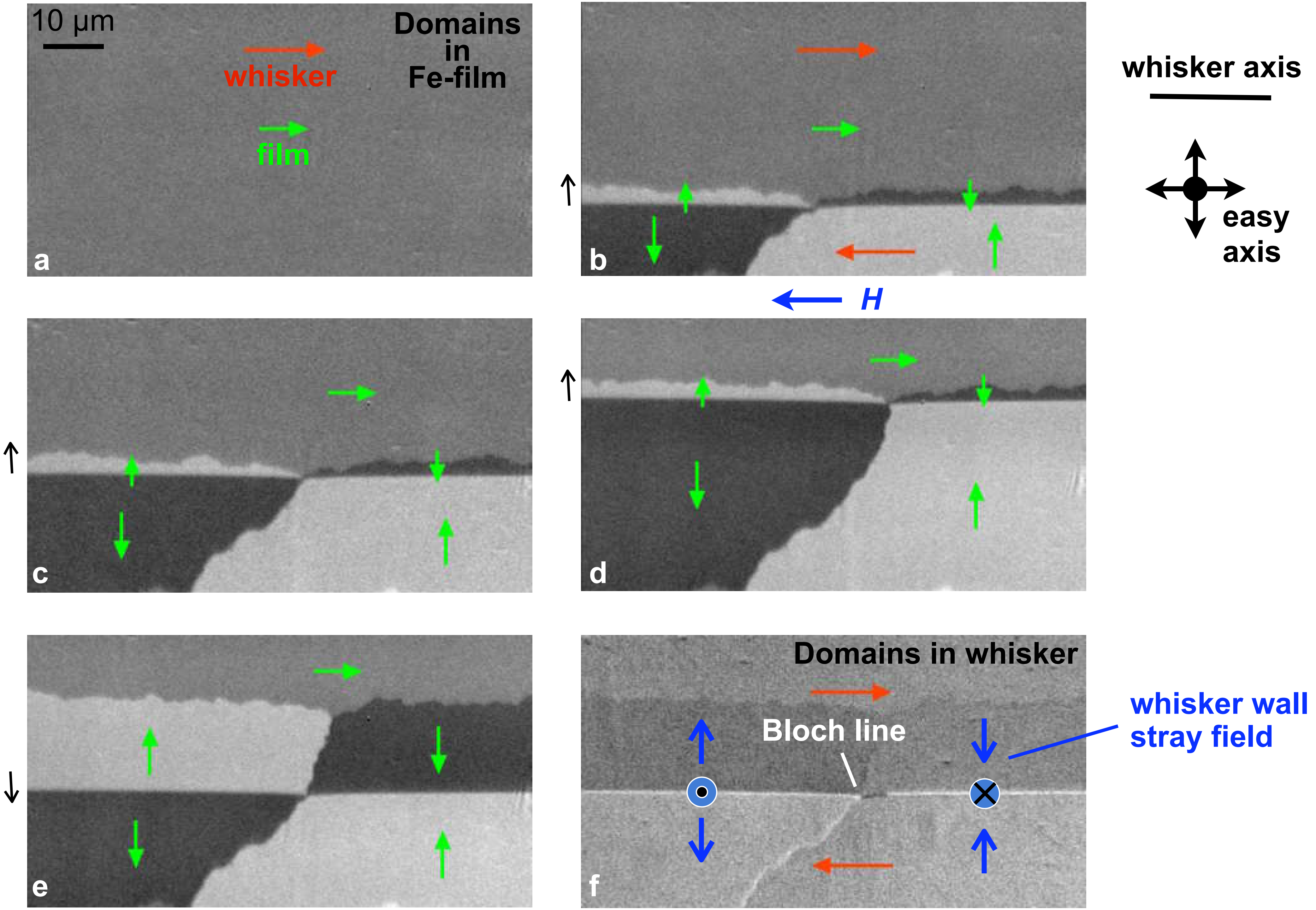

Time-resolved Kerr microscopy

Dynamic imaging at low speed

Permalloy, 240 nm thick

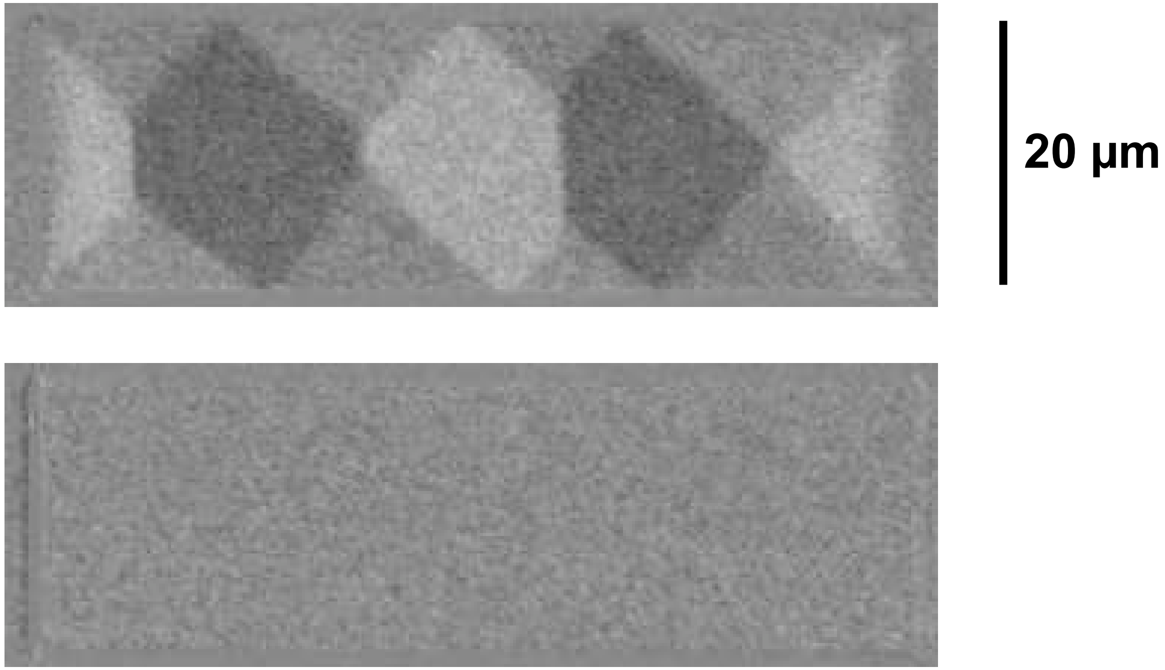

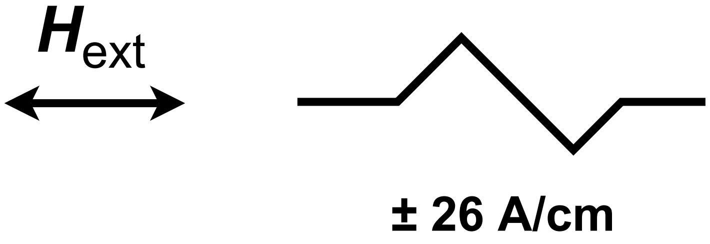

Time resolved Kerr microscopy

Time-resolved observation of periodic processes

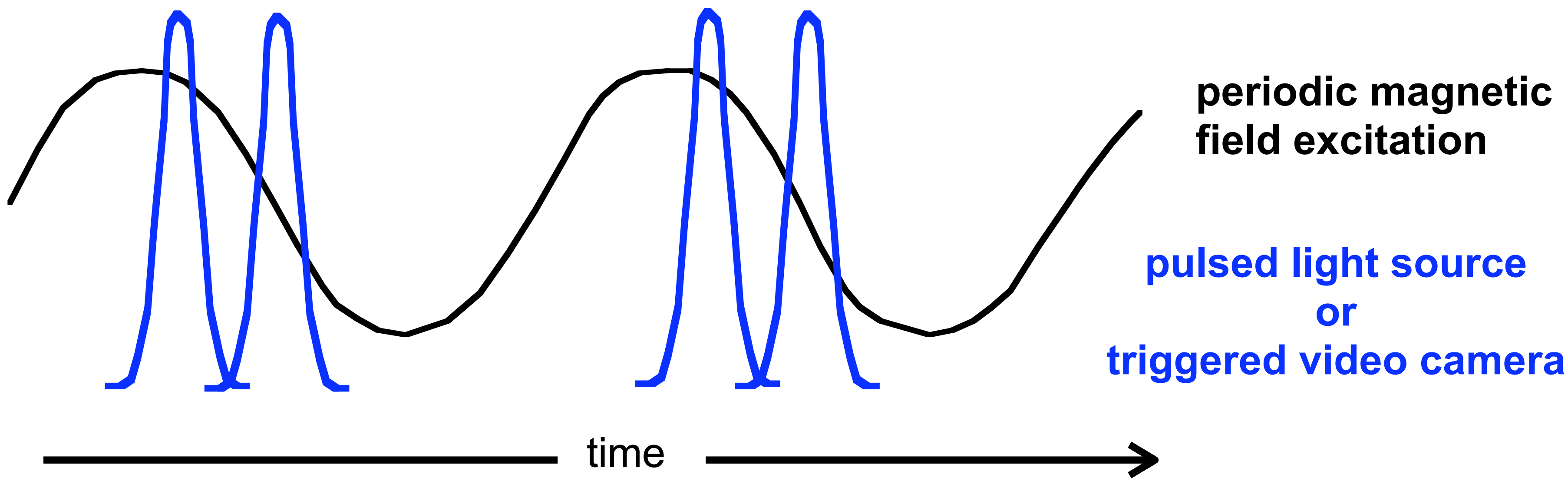

- W. Drechsel, Z. Phys. 164 (1961)
- R. Conger, G. Moore, J. Appl. Phys. 34 (1963)
- B. Passon, Z. Angew. Phys. 25 (1968)
- L.Gál, G. J. Zimmer, F. B. Humphrey, Phys. Stat. Sol. A30 (1975)
- B. Petek, P. Trouilloud, B. Argyle, IEEE Trans. Magn. 26, 1328 (1990)
- F. Liu, M. Schultz, M. Kryder, IEEE Trans. Magn. 26, 1340 (1990)
- M. Freeman and W. K. Hiebert: Stroboscopic microscopy of magnetic dynamics, in “Spin Dynamics in confined magnetic structures I”, Springer Berlin (2002)
- J.P. Park, P. Eames, D.M. Engebretson, J. Berezovsky, and P.A. Crowell, Phys. Rev. B 67, 020403R (2003)

Time resolved Kerr microscopy, setup

High Speed Camera
(Picostar© from Lavision)

Gated intensifier

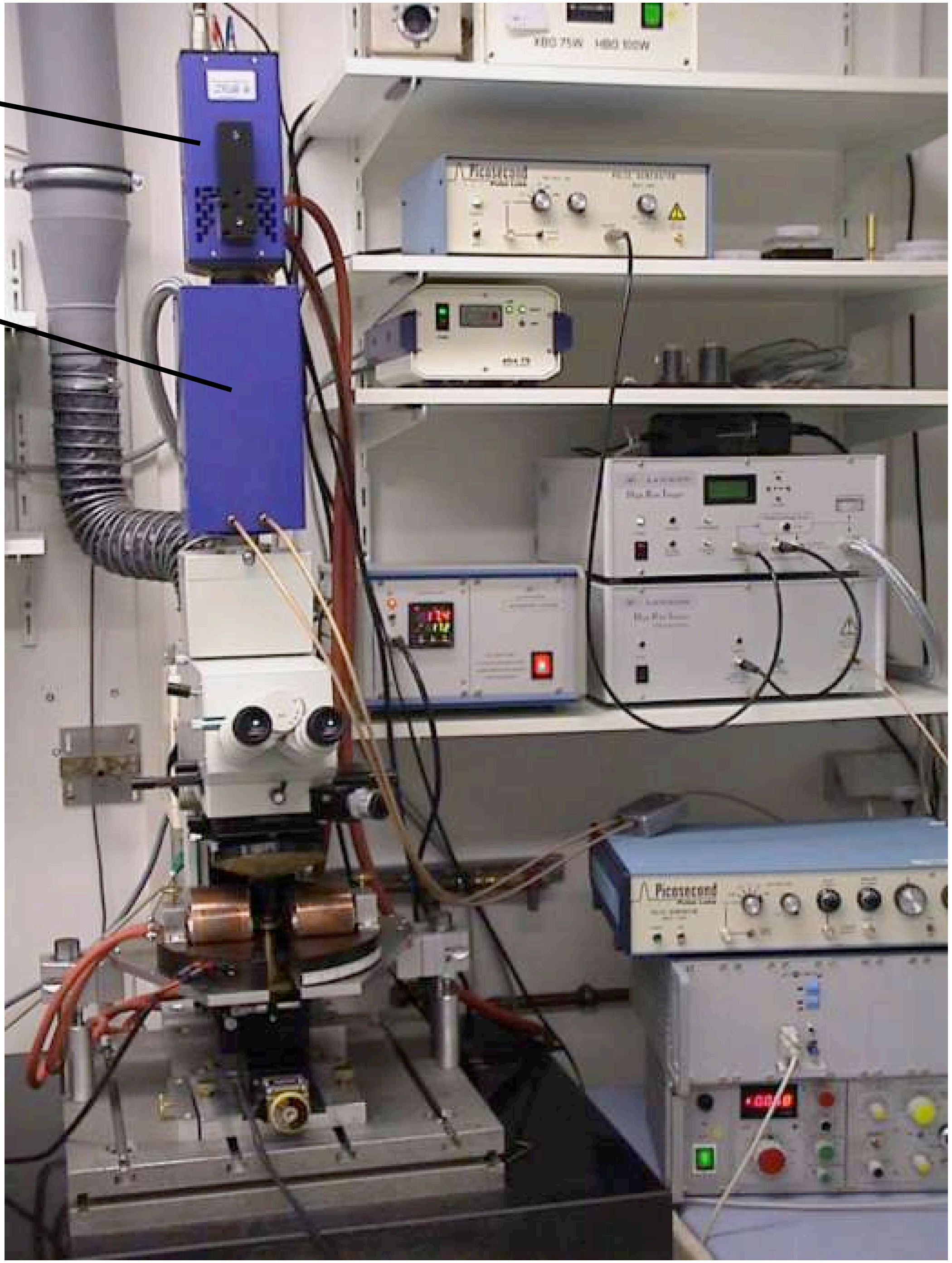

max. repetition rate: 80 MHz

opening gate: 250 ps – DC

Time resolved Kerr microscopy, setup

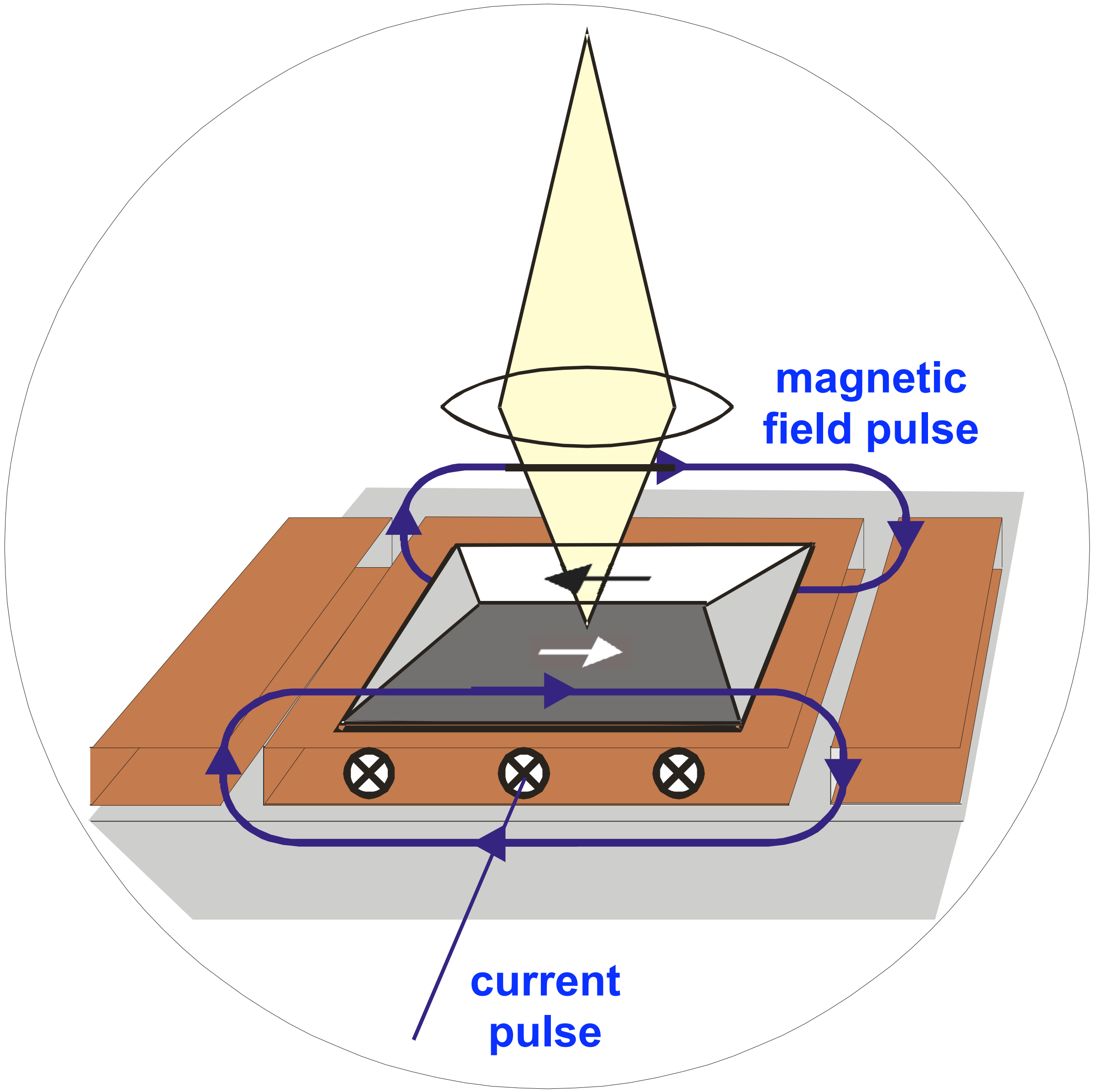

- coplanar waveguide
- fast field excitation
- patterned magnetic element

sample preparation:
R. Kaltofen, C. Krien, I. Mönch, H. Vinzelberg, C.M. Schneider (IFW Dresden)

Time resolved Kerr microscopy, setup

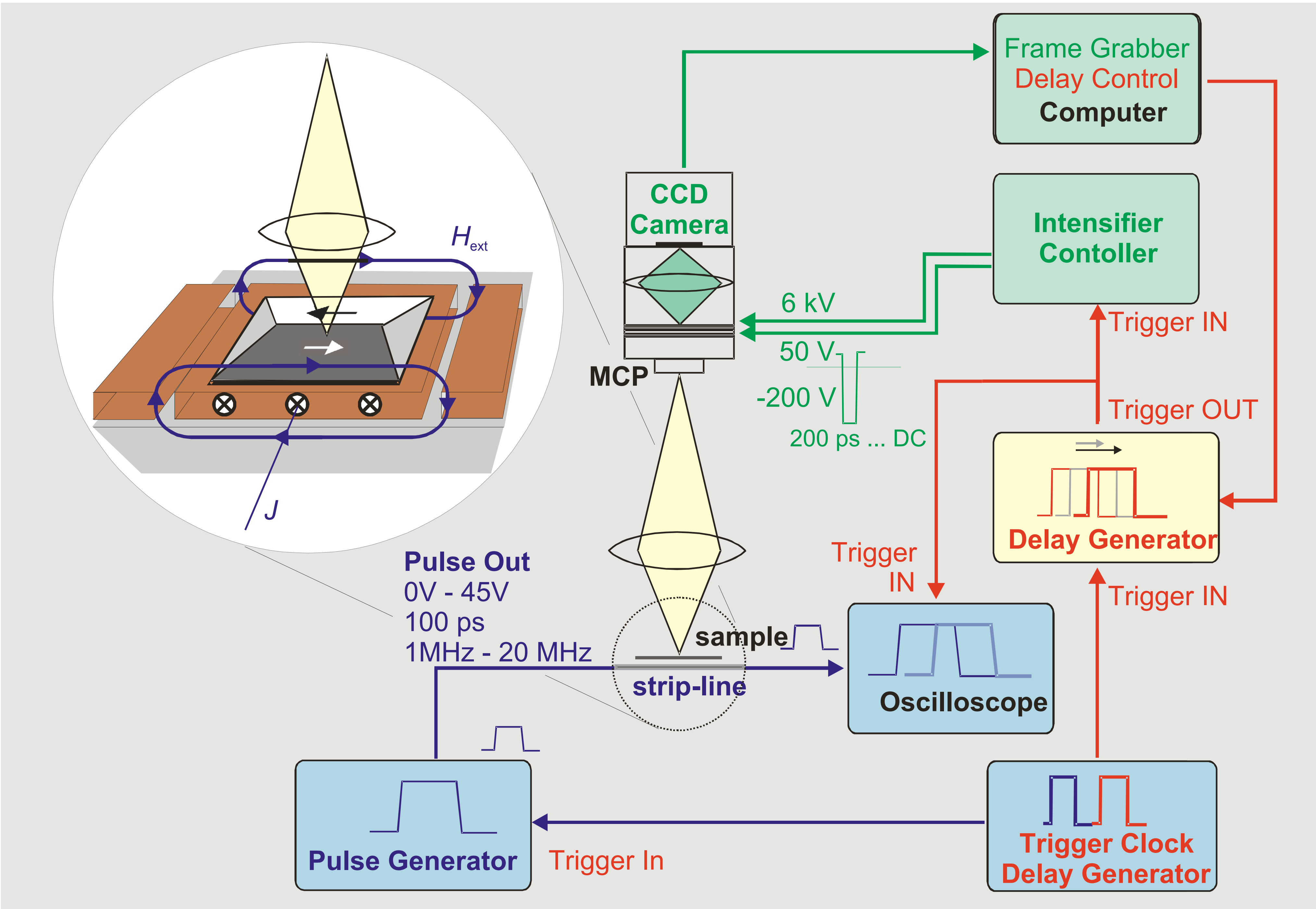

Time resolved Kerr microscopy

Advantage of wide-field setup

- combination with static imaging
- flexible gating time, repetition rate

Limitations

- limited repetition rate, limited illumination intensity

  → no single shot imaging possible

  → accumulation of large number of independent events necessary (at fixed time after pulse)

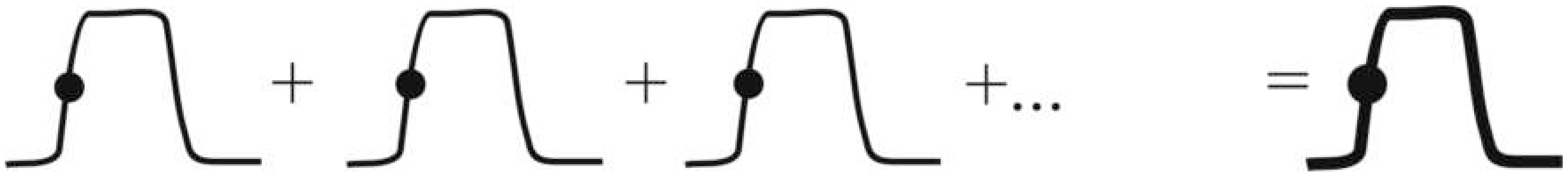

  → requires repetitive magnetization processes!!

- only elements larger than some micrometer can be imaged

quasistatic

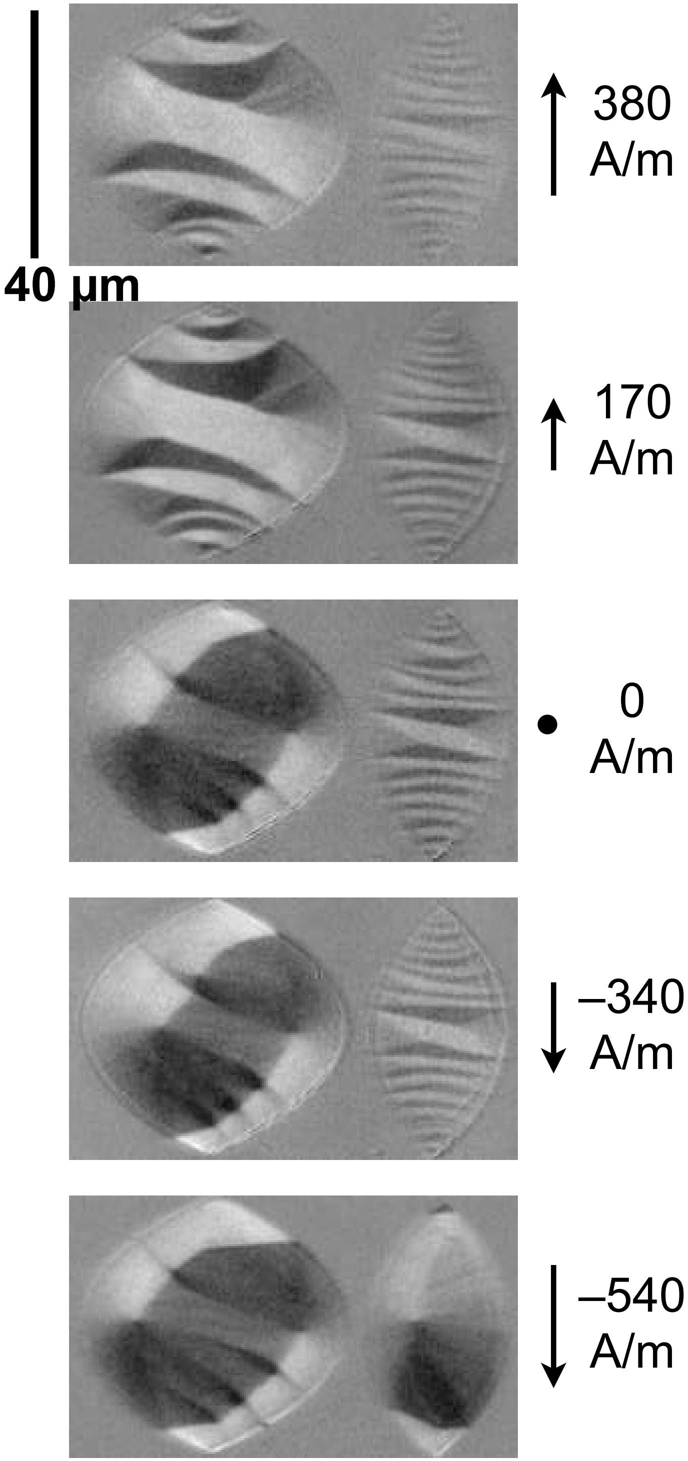

dynamic switching

Permalloy,
40 nm thick

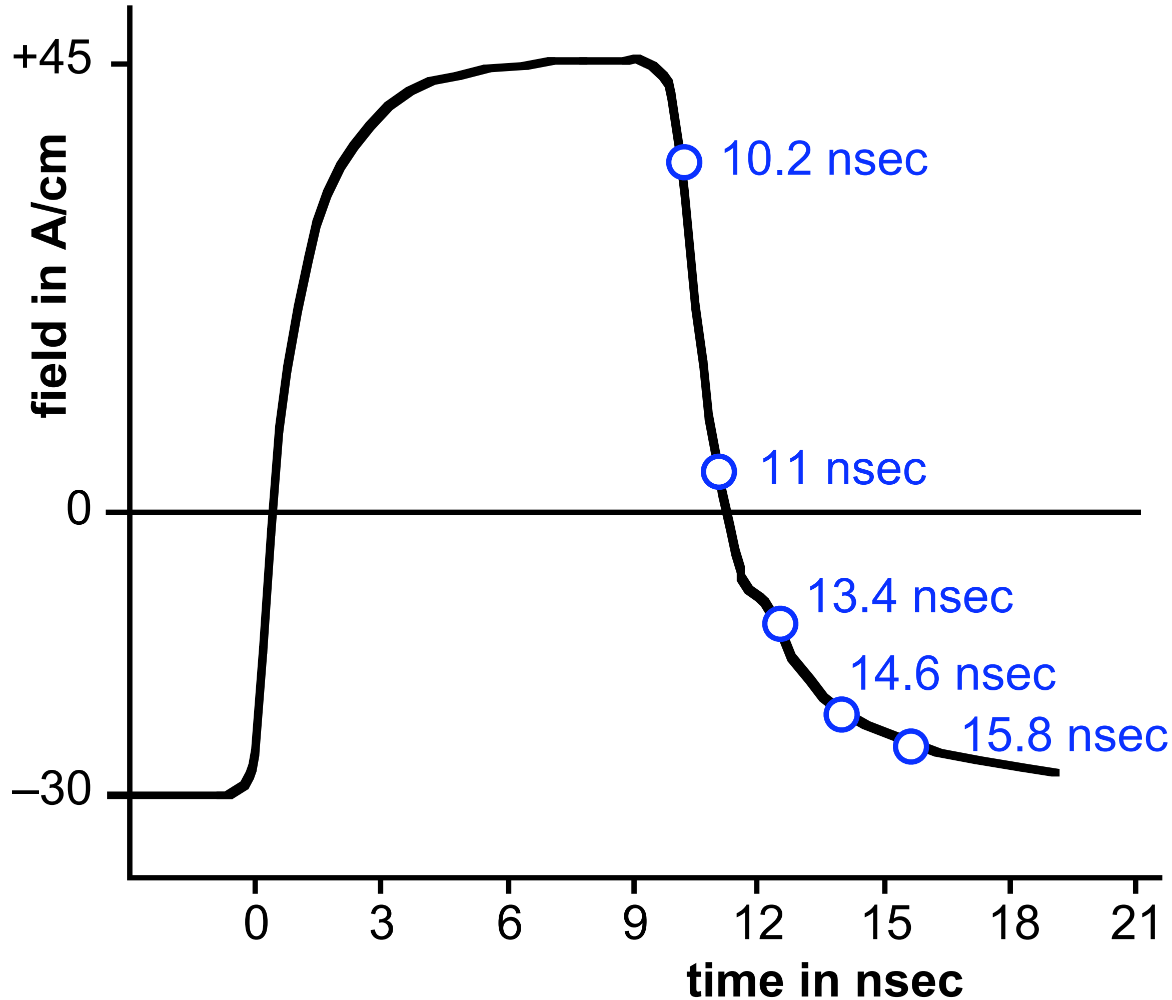

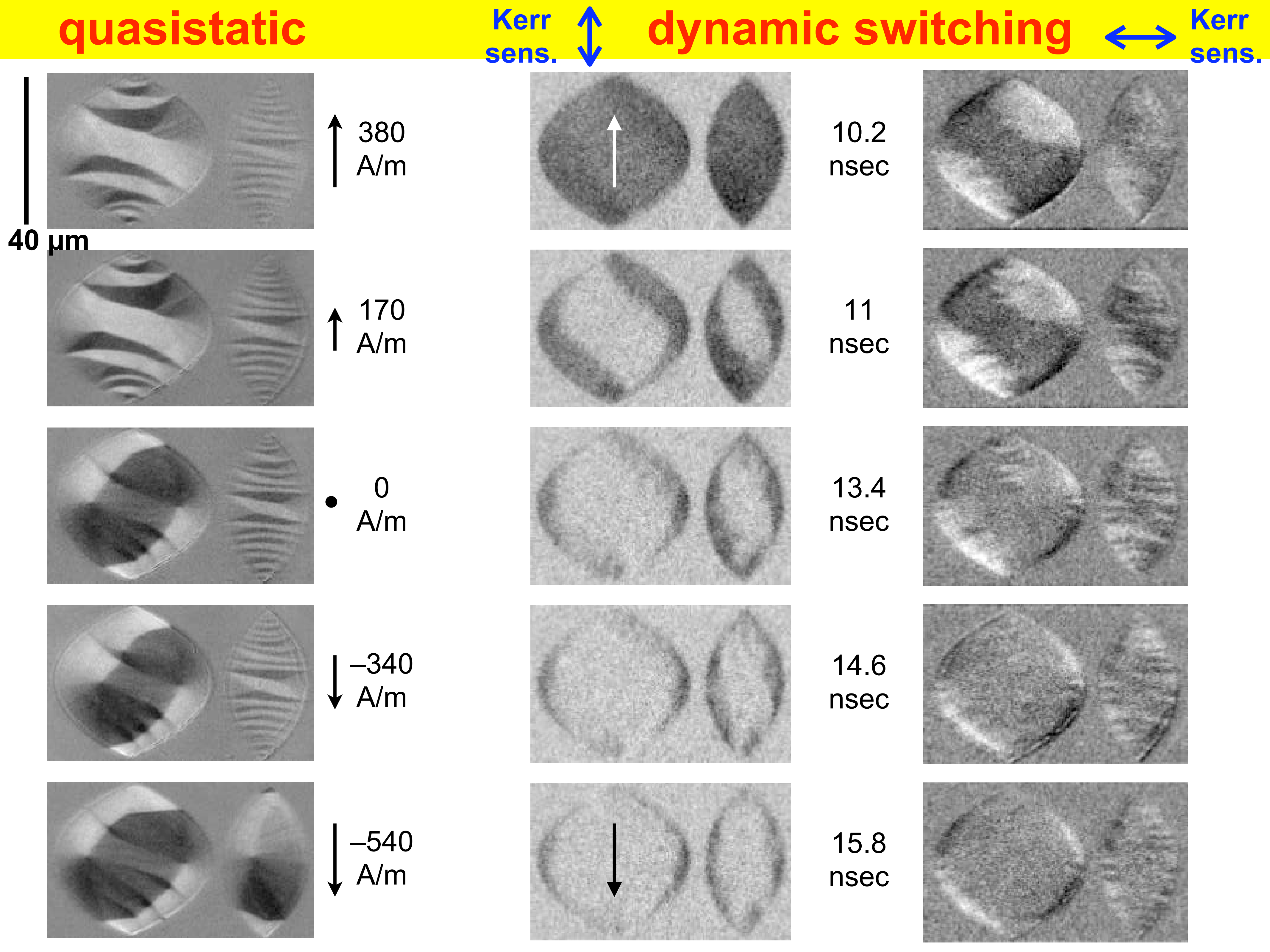
quasistatic
Kerr sens.
dynamic switching
Kerr sens.
40 µm
380 A/m
170 A/m
0 A/m
–340 A/m
–540 A/m
10.2 nsec
11 nsec
13.4 nsec
14.6 nsec
15.8 nsec

Switching of Permalloy element (40 x 30 µm^2, 50 nm thick)

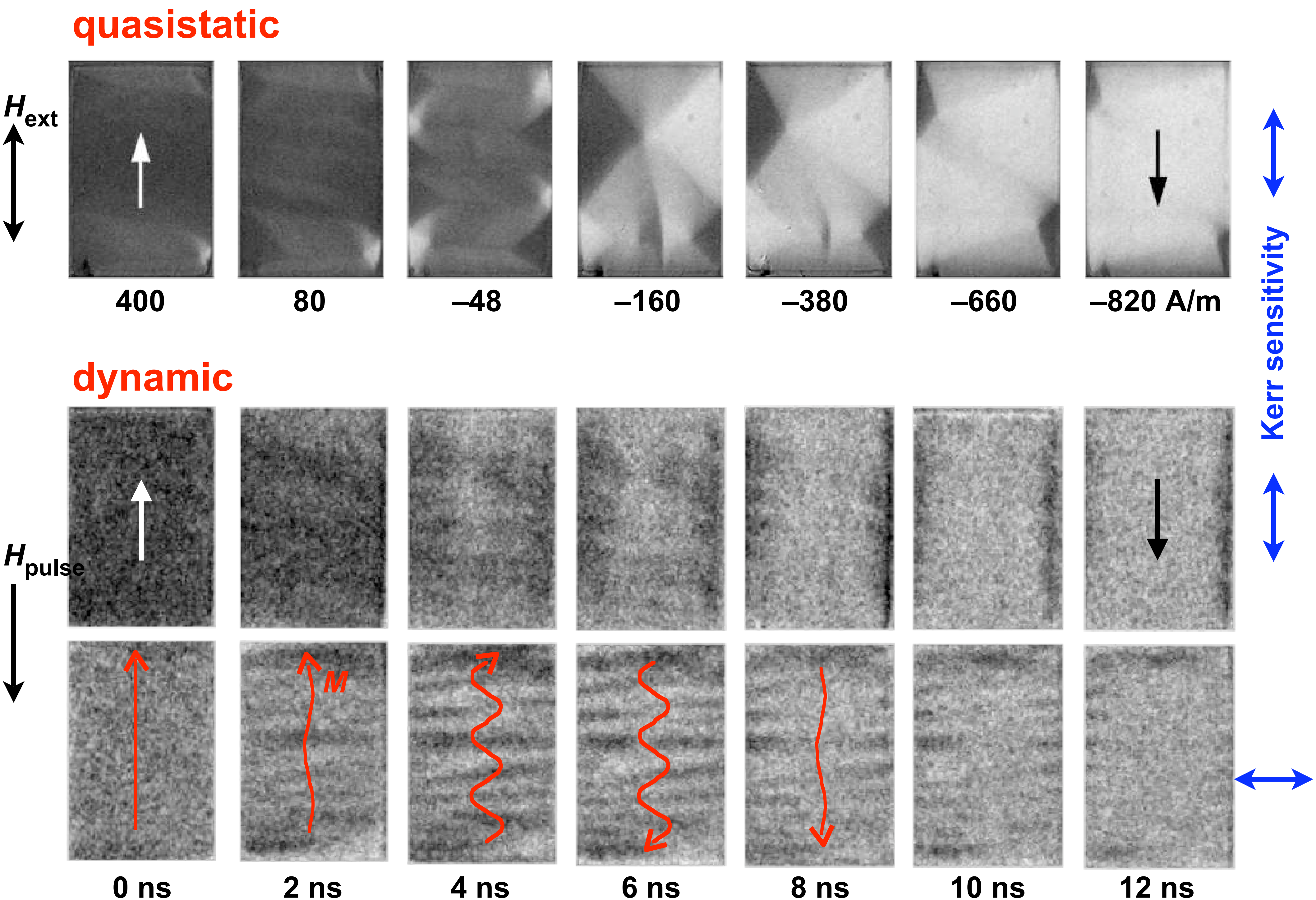

2. Kerr microscopy

Advantages

- sample manipulation easy: arbitrary sample shape and size, arbitrary magnetic fields, cooling, heating, fast
- simultaneous measurement of hysteresis curves
- direct imaging of magnetization vector
- quantitative method
- information depth 20 nm, depth-selective imaging possible in multilayers
- imaging of dynamic processes at high speed

Drawbacks

- optical resolution: 300 nm (domains larger than 150 nm are resolved)
- only surface domains can be seen

3. Non-linear magnetooptics: Second harmonic Kerr microscopy

3. Second harmonic microscopy

Kerr effect (linear effect): $\boldsymbol{D}_i(\omega) = \varepsilon_{ij} E_j(\omega)$

Second harmonic effect: $\boldsymbol{D}_i(2\omega) = \chi_{ijk} E_j(\omega) E_k(\omega)$

- Symmetry analysis
  $\Rightarrow$ effects from bulk of regular, high symmetry materials are forbidden

- However, symmetry is broken at surface (or interfaces in multilayers)
  $\Rightarrow$ SH-amplitudes originate mainly from first atomic layers
  $\Rightarrow$ True *surface* (interface) microscopy

- Experiment: short laser pulses generate second harmonic, excited non-linear light amplitude is separated from incident light by spectroscopic means

3. Second harmonic microscopy

Courtesy T. Rasing

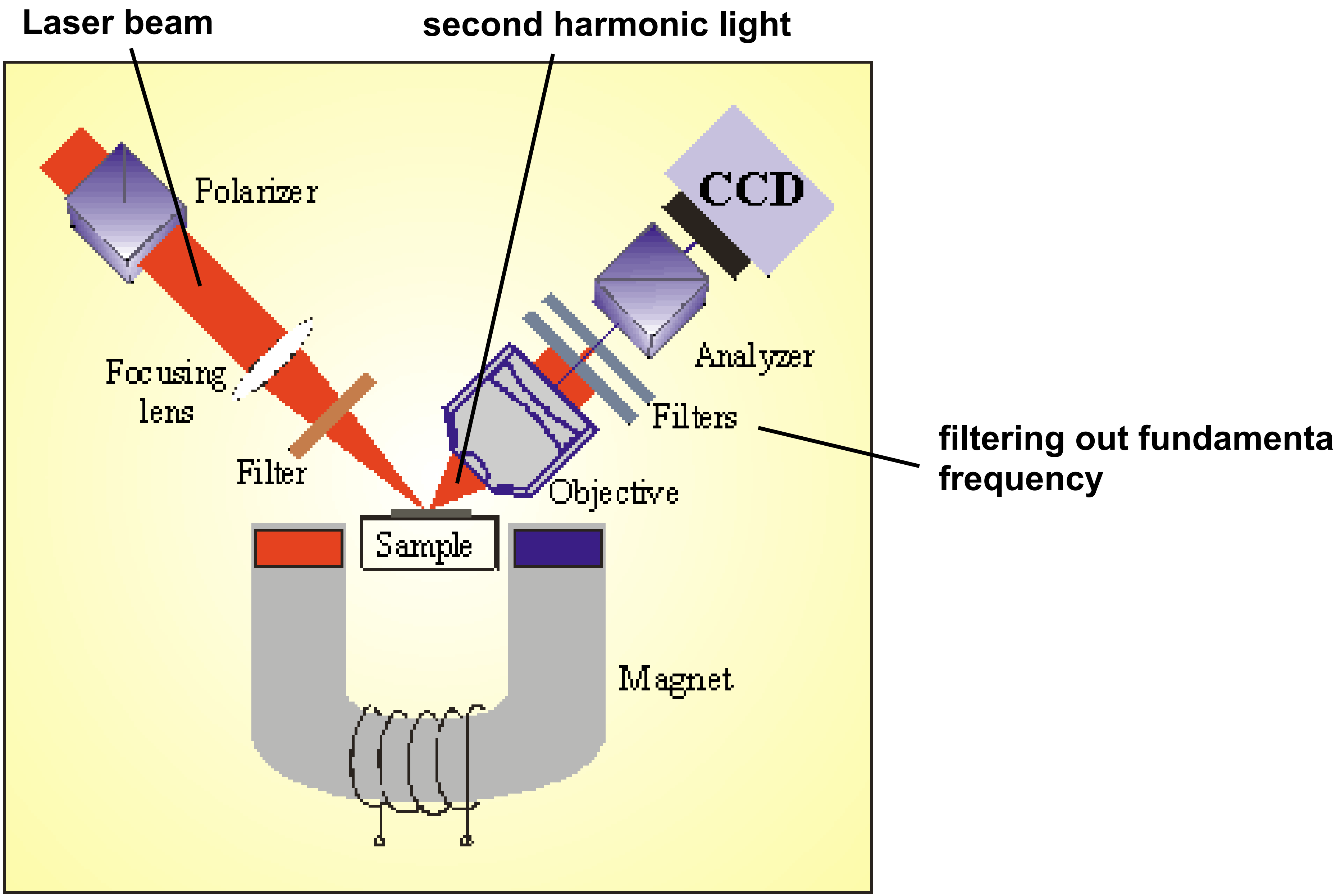

3. Second harmonic microscopy

Courtesy T. Rasing

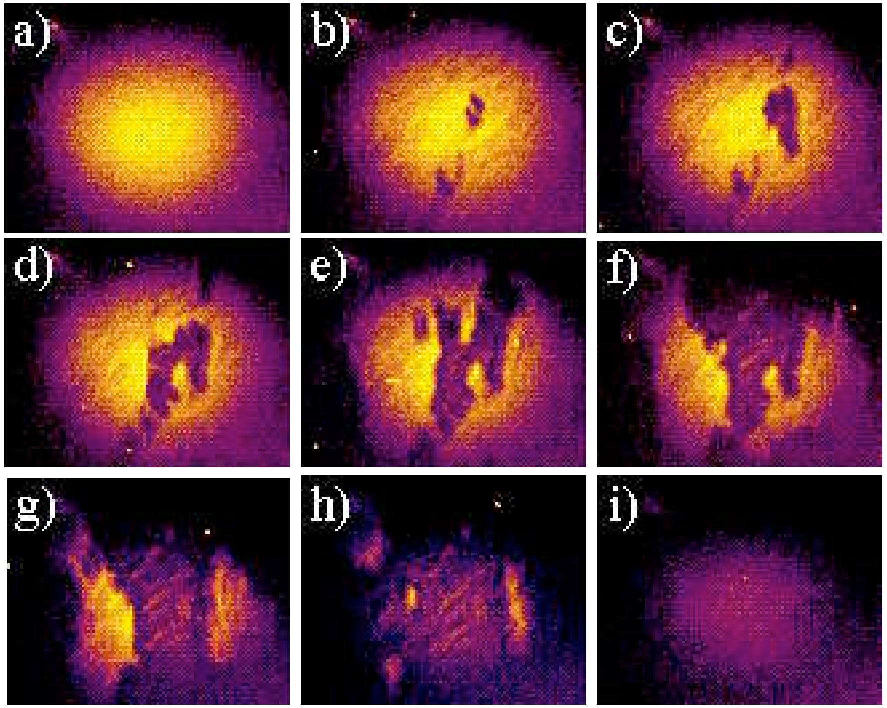

CoNi film (9 nm thick), sandwiched by Pt

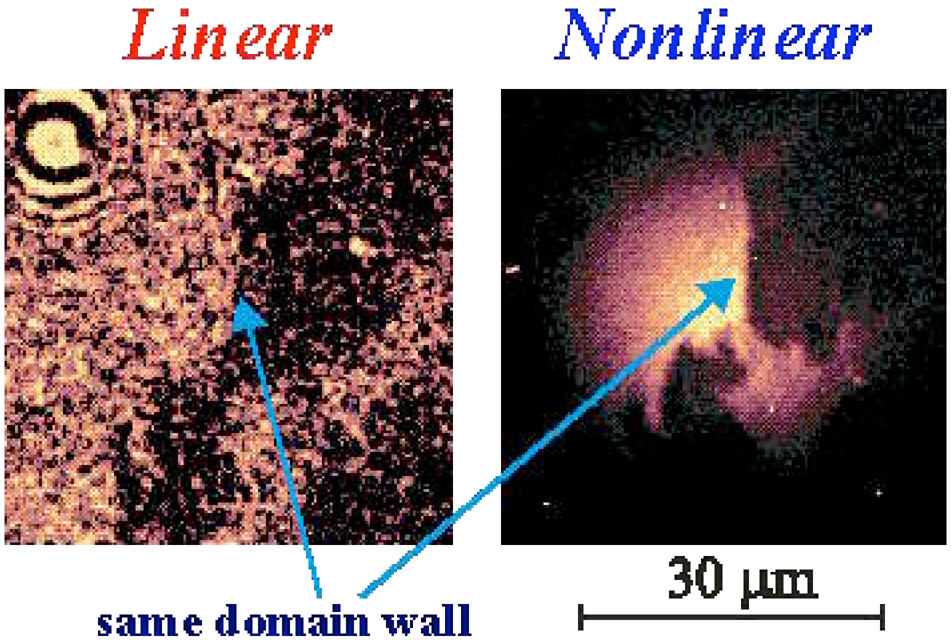

Comparison of linear and SH contrast
- Linear image: use of analyser, contrast due to whole layer
- Second harmonic: no polarization analysis required, because SH-intensity is changed by magnetization reversal, contrast from interface

4. X-ray Spectroscopy

X-ray Spectroscopy

- Based on X-ray circular dichroism
  (magnetization-dependent absorption of circularly polarized light)
- Interaction with core electrons
  - Radiation-induced transition into unoccupied or free states
  - Element specifity

Iron whisker
(courtesy C.M. Schneider)

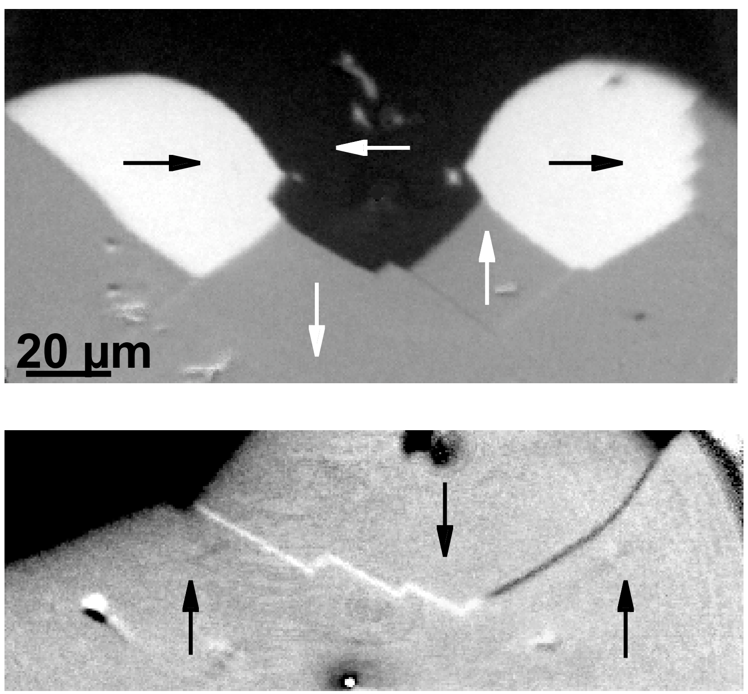

Imaging of excited photoelectrons in Photo Emission Electron Microscope
PEEM method

Amorphous FeGd film
(courtesy P. Fischer and G. Schütz)

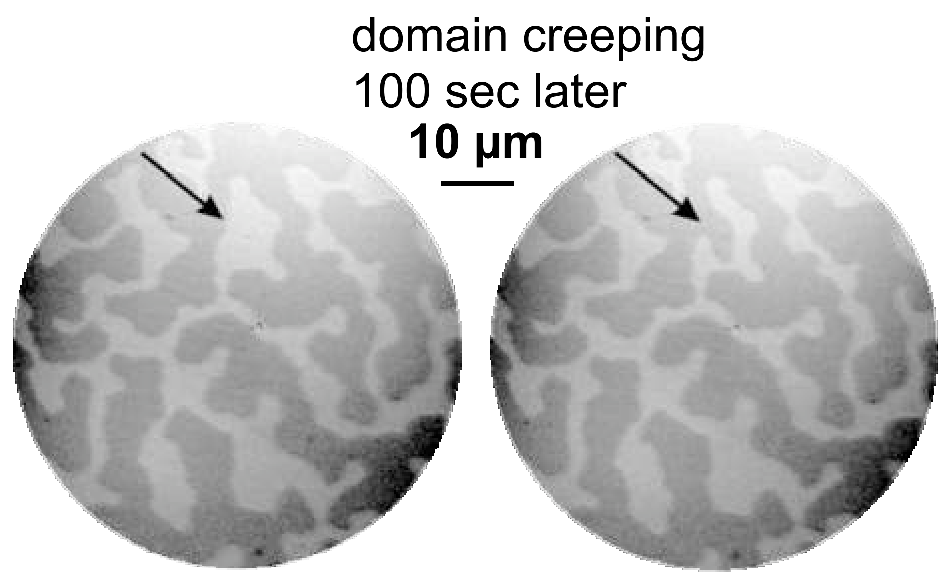

resolution: some 10 nm

Imaging of X-ray absorption in X-ray microscope
X-ray microscopy

Element-specific PEEM imaging on Fe-Cr-Co layer system

(courtesy C.M. Schneider)

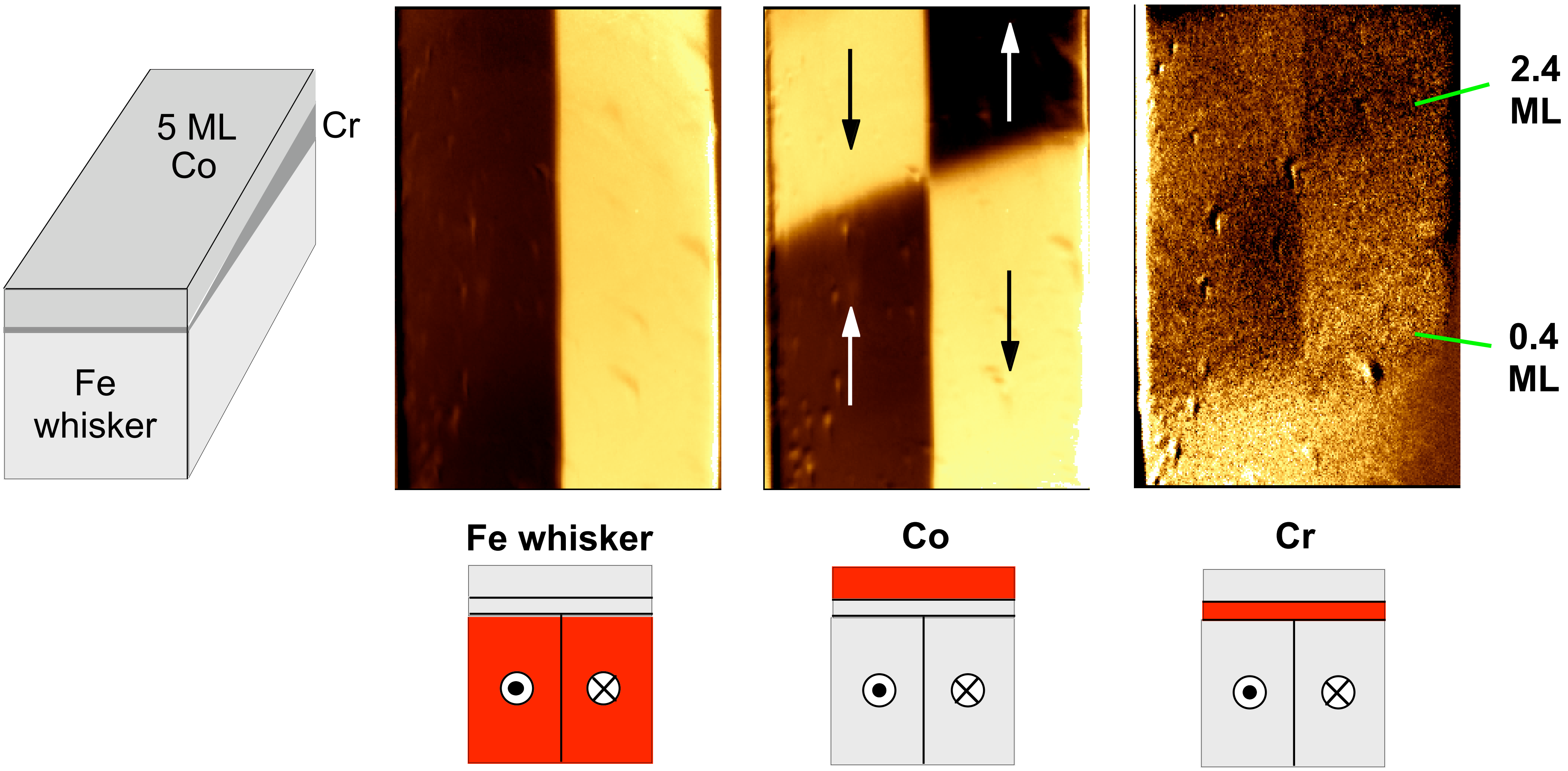

X-ray Spectroscopy

X-MCD: absorption of circularly polarized x-rays depends on projection of *M* on helicity of photons, change of sign by reversing *M*

Physical origin:

if energy of absorbed photon exceeds binding energy of an inner core level (e.g. spin-orbit split $p_{1/2}$ and $p_{2/3}$ states)
⟶ transition into unoccupied spin-split states above Fermi level (e.g. into 3d band)

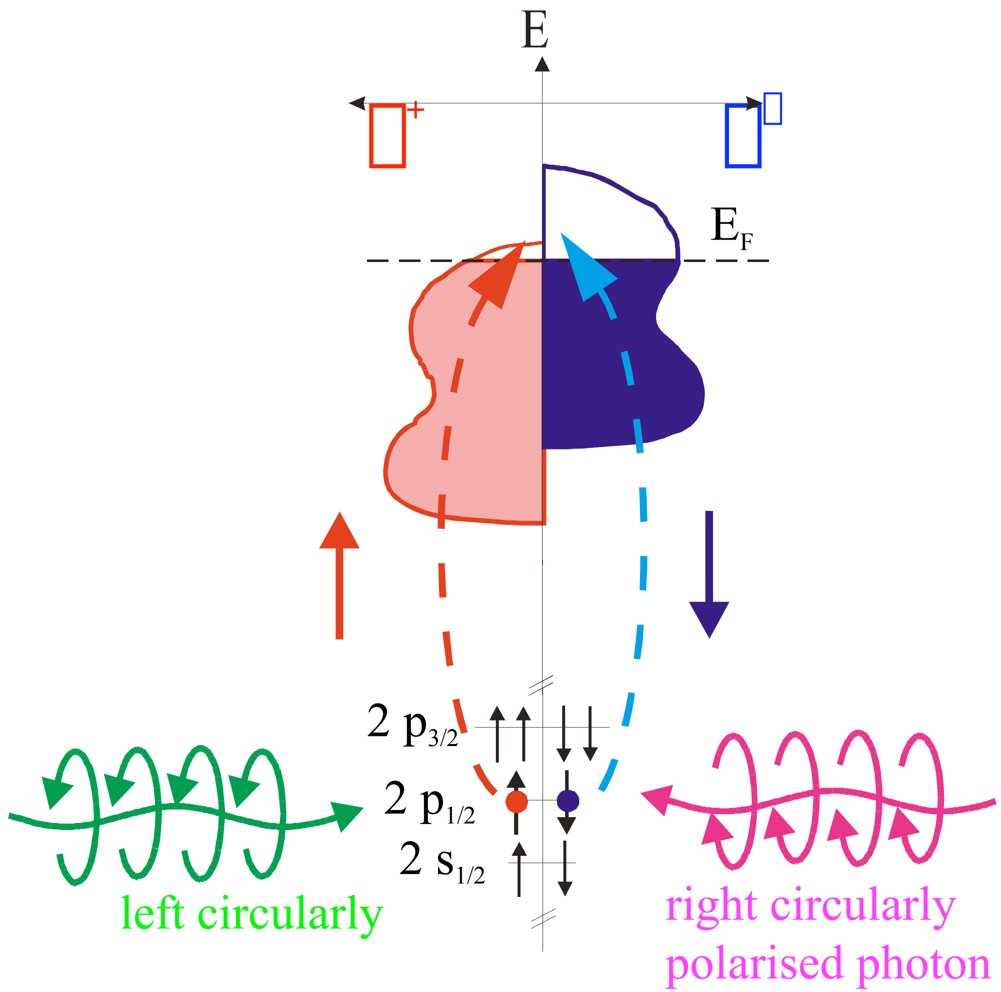

Initial states are well defined inner-core levels
⟶ X-MCD is element selective

Fermi's golden rule: transition probability of absorption process is related to density of unoccupied states, which are different for minority and majority bands due to exchange interaction
⟶ X-MCD signal is proportional to magnetic moment of absorbing atom
⟶ sensing of magnetization of sample

Spin and orbital contributions of magnetic moments can be extracted (by relating data from corresponding spin-orbit split states (e.g. L_2 and L_2 edges) and applying sum rules

X-ray Spectroscopy

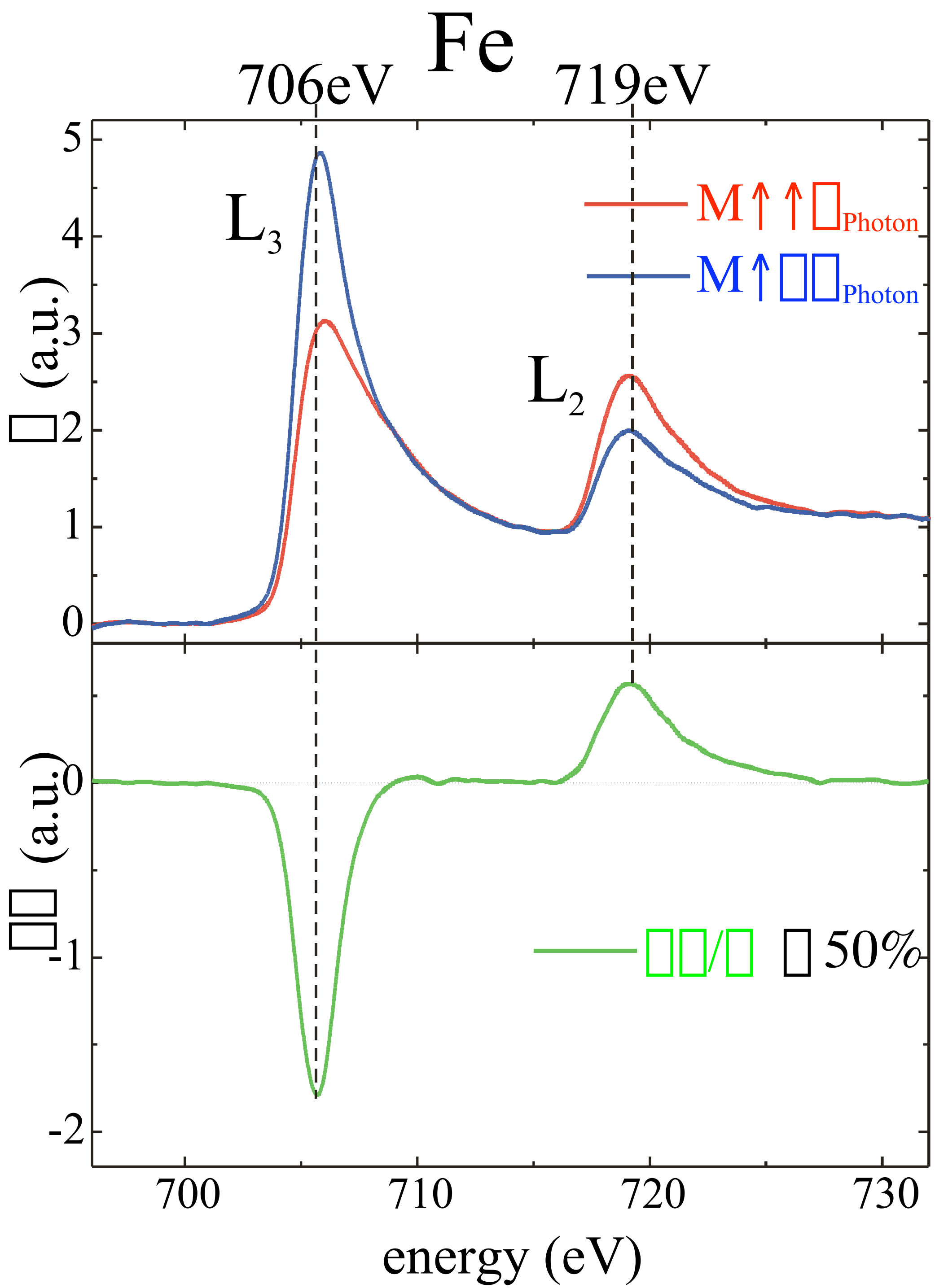

Large dichroic effects occur at L_3 and L_2 edges (2p ⟶ 3d)

X-ray Microscopy

X-ray Microscopy

Courtesy P. Fischer, Th. Eimüller

Magnetic contrast in MTXM

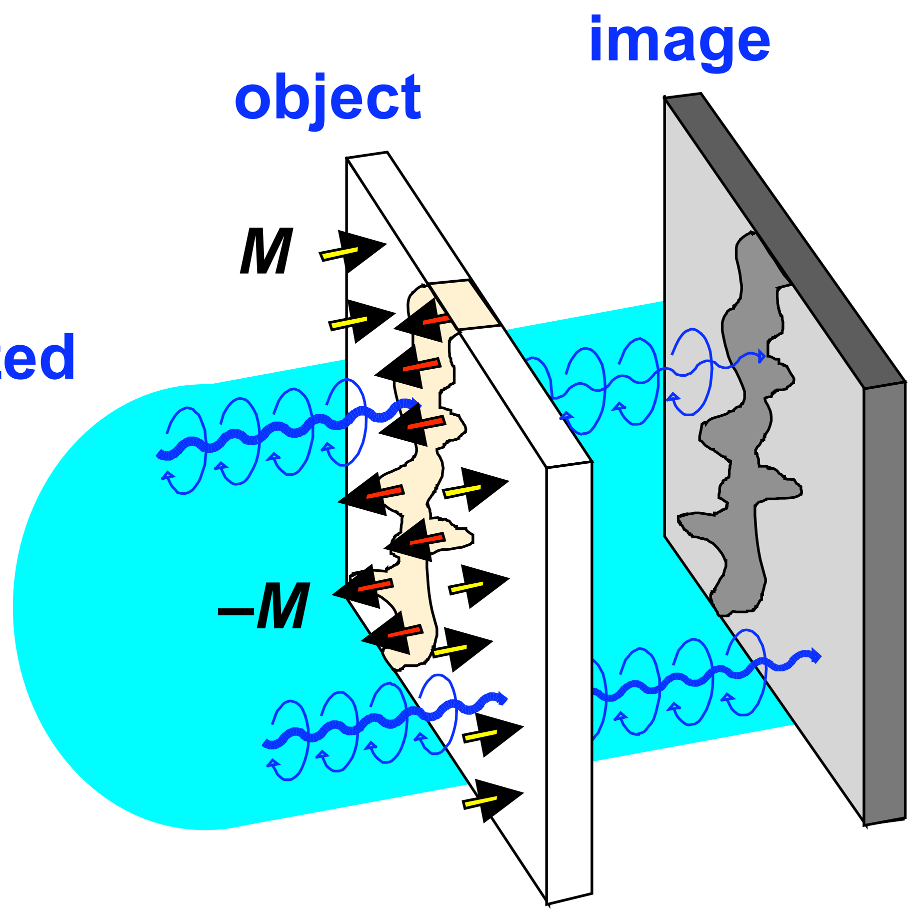

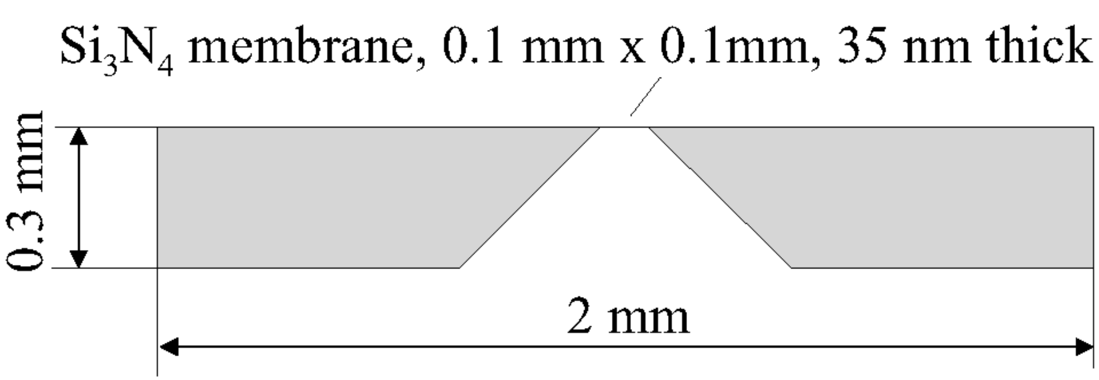

large absorption of soft X-rays (energy < 1 keV)

- **film thickness < 100 nm**
- **thin substrates (Si_3N_4)**

X-ray Microscopy

Courtesy P. Fischer, Th. Eimüller

High lateral resolution

- determined by the micro zone plate
- currently: 25 nm

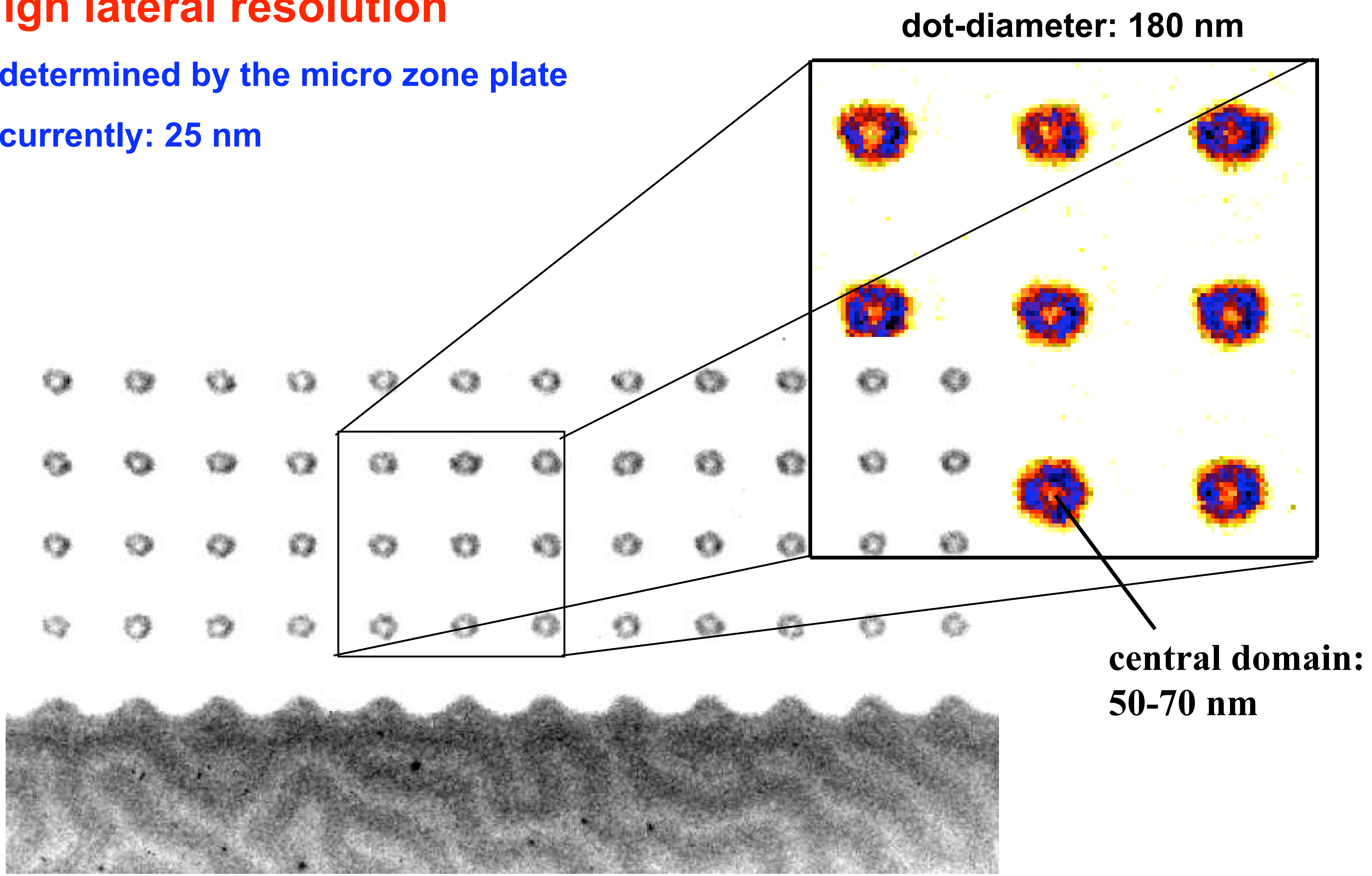

Fe/Gd multilayer, structured with electron beam lithography

X-ray Microscopy

Courtesy P. Fischer, Th. Eimüller

M-TXM images in varying applied external fields

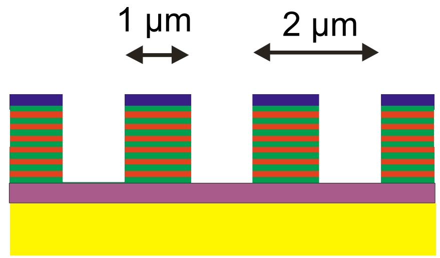

Switching of Fe/Gd multilayered dots

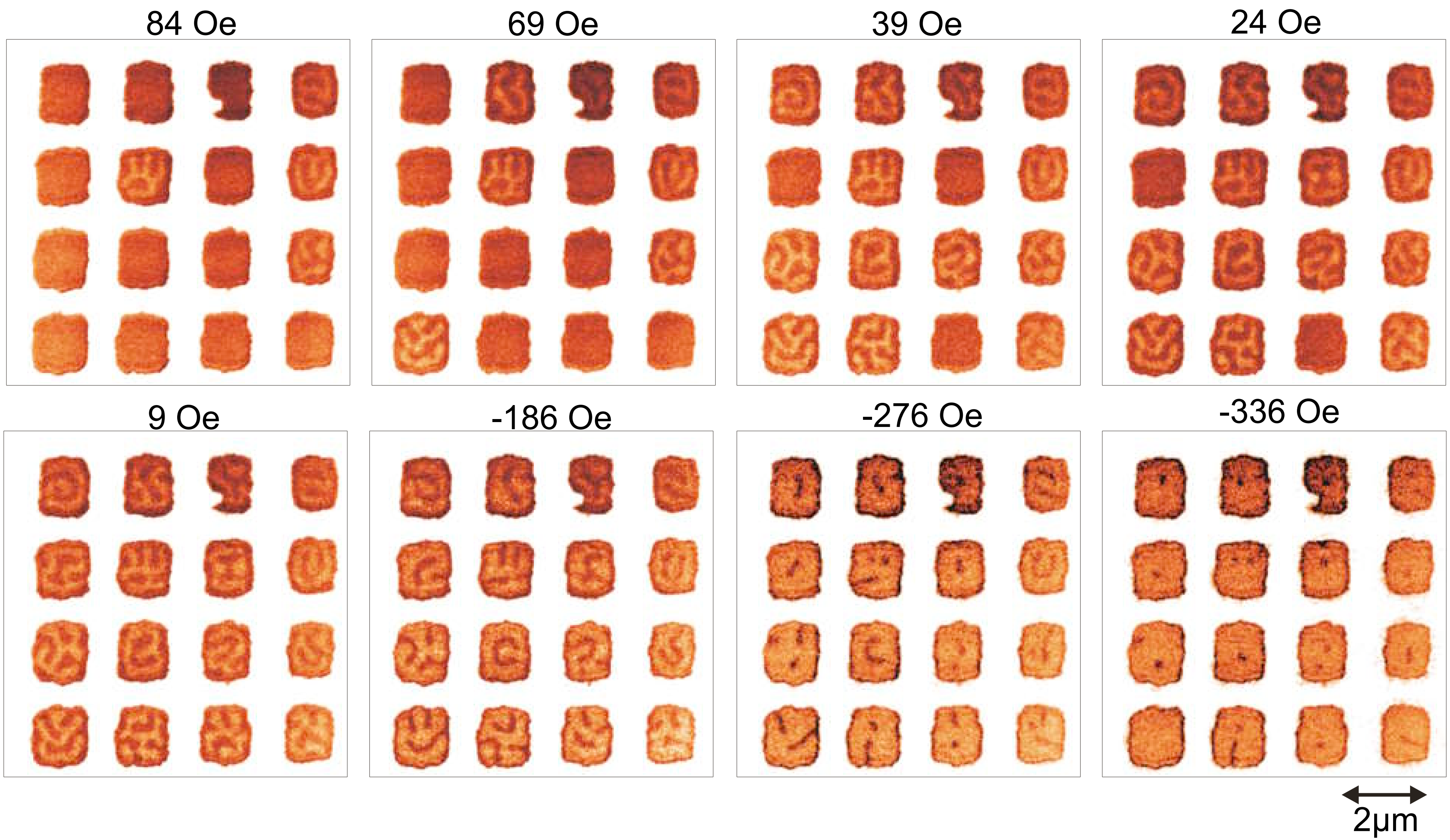

X-ray Microscopy

Courtesy P. Fischer, Th. Eimüller

In-plane imaging

Dichroic contrast: given by projection of M on photon propagation direction. In-plane imaging by tilting the sample (30°):

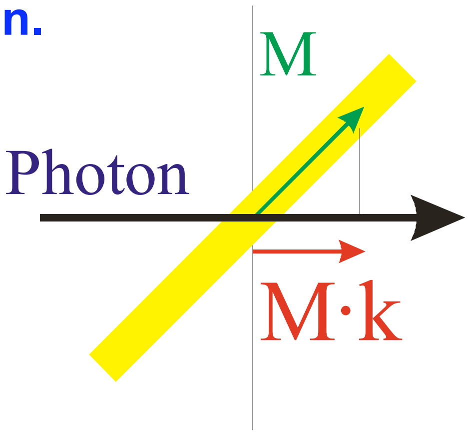

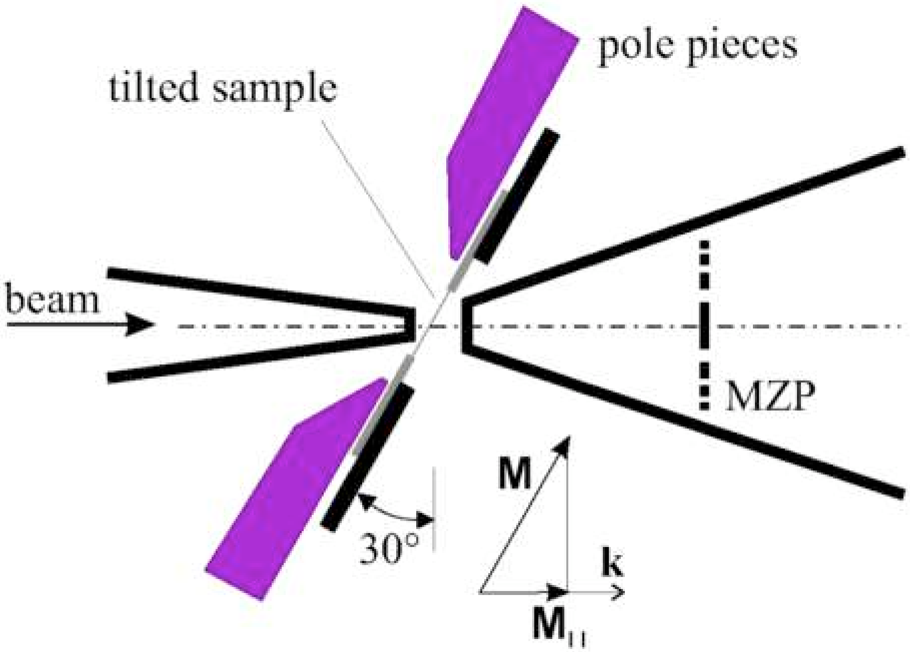

Co elements (35 nm thick)

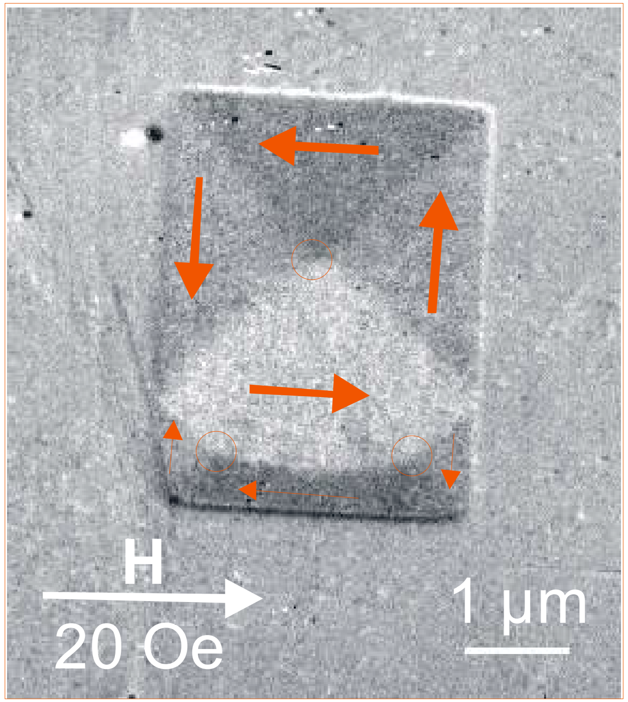

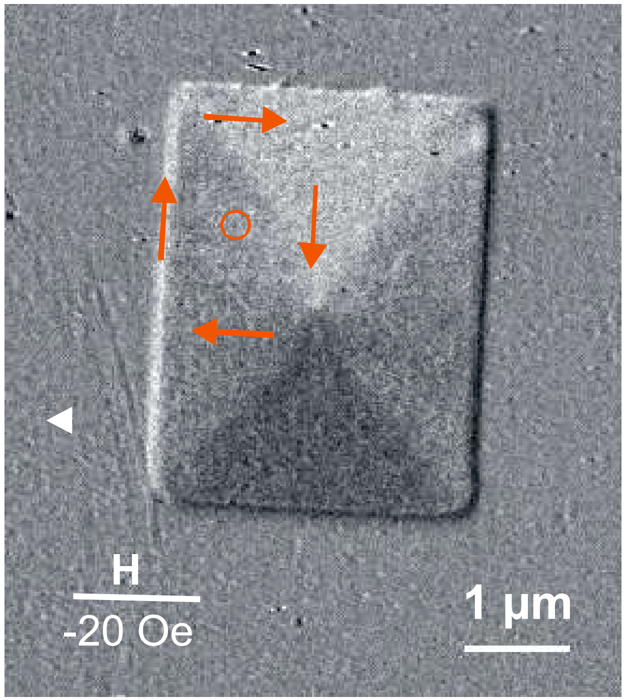

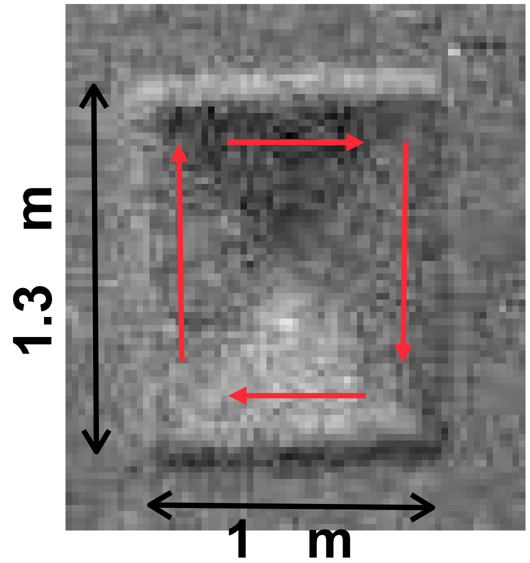

$Ni_{80}Fe_{20}$ (50 nm) @ Ni L_3 edge

X-ray Microscopy

Stroboscopic pump- and probe imaging

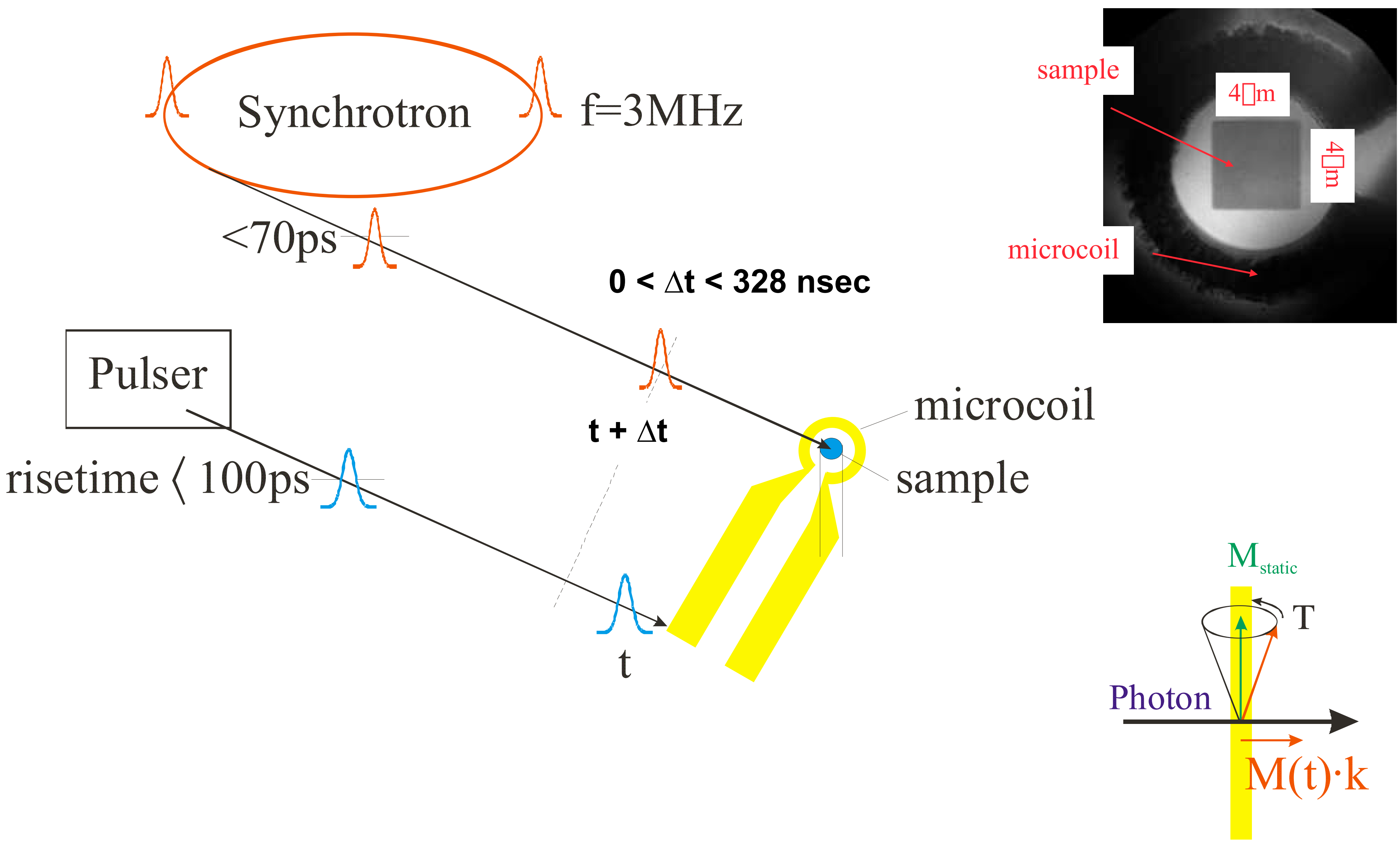

X-ray Microscopy

Courtesy P. Fischer

Stroboscopic pump- and probe imaging

Δt= −400ps

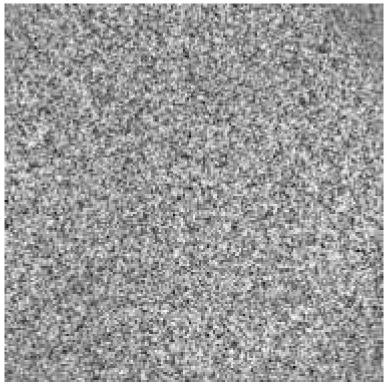

Δt=+200ps

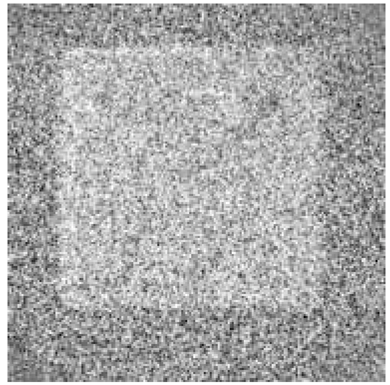

Δt=+400ps

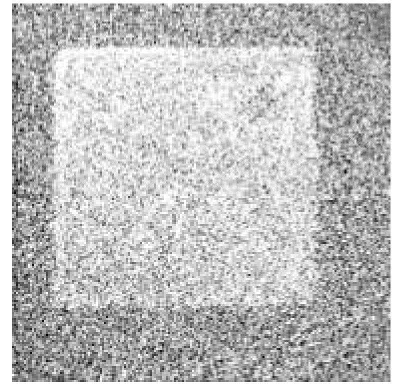

Δt=500ps

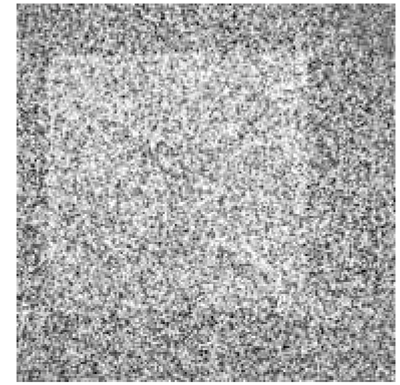

Δt=+600ps

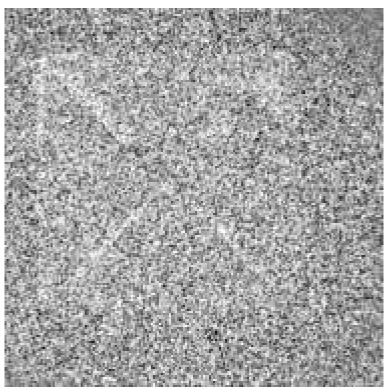

Δt=900ps

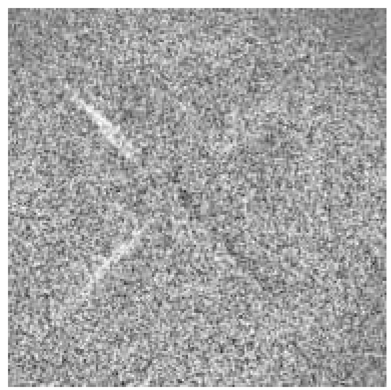

Δt=+1000ps

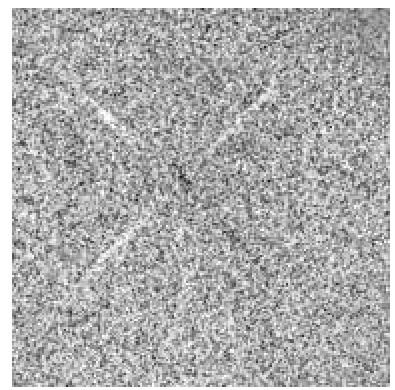

Δt=+1200ps

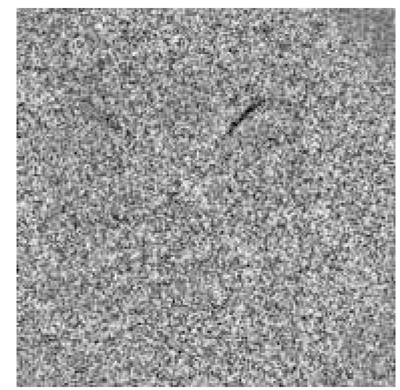

Δt=+1600ps

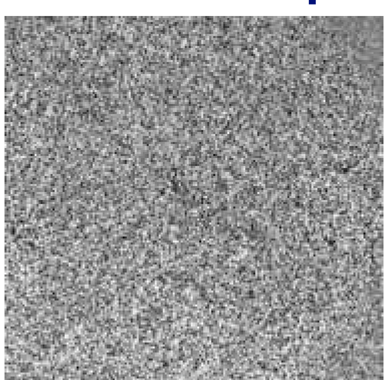

Δt=2400ps

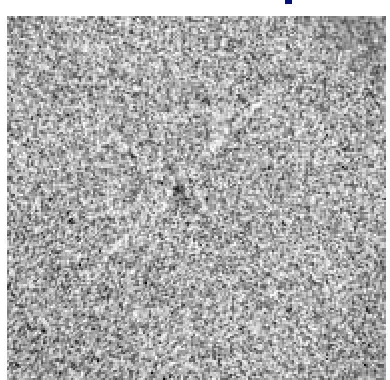

Δt=3200ps

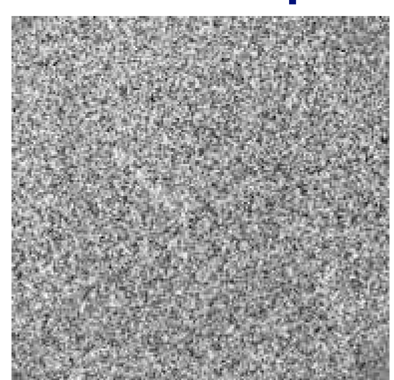

(4 x 4) m^2
3nm Al/
50nm PY/
2nm Cu/
50nm Co/
substrate

 Courtesy P. Fischer, Th. Eimüller

Summary

Advantages

- lateral resolution at (currently) 25 nm
- imaging in applied magnetic fields (currently some kOe)
- quantitative (contrast proportional to *M*)
- probing of in- and out-of-plane magnetization
- time resolution in the sub-ns regime
- element specific imaging
- high sensitivity to few nm layers (for Fe: < 2 nm)

Disadvantages

- sample must be transparent (*d* < 100 nm)
- thin substrates
- synchrotron radiation necessary

PEEM

Courtesy H.Ohldag

X-Ray Absorption Spectroscopy and Total Electron Yield

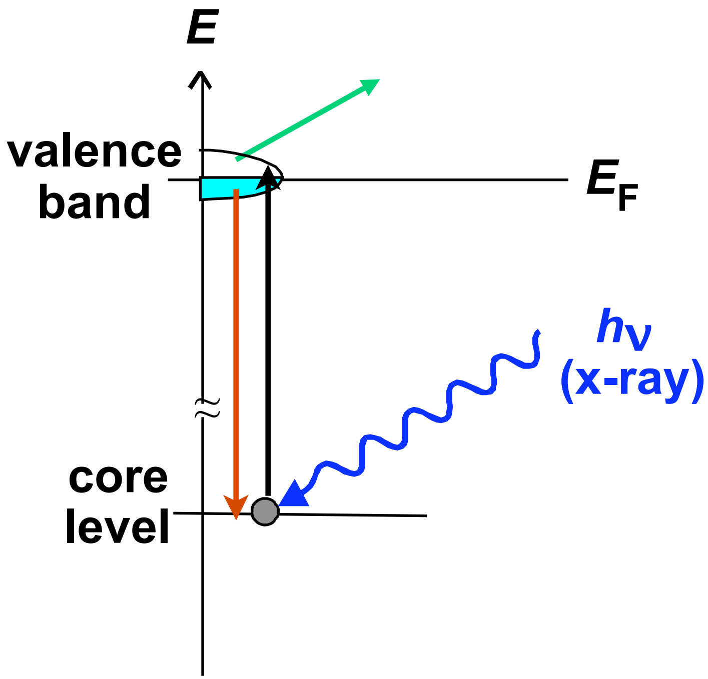

Excitation of a core electron into an empty valence state by the incoming x-ray

Recombination for example via an Auger decay

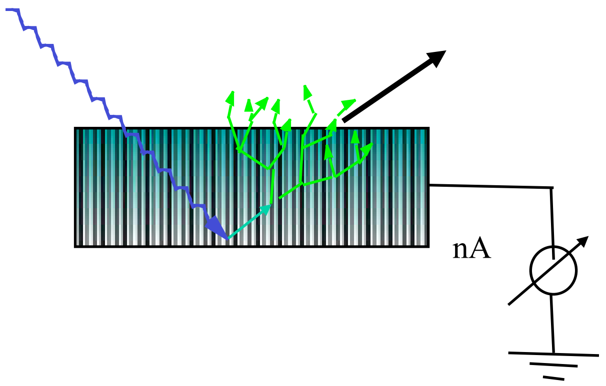

Inelastic scattering of the original photoelectron and auger electron leads to emission of secondary electrons

Electron yield ~ x-ray absorption coefficient

Probing depth ~ electron escape length exp(-λt) (λ~2nm)

PEEM technique

Full field microscope with ~50nm spatial resolution

Electrostatic lenses magnify spatial variation of TEY onto a screen

Probing depth: 2 nm

1.) Accelerating field → Topography
2.) X-ray energy → Chemistry
3.) X-ray polarization → Magnetism

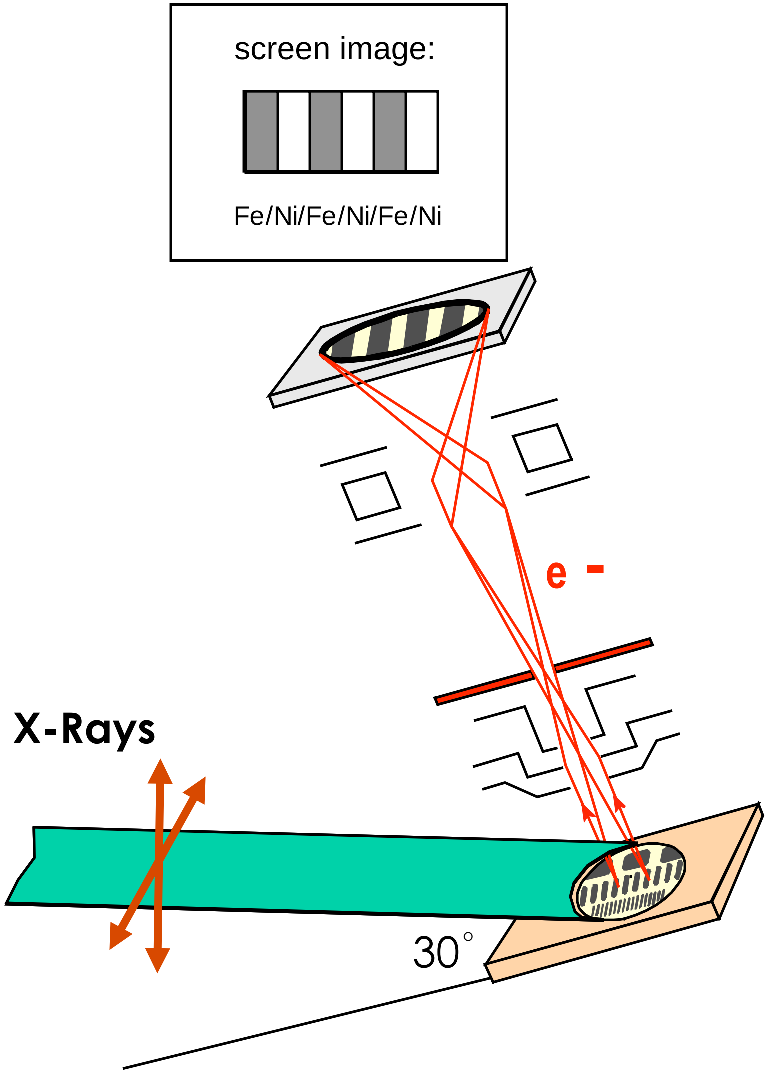

PEEM

Courtesy H.Ohldag

Polarization Dependence of XAS - Circular Dichroism

Circular polarized x rays

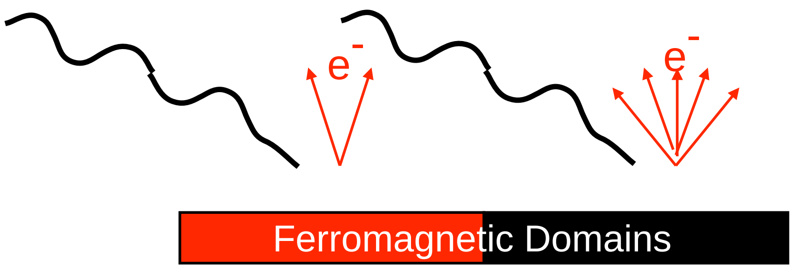

Circular polarization

TEY sensitive to direction of magnetic moment

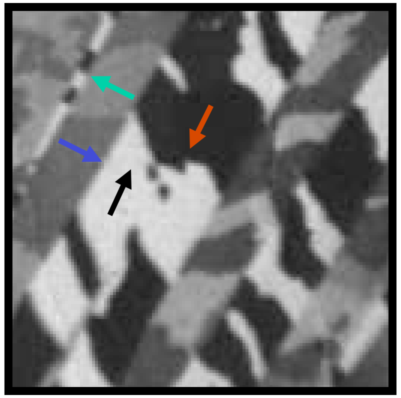

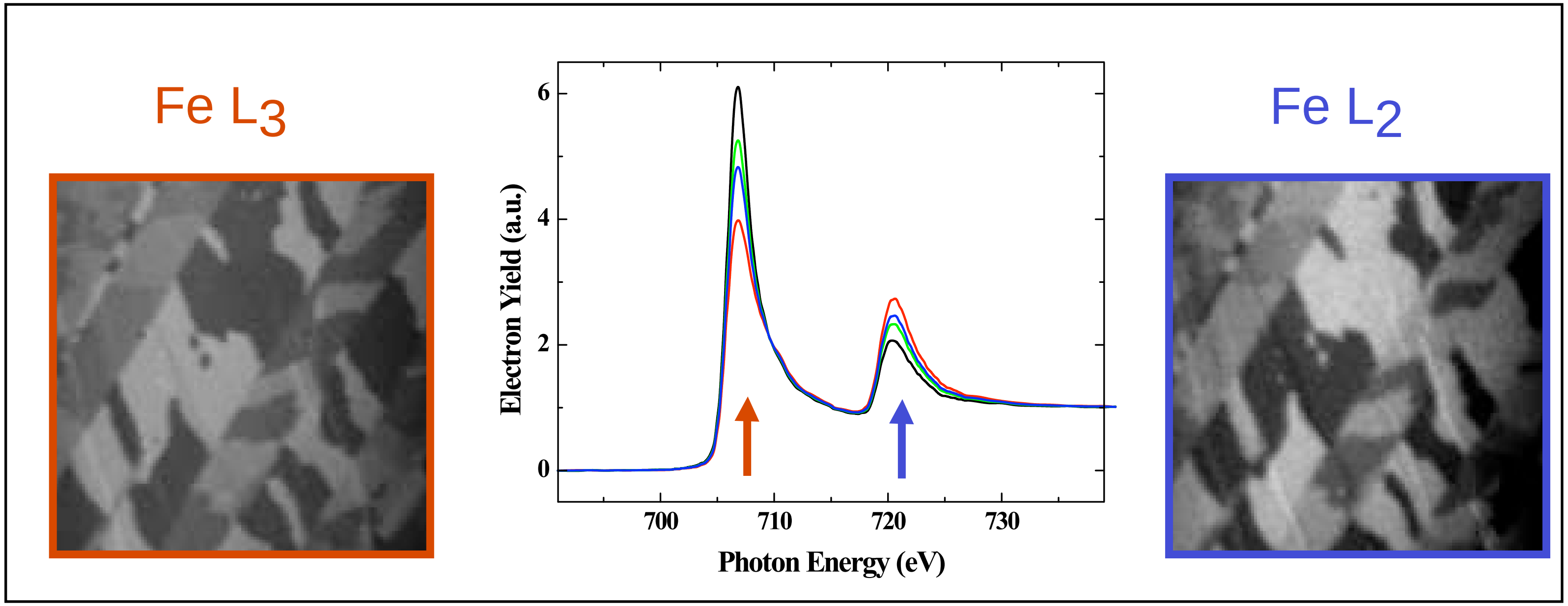

Courtesy H.Ohldag

Polarization Dependence of XAS - Linear Dichroism

Linear polarized x rays

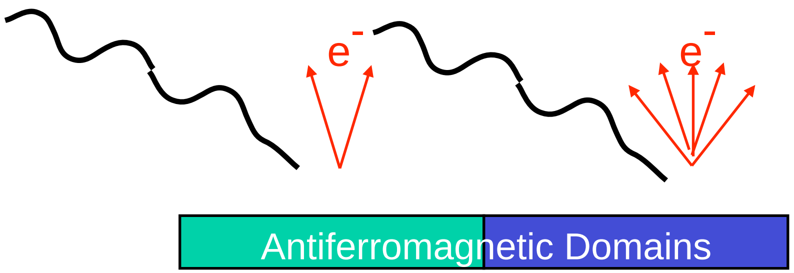

Linear polarization → Sensitive to axis of magnetic moments

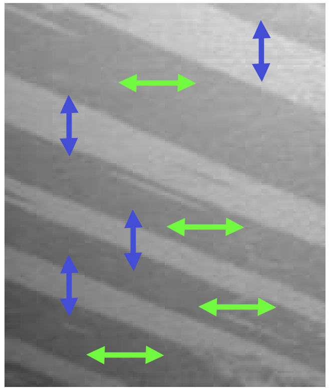

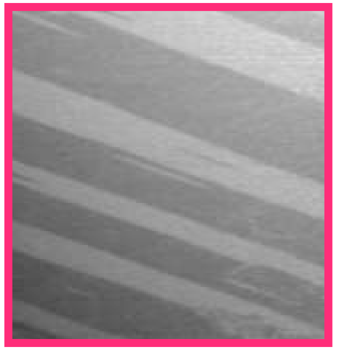

NiO L_{2A}

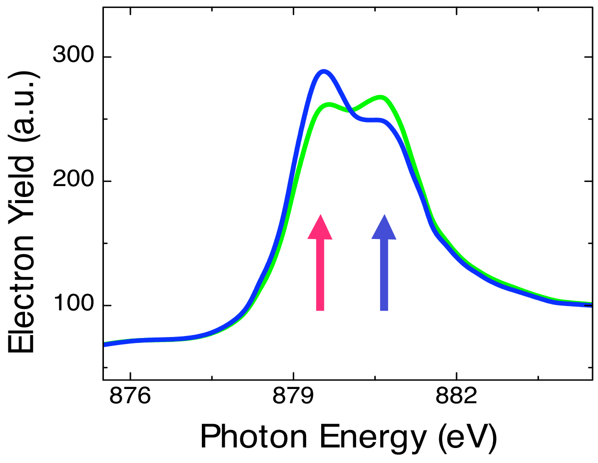

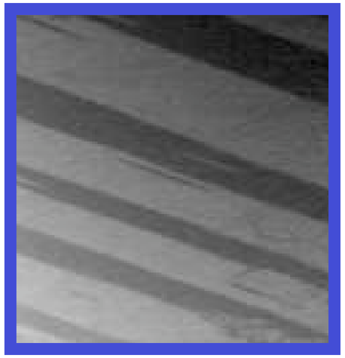

NiO L_{2B}

Courtesy H.Ohldag

Element Specific Magnetic Imaging of Thin Films

The sample is an exchange coupled cobalt layer (2nm) on a NiO(001) single crystal surface.

PEEM can image:

- Ferromagnetic Domains of top cobalt layer
- Antiferromagnetic Domains of bottom NiO crystal
- Ferromagnetic polarization of NiO at the buried interface to the cobalt layer.

Comparison of X-ray microscopy with PEEM imaging

equal	• XMCD as contrast • element-specific • quantitative • in- and out-of-plane
advantages of PEEM	• no sample thinning • higher sensitivity • higher spectral resolution
disadvantages of PEEM	• imaging in fields difficult • time consuming adjustment • lower standard resolution • UHV conditions

5. Transmission Electron Microscopy

5. Transmission Electron Microscopy

Principle

- **Electrons are deflected by Lorentz force**

$$\boldsymbol{F}_L = q_e (v_e \times \boldsymbol{B})$$

q_e: electron charge
v_e: electron velocity
$\boldsymbol{B}$: magnetic flux density

- **Stray fields outside the sample contribute to contrast**

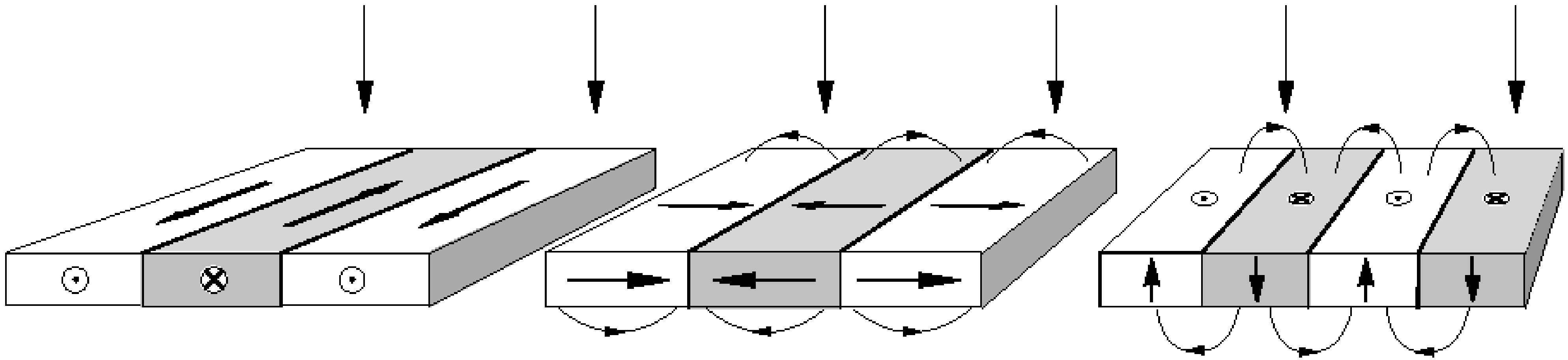

net deflection of electrons

deflection by magnetization is cancelled by deflections due to stray field

no deflection by magnetization, stray field deflection cancells

- **Tilting of sample may be required**
- **maximum sample thickness: some 100 nm**

5. Transmission Electron Microscopy

5.1 Fresnel technique (defocused mode imaging)

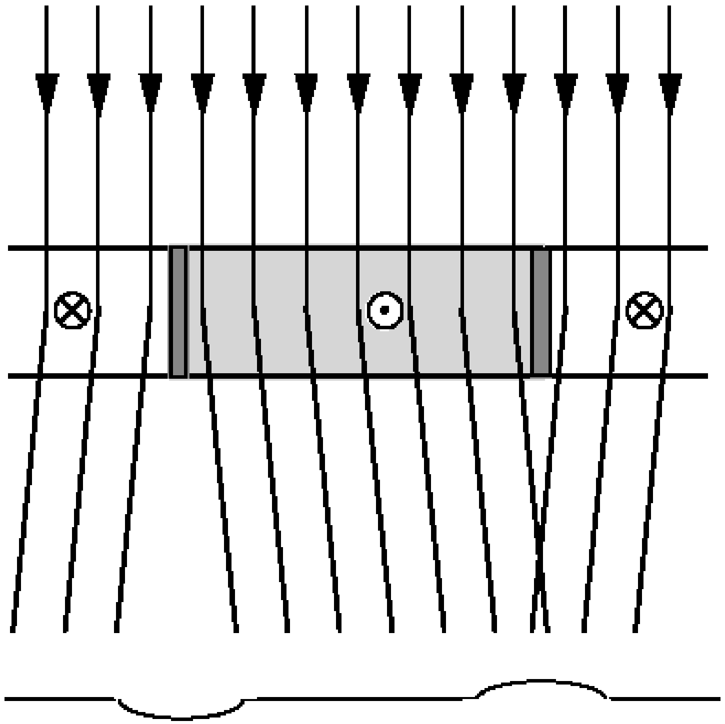

Metallic glass, partially crystallized
(courtesy J. Chapman)

- Out-of-focus: shadow effects delineate domain boundaries
- Magnetization direction can be derived from ripple (if present)

5.1 Fresnel technique

Fresnel imaging of differently sized magnetic particles

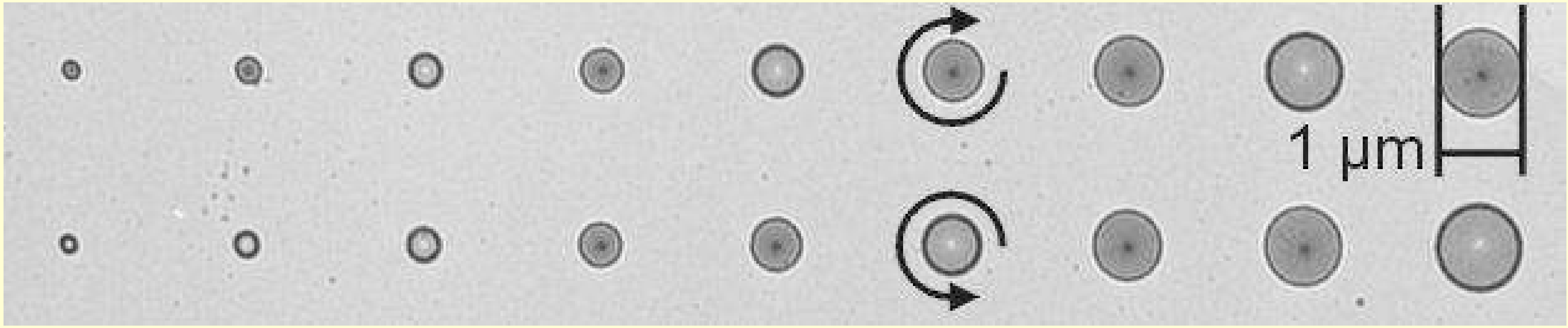

5. Transmission Electron Microscopy

courtesy J. Zweck

5.1 Fresnel technique

Fresnel imaging of differently sized magnetic particles

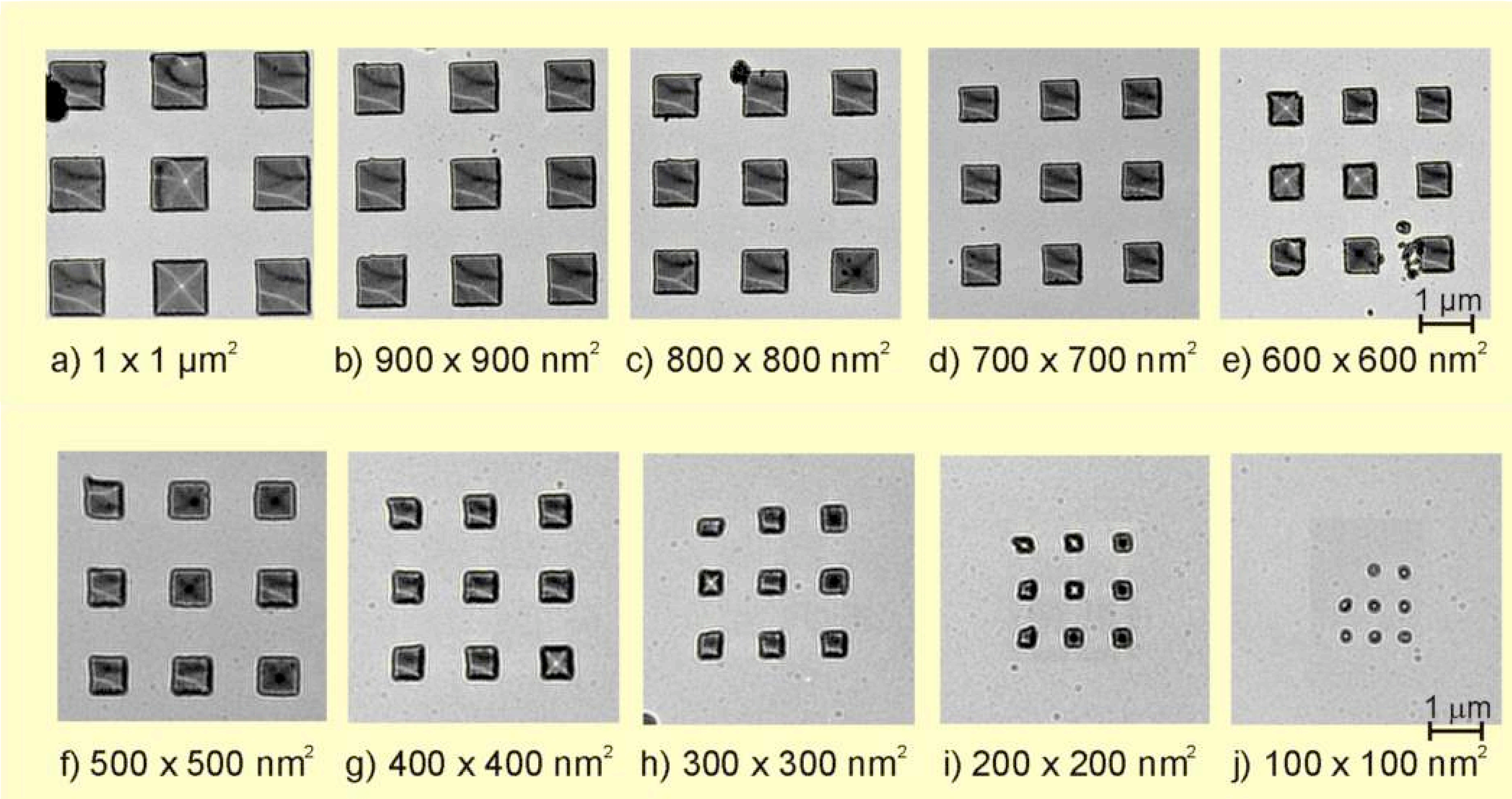

5. Transmission Electron Microscopy

5.2 Foucault technique (in-focus)

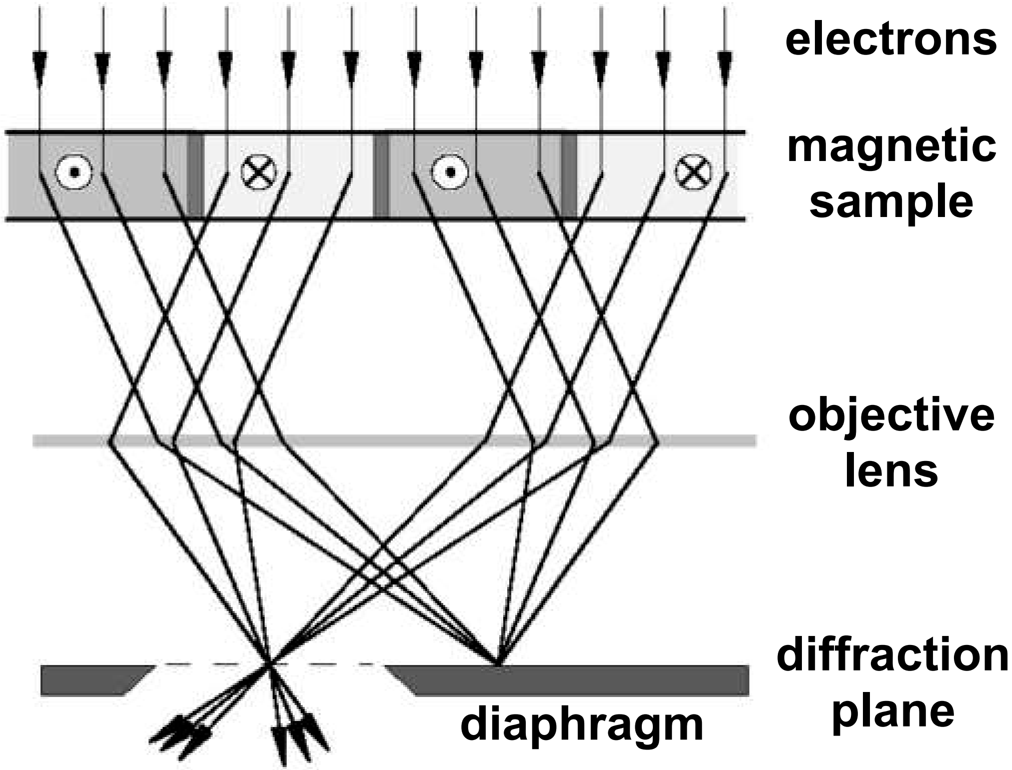

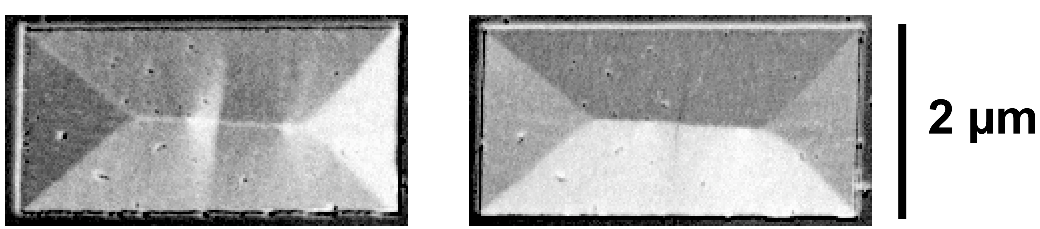

Permalloy, 24 nm thick
(courtesy J. Chapman)

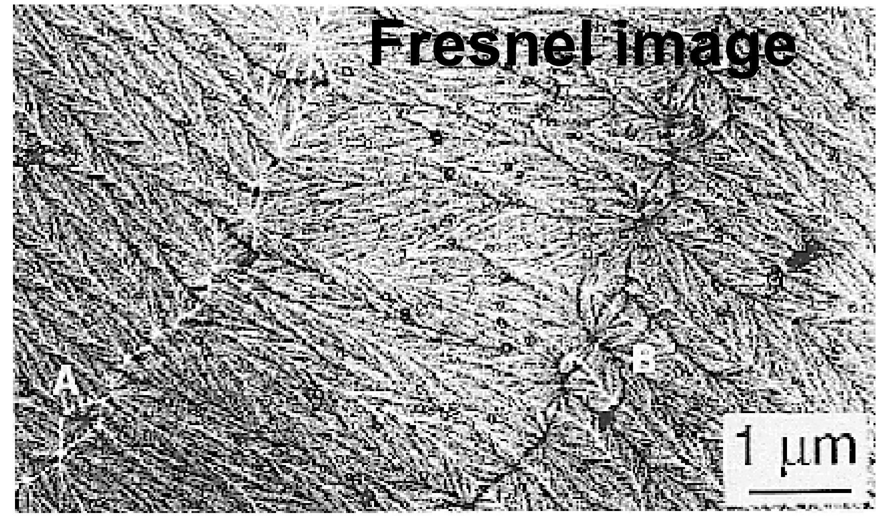

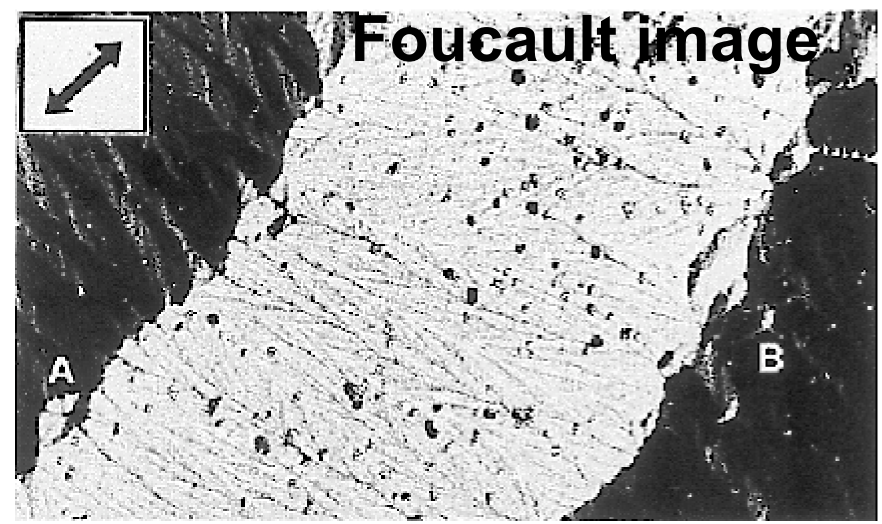

Metallic glass, partially crystallized
(courtesy J. Chapman)

5. Transmission Electron Microscopy

courtesy J. Zweck

5.2 Foucault technique (in-focus)

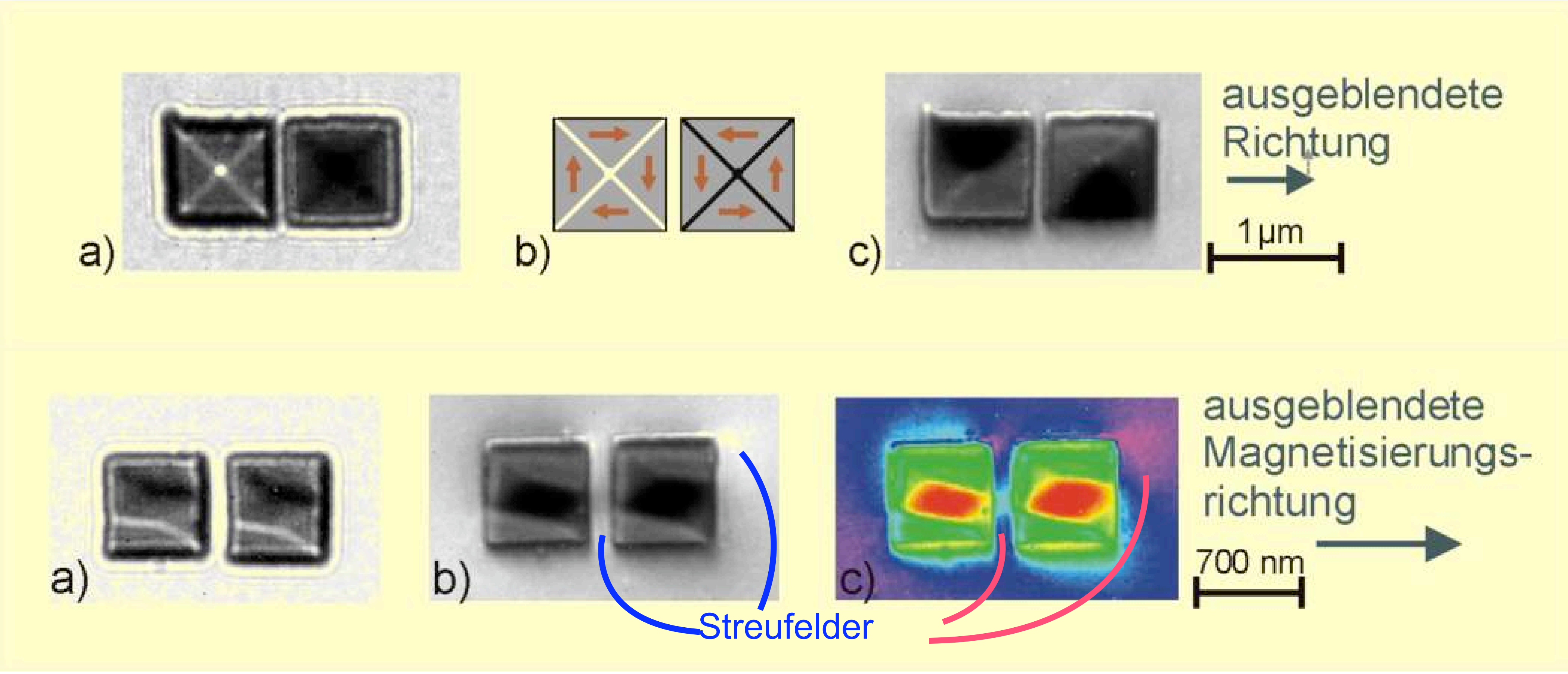

courtesy J. Zweck

5.2 Foucault technique (in-focus)

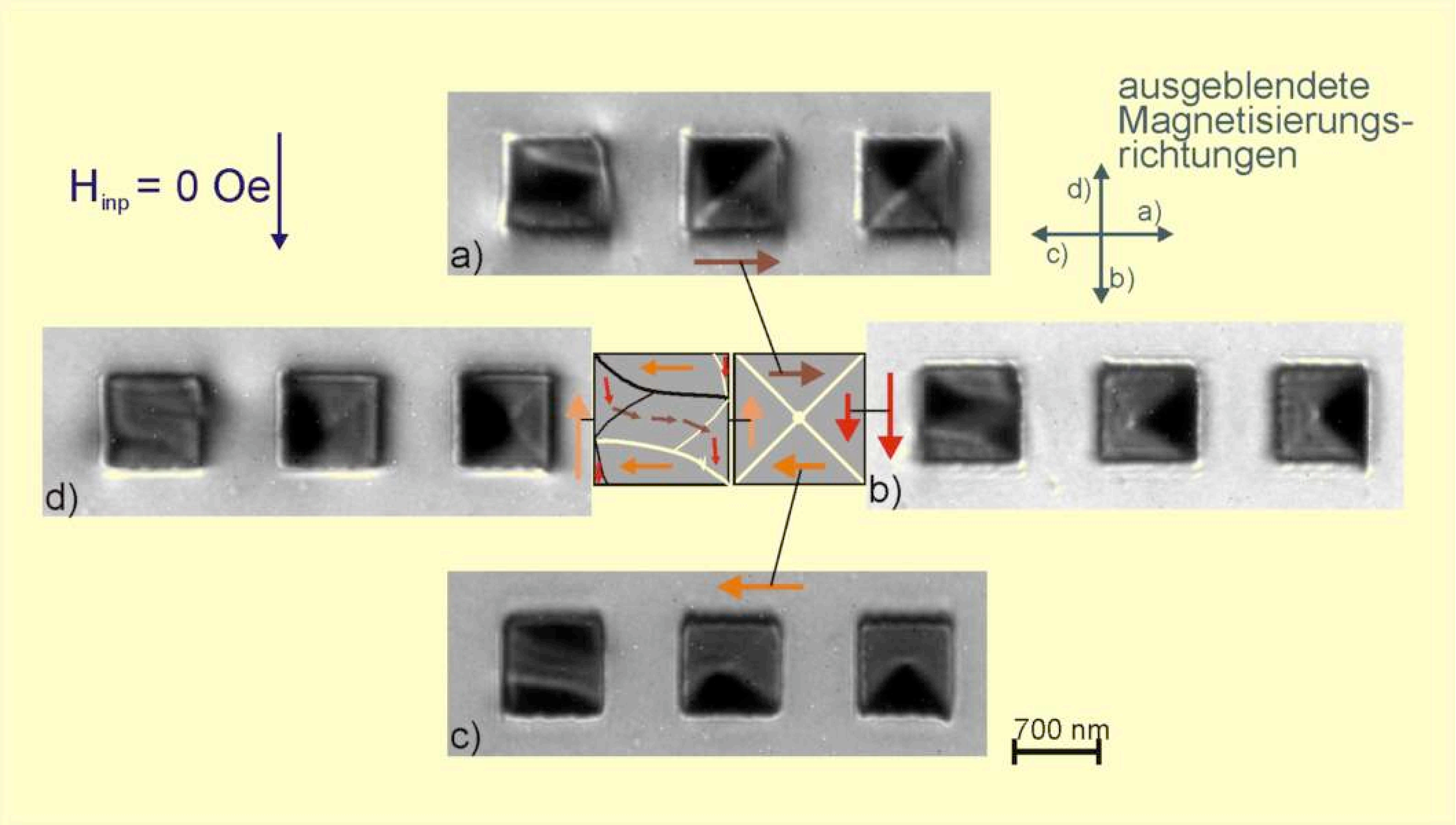

5. Transmission Electron Microscopy

5.3 Differential Phase Contrast (DPC) Microscopy

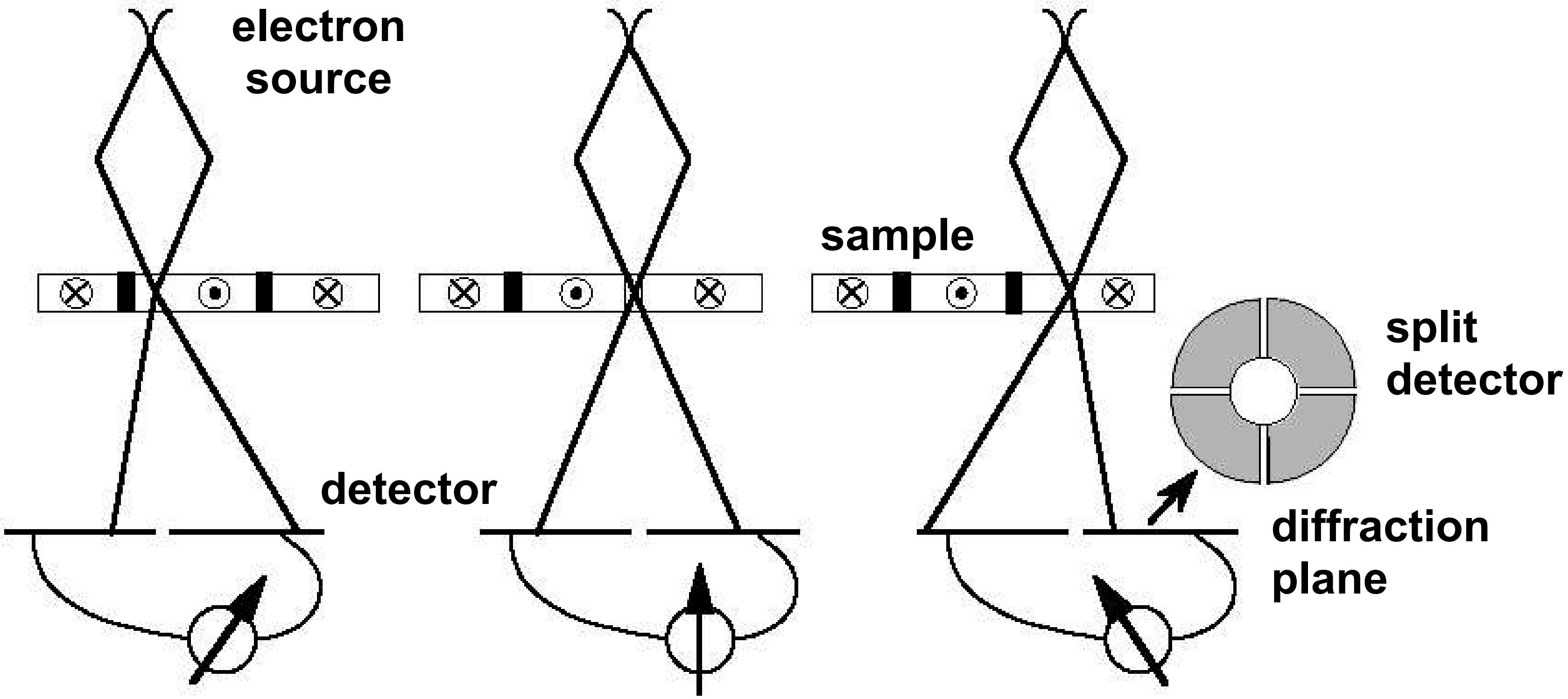

- Domain contrast like in Kerr microscopy
- Resolution better than 10 nm
- Quantitative determination of magnetization direction (by combining signals of a quadrant detector)

5. Transmission Electron Microscopy

5.3 Differential Phase Contrast (DPC) Microscopy

In a scanning TEM

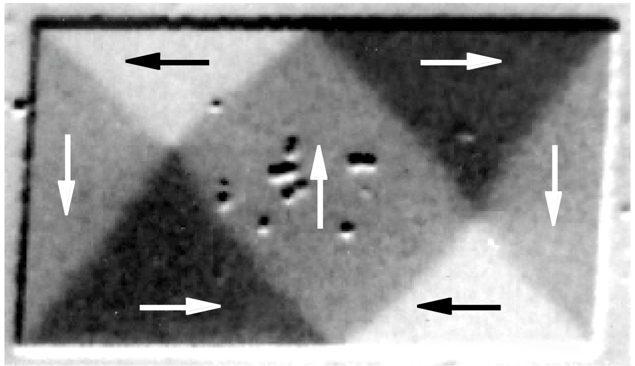

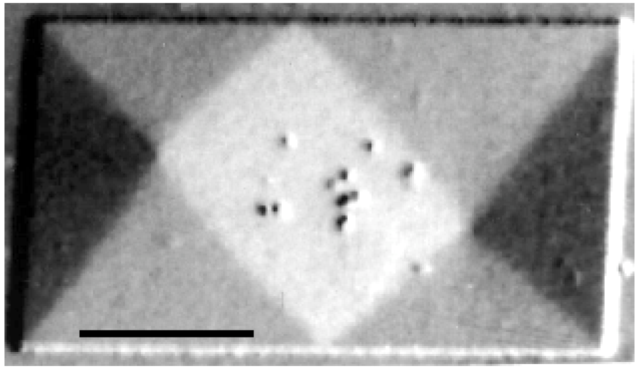

Permalloy, 60 nm thick
(courtesy J. Chapman)

In a conventional TEM

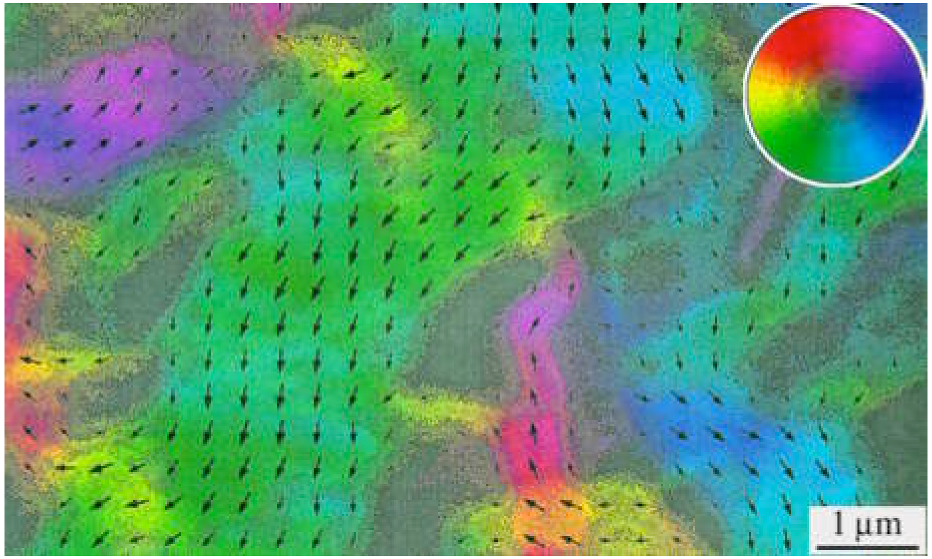

AFM coupled Co-Cr-Co sandwich
(courtesy J.P. Jakubovics)

Difference between Foucault images, obtained at different angles of incidence

5.4 Electron Holography

Principle

$$\mathrm{grad}\,\square_e = (2\ \mathrm{p}\ q_e\, D/h)\,\boldsymbol{B}_0 \times \boldsymbol{s}_b$$

phase of electron wave | **film thickness** | **magnetic flux density perpendicular to beam direction** | **beam direction**

- Magnetization influences *phase* of electron wave
- Phase gradient is perpendicular to $\boldsymbol{B}_0$
- Lines of constant phase are parallel to $\boldsymbol{B}_0$
- Flux between two lines is equal to flux quantum h/q_e

Electron Holography:

- Interference pattern of 2 electron waves shifted in phase
- Evaluation in optical interferometer

5. Transmission Electron Microscopy

5.4 Electron Holography

Off-axis holography (*Tonomura et al. 1980*)

Generation of hologram

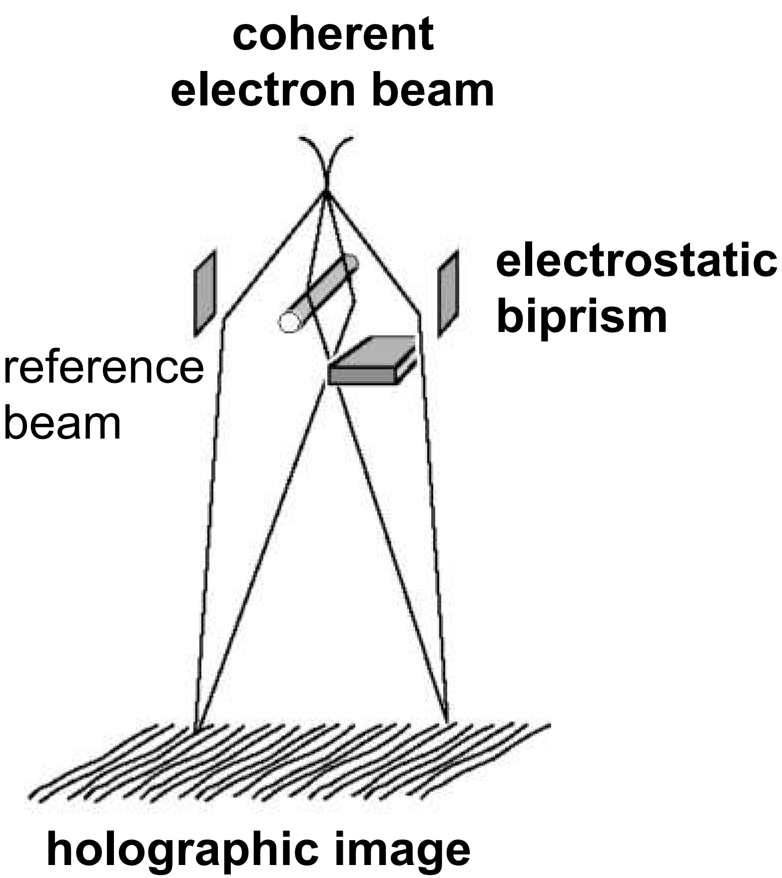

Optical reconstruction

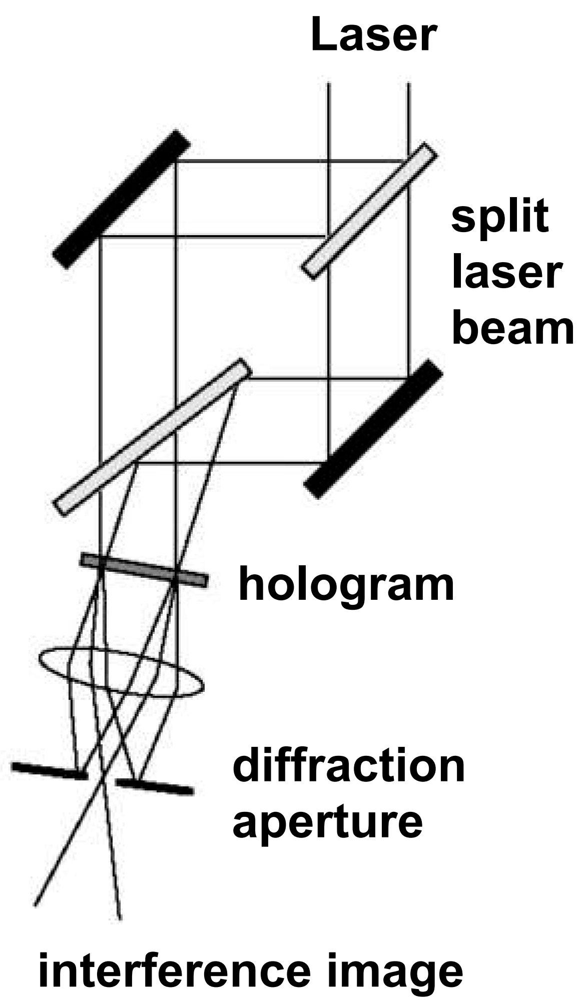

Image shows lines of constant phase

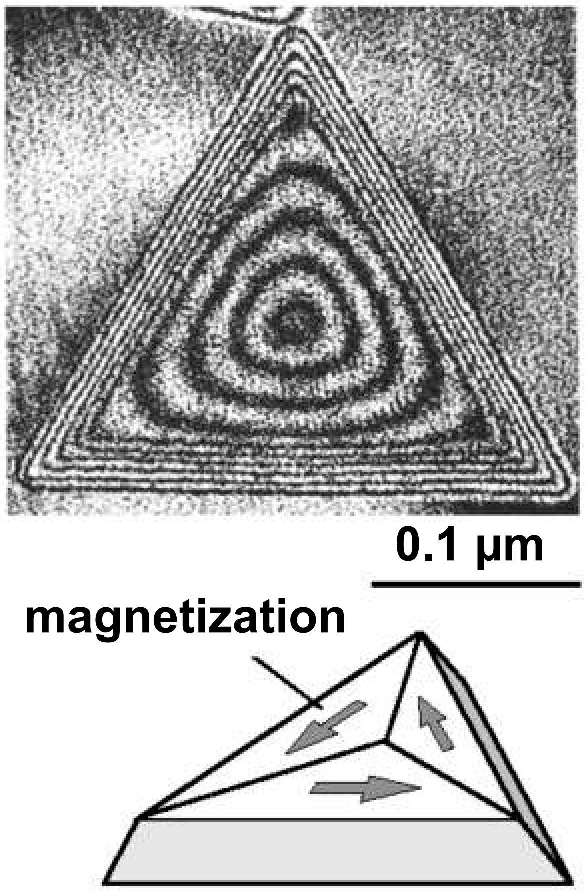

5. Transmission Electron Microscopy

5.4 Electron Holography

Differential Holography (*Mankos et al. 1994*)

• Both interfering beams pass through sample along slightly different paths (distance: 10 nm)

• Reconstruction contains information about their phase difference

⟶ phase gradient is recorded, which is proportional to magnetization

⟶ "real" domain images like in Kerr microscopy

• Quantitative information about magnetization direction at high resolution

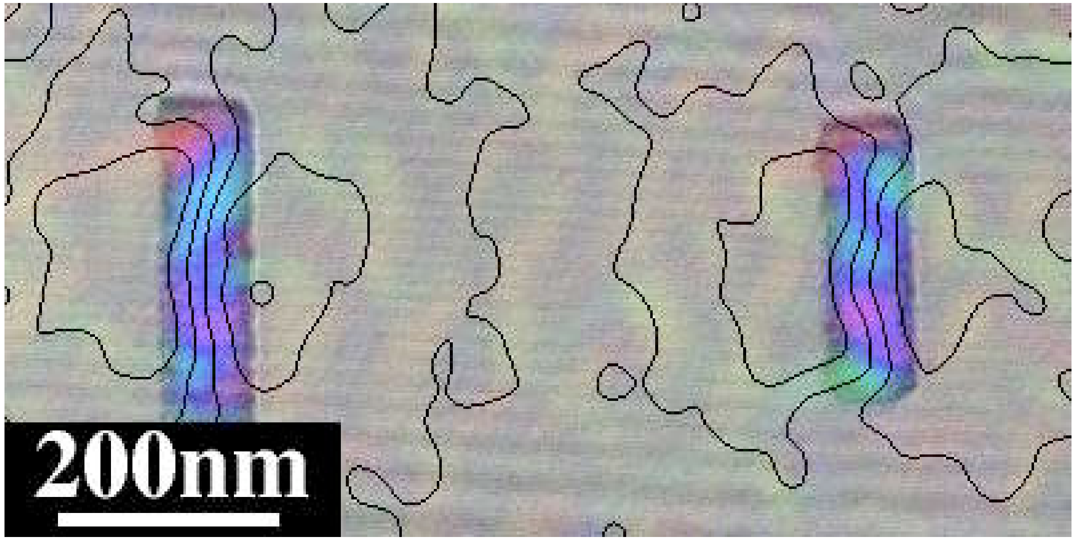

Co/Au/Ni/Al multilayer
(courtesy M. McCartney)

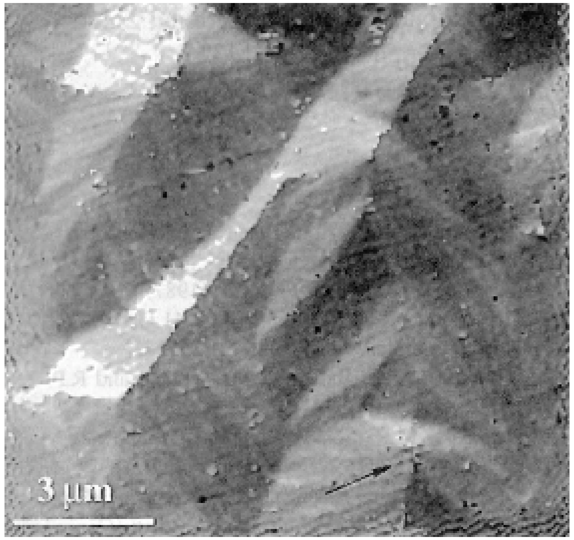

30 nm Co film
(courtesy M. Scheinfein)

6. Electron Reflection Microscopy

6. Electron Reflection Microscopy

Principle

- Based on Scanning Electron Microscope
- Electrons hit sample with energies in 10 - 100 kV range
- Two kinds of re-emitted electrons:
    - *backscattering* from nuclei of atoms (elastic or inelastic scattering)
    - *secondary electrons*: emitted from atoms that have been excited by primary beam, energy range: some 10 eV
- all electrons somehow deflected by magnetization and stray fields
- additionally: polarization of secondary electrons can be analysed

- Three modes of domain observation:
    - **Secondary Electron Contrast (Type I)**
    - **Backscattering Contrast (Type II)**
    - **Electron Polarization Analysis**

6. Electron Reflection Microscopy

6.1 Secondary Electron Contrast (Type I)

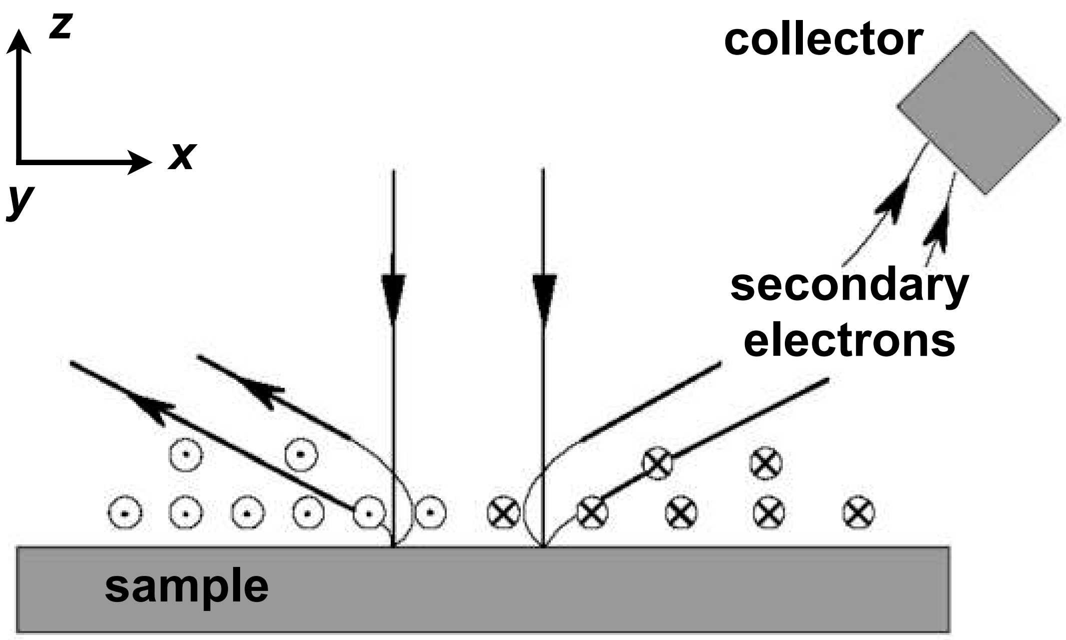

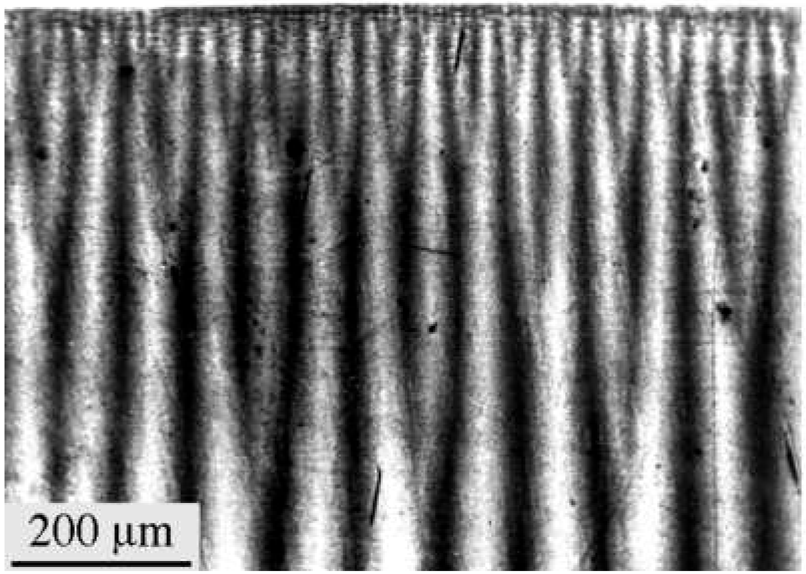

Cobalt crystal
(courtesy J. Jakubovics)

- Collection of secondary electrons in asymmetric arrangement
- Intensity depends on magnetic field component $\boldsymbol{H}_y(\boldsymbol{r})$
- Displayment of fundamental harmonic of domain pattern
- Diffuse image

6. Electron Reflection Microscopy

6.2 Backscattering Contrast (Type II)

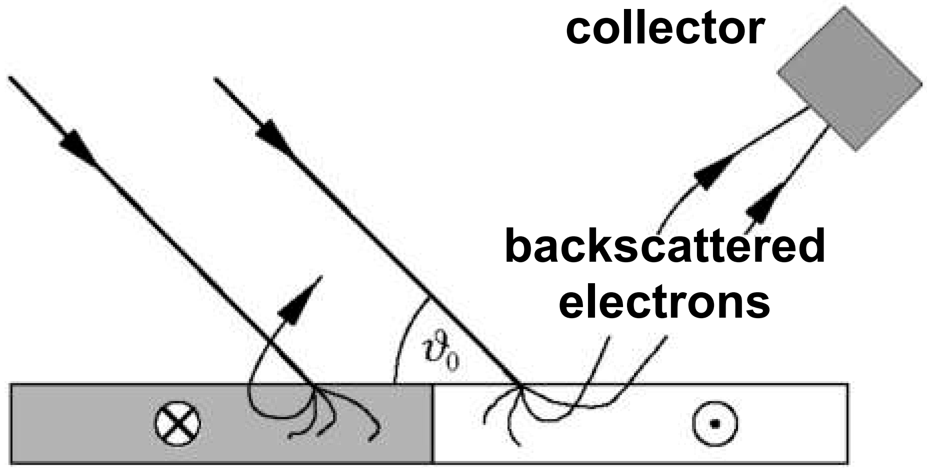

- Deflection of electrons by magnetic induction, either towards or away from surface
- Low resolution
- Tunable depth sensitivity from 1 to 20 µm by varying electron energy

Domain observation through insulation coating on transformer steel
(courtesy T. Nozawa)

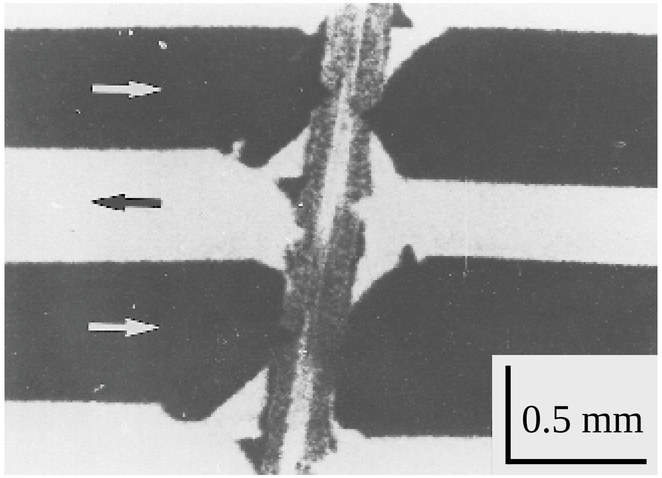

Depth selective imaging on the 2 Permalloy yoke layers of thin film recording head
(courtesy R. Ferrier)

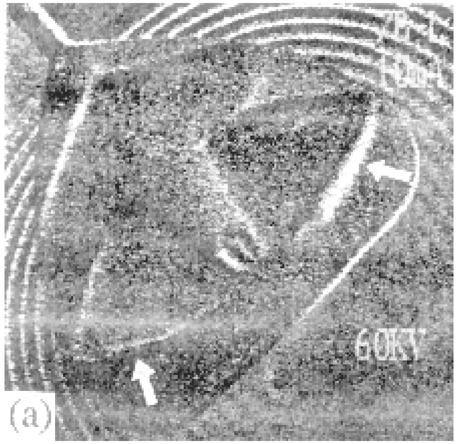

60 kV: upper yoke

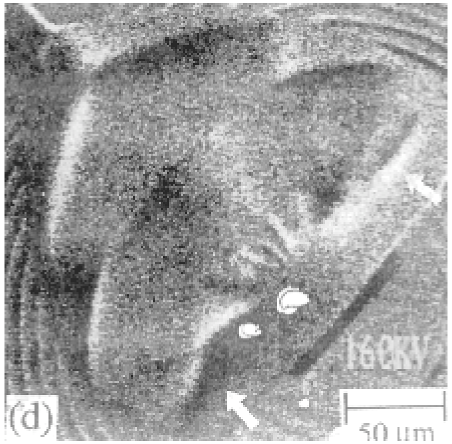

160 kV: lower yoke

6. Electron Reflection Microscopy

6.3 Electron Polarization Analysis

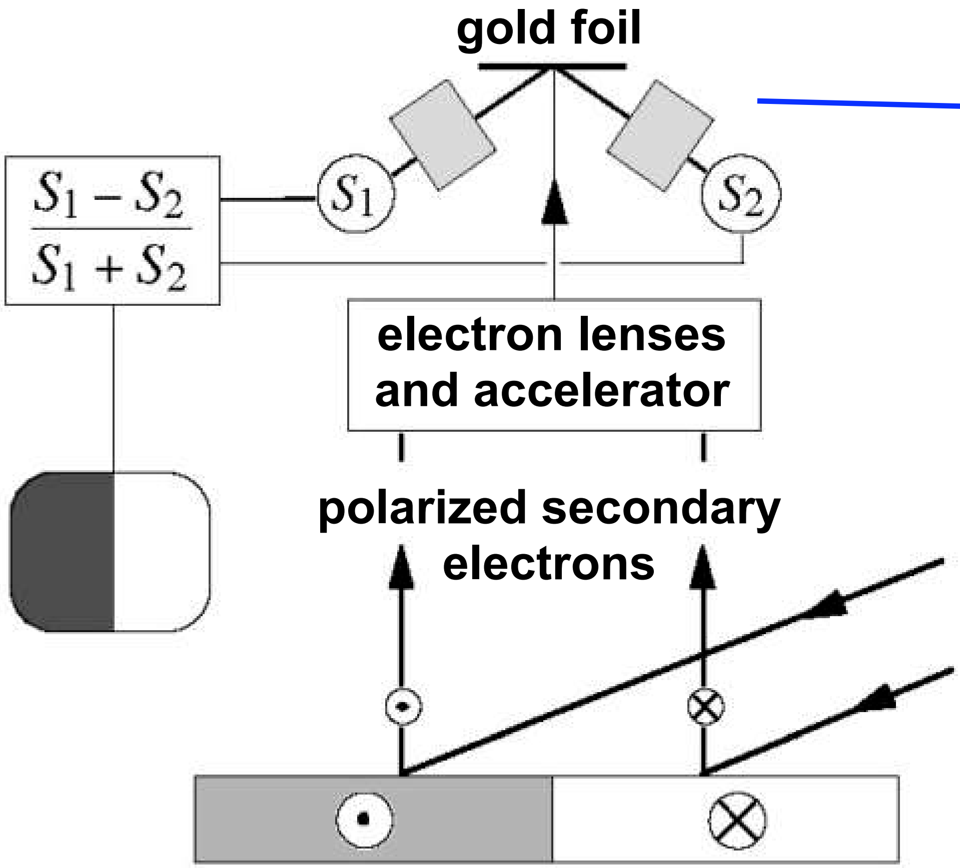

Mott detector:

Scattering of polarized electrons by gold foil is asymmetric (spin-orbit coupling effects)

- Secondary electrons are spin polarized, moment along magn. direction
- Surface sensitive (secondary electrons emerge from top nanometer)
- Quantitative (independent measurement of 3 magn. components)
- Resolution in 10 nm range

6. Electron Reflection Microscopy

6.3 Electron Polarization Analysis

(courtesy J. Unguris)

Basal plane of Co crystal

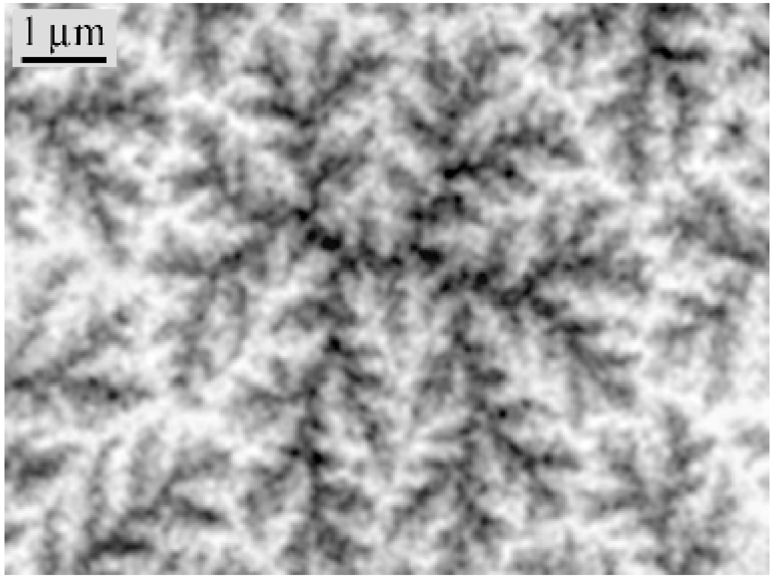

polar components

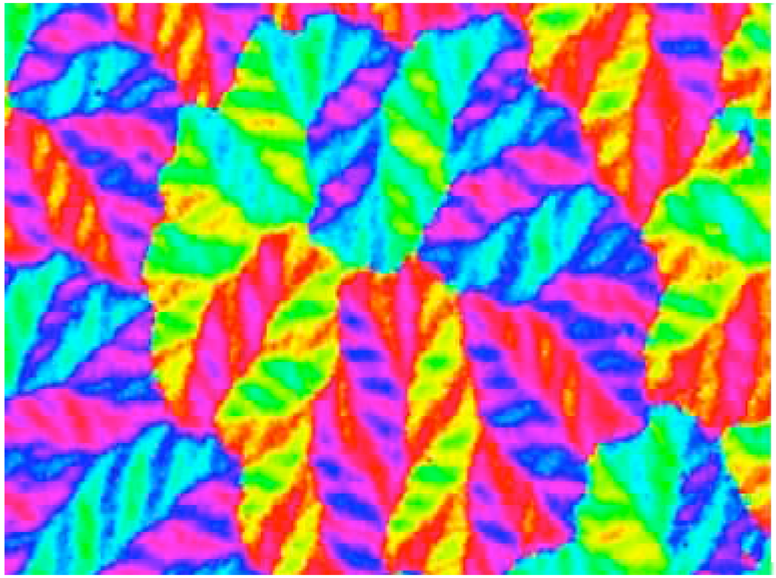

in-plane components

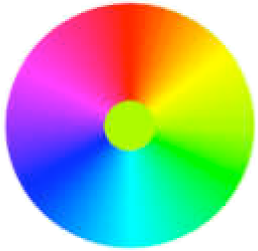

“Wheel side” of amorphous ribbon

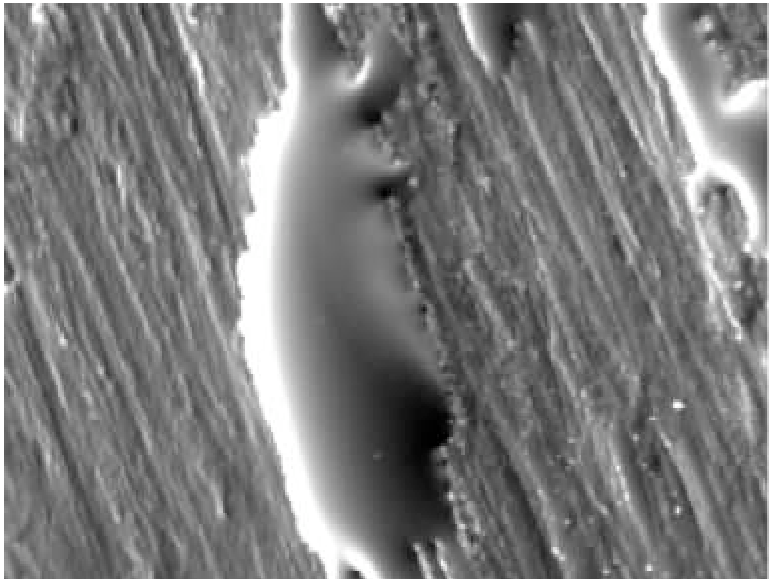

topography

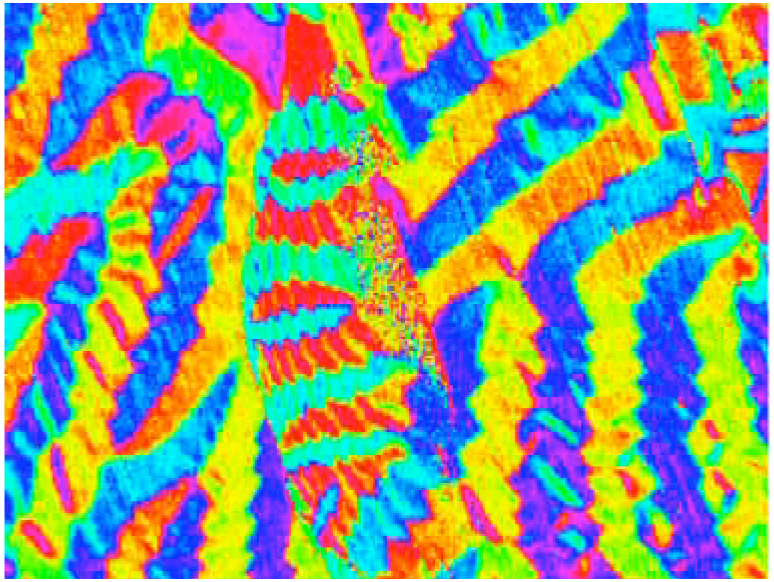

in-plane components

7. Mechanical Microscanning Techniques

7. Mechanical Microscanning Techniques

Overview

- Magnetic Force Microscopy
- Near-Field Scanning Microscopy
- Spin-Dependent Tunneling Microscopy
- Magnetic Field Sensor Scanning

7.1 Magnetic Force Microscopy

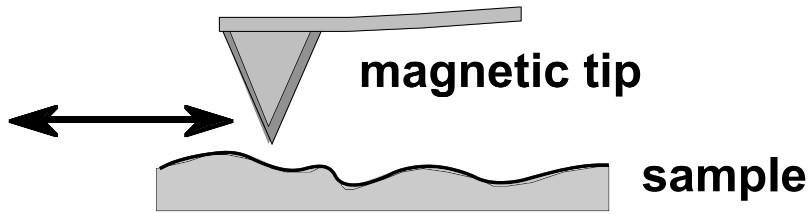

Data track on hard disk

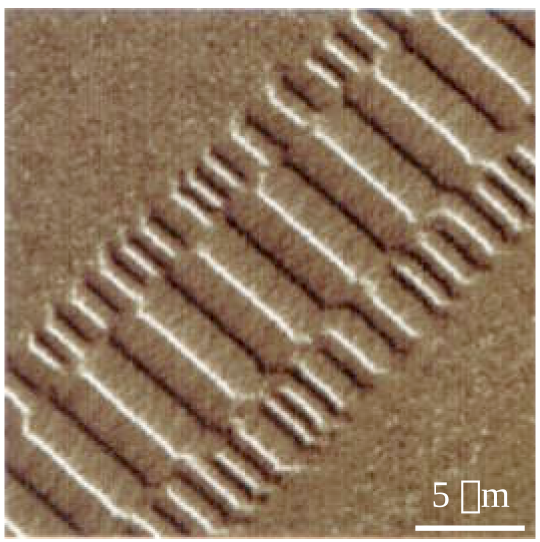

Co elements

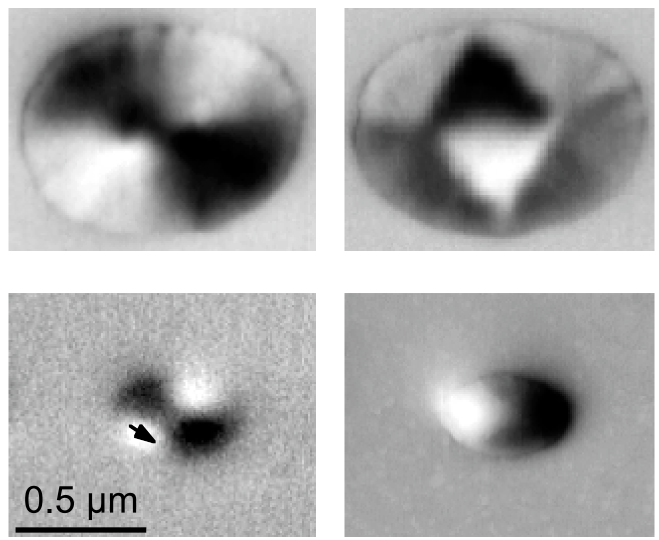

Courtesy: A. Fernandez

(111) Fe surface

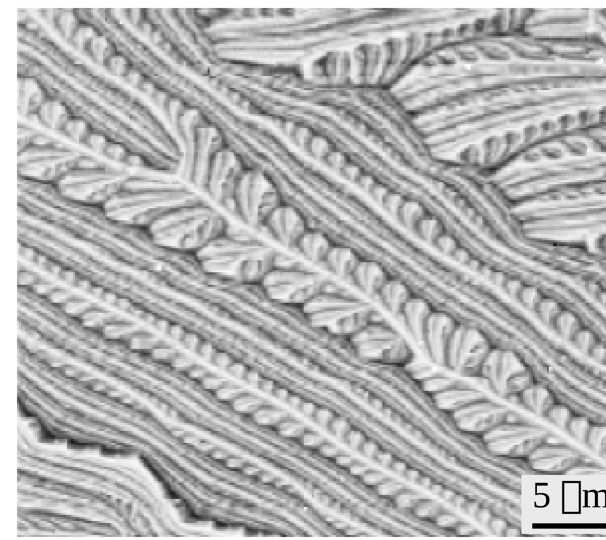

Courtesy: J. Miltat

7. Mechanical Microscanning Techniques

7.1 Magnetic Force Microscopy

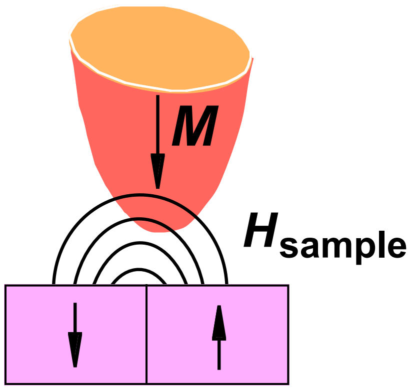

tip magnetization =
stray field sensor

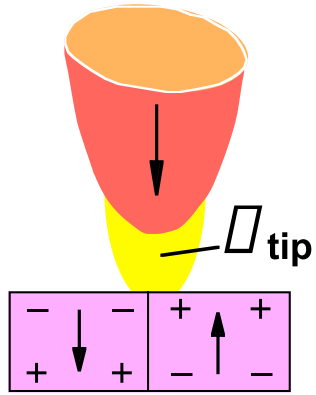

tip potential =
charge sensor

Charge and Susceptibility Contrast

- Weak interaction: *Charge contrast*
- Reversible interaction: *Susceptibility contrast*
- Separartion of contrasts by difference and sum images with inverted tip polarization

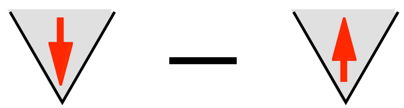

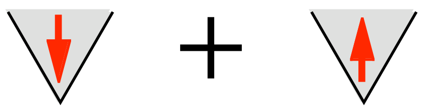

NdFeB twin boundary

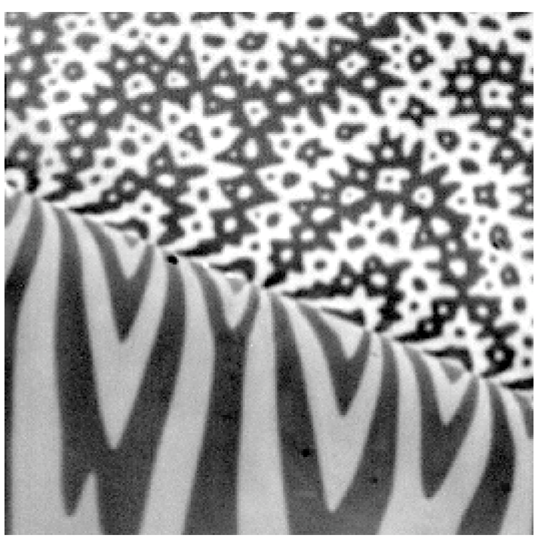

Kerr image

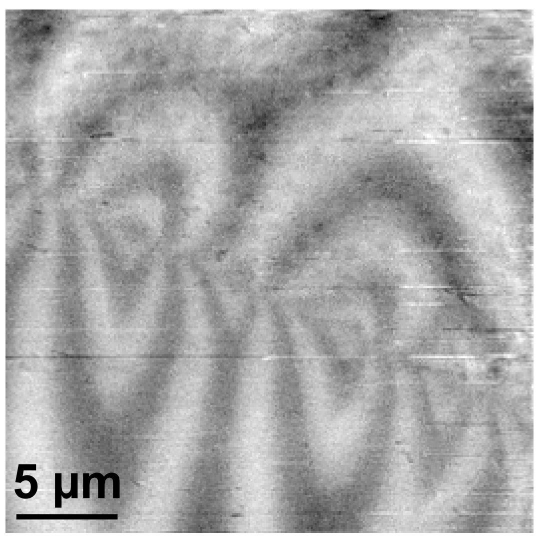

MFM: charge contrast

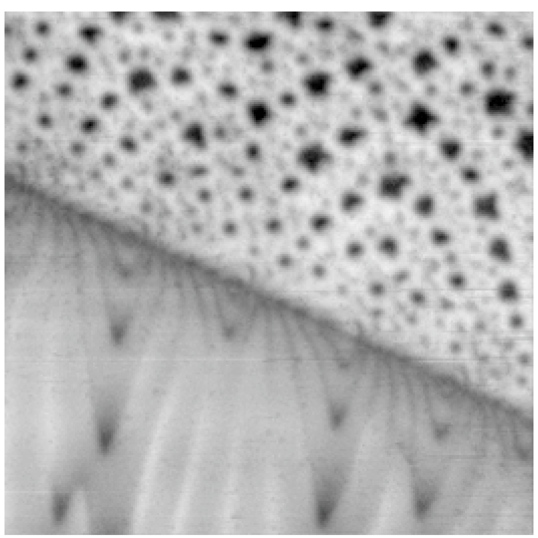

susceptibility contrast

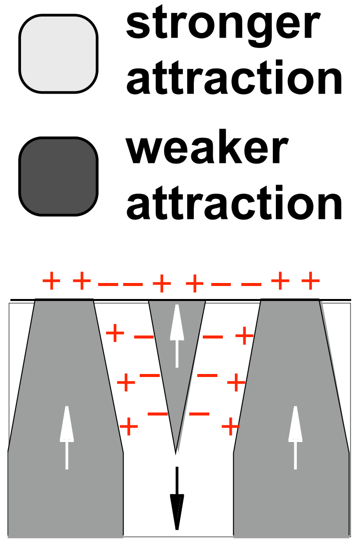

7. Mechanical Microscanning Techniques

7.1 Magnetic Force Microscopy

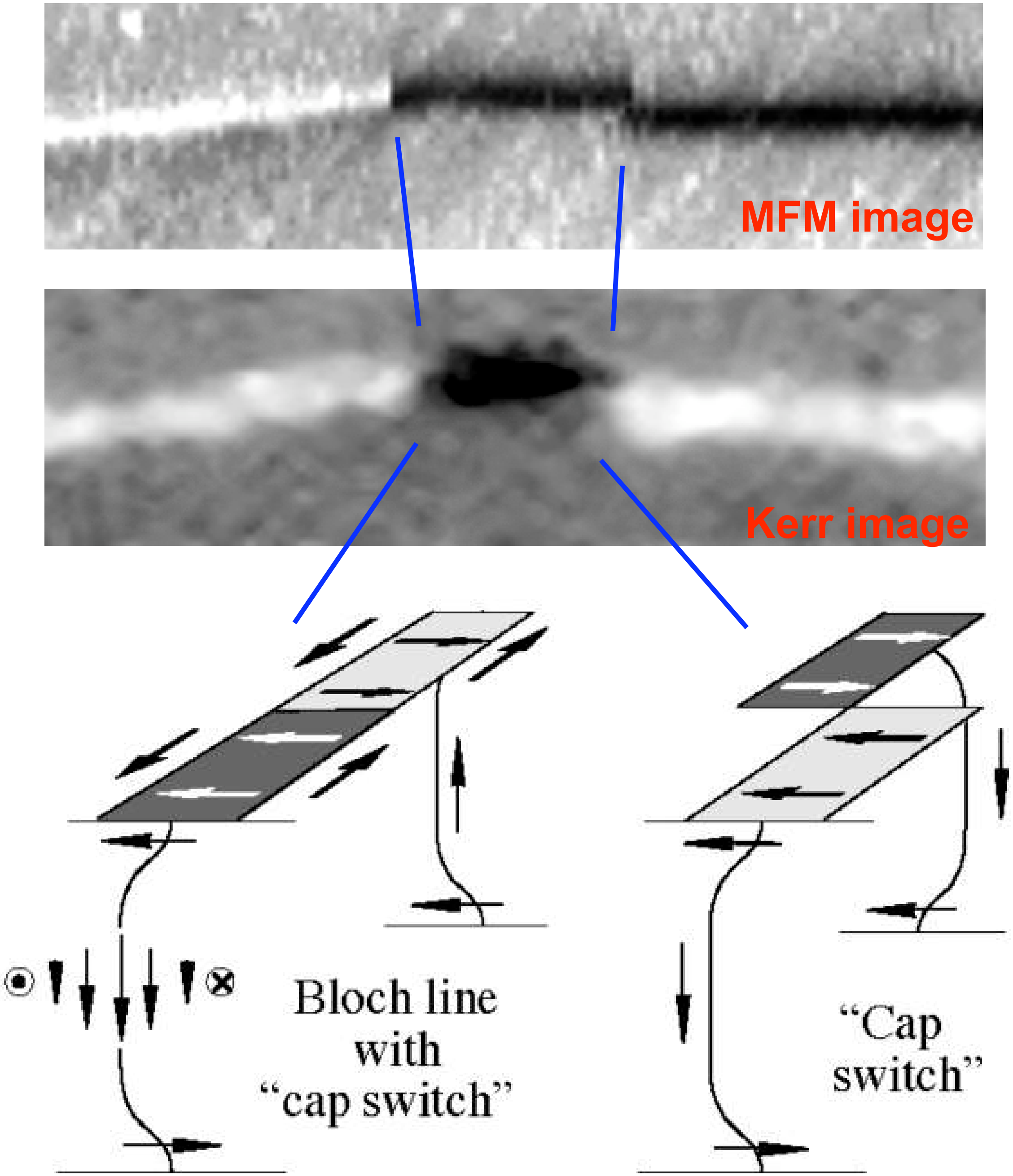

Asymmetric vortex wall on Fe whisker

Wall imaging

MFM:
sensitive to interior magnetization of the wall

Kerr:
sensitive to surface magnetization

7. Mechanical Microscanning Techniques

7.2 Spin-polarized Tunneling Microscopy

- Tunneling of spin-polarized current between tip and sample surface
- Tunneling resistance depends on relative orientation of current polarity and domain magnetization
- Extreme resolution

7. Mechanical Microscanning Techniques

7.2 Spin-polarized Tunneling Microscopy

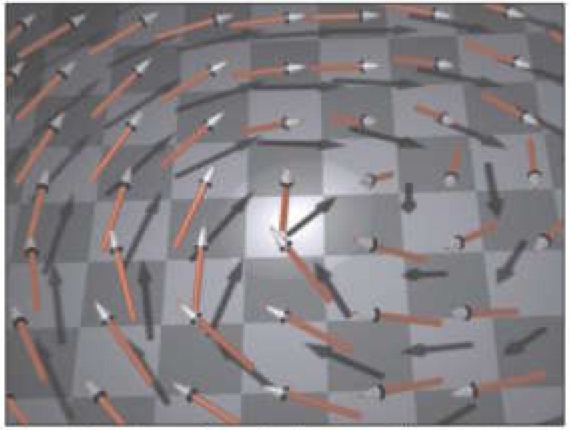

Fig. 1. Schematic of a vortex core. Far away from the vortex core the magnetization continuously curls around the center with the orientation in the surface plane. In the center of the core the magnetization is perpendicular to the plane (highlighted).

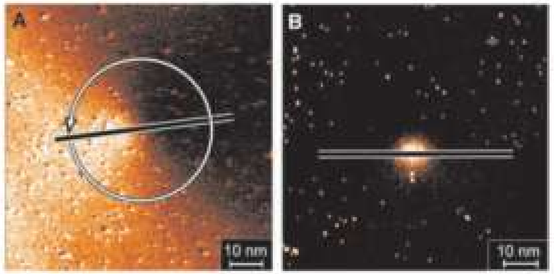

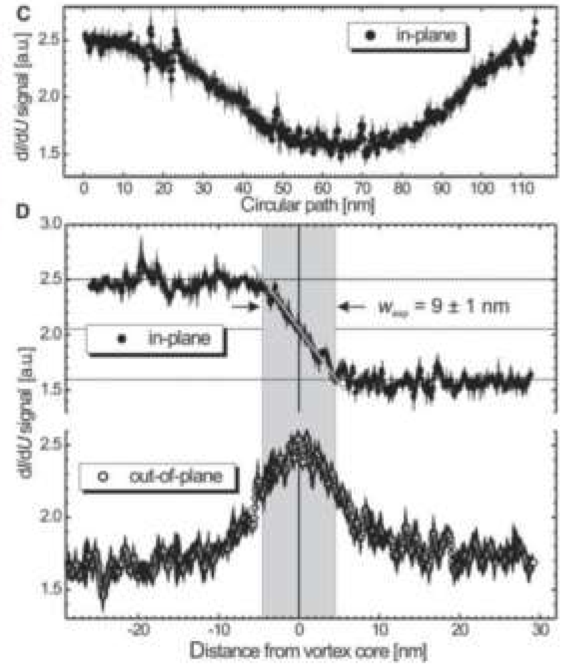

Fig. 3. Magnetic dI/dU maps as measured with an (**A**) in-plane and an (**B**) out-of-plane sensitive Cr tip. The curling in-plane magnetization around the vortex core is recognizable in (A), and the perpendicular magnetization of the vortex core is visible as a bright area in (B). (**C**) dI/dU signal around the vortex core at a distance of 19 nm [circle in (A)]. (**D**) dI/dU signal along the lines in (A) and (B). The measurement parameters were (A) $I = 0.6$ nA, $U_0 = -300$ mV and (B) $I = 1.0$ nA, $U_0 = -350$ mV.

Direct Observation of Internal Spin Structure of Magnetic Vortex Cores

A. Wachowiak et al.

Science **298** (2002)

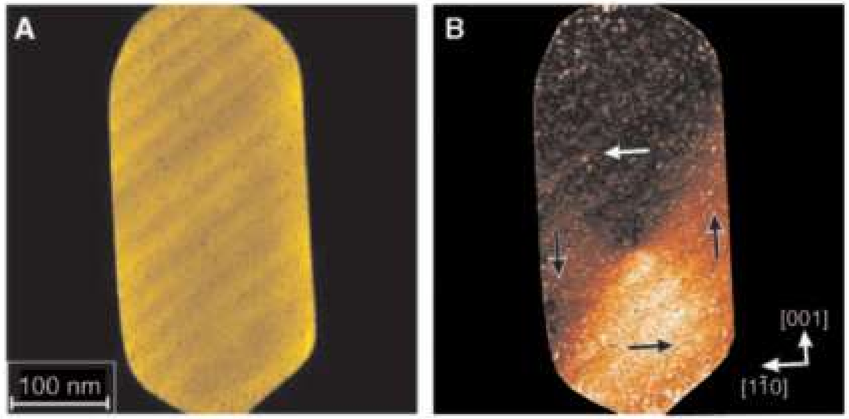

Fig. 2. (**A**) Topography and (**B**) map of the dI/dU signal of a single 8-nm-high Fe island recorded with a Cr-coated W tip. The vortex domain pattern can be recognized in (B). Arrows illustrate the orientation of the domains. Because the sign of the spin polarization and the magnetization of the tip is unknown, the sense of vortex rotation could also be reversed. The measurement parameters were $I = 0.5$ nA and $U_0 = +100$ mV. The crystallographic orientations were determined by low-energy electron diffraction.

8. X-ray and neutron topography

8. X-ray and Neutron topography

8.1 X-ray Topography

- Plane parallel X-ray beam, restricted to narrow strip
- Bragg condition fulfilled for some set of lattice planes
- Diffracted beam recorded by photographic plate
- Crystal and plate are advanced synchronously (scanning)

Contrast mechanism:

- Magnetostrictive strains disturb Bragg reflection
- Contrast at those positions, where rotation or spacing of lattice *changes*

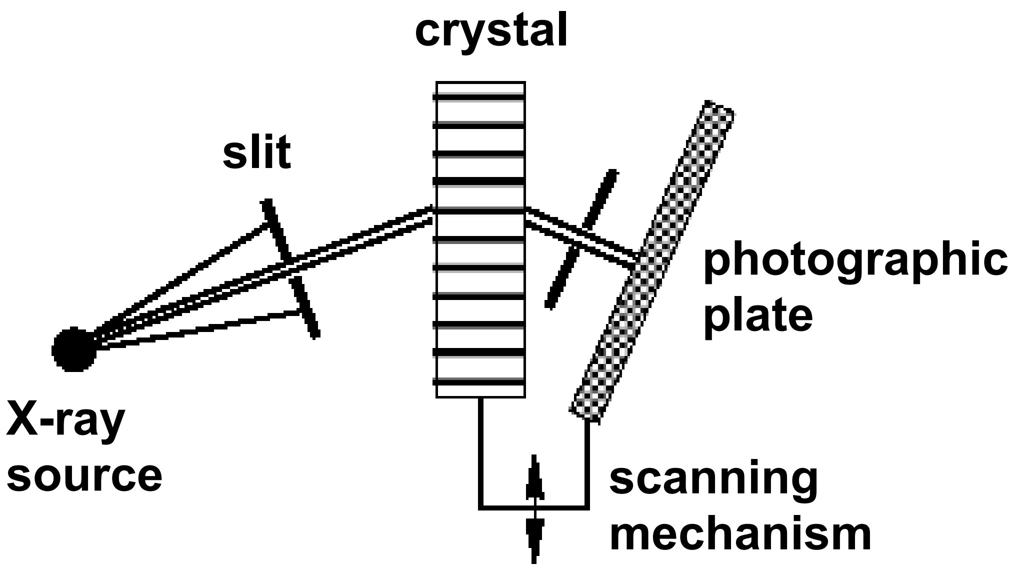

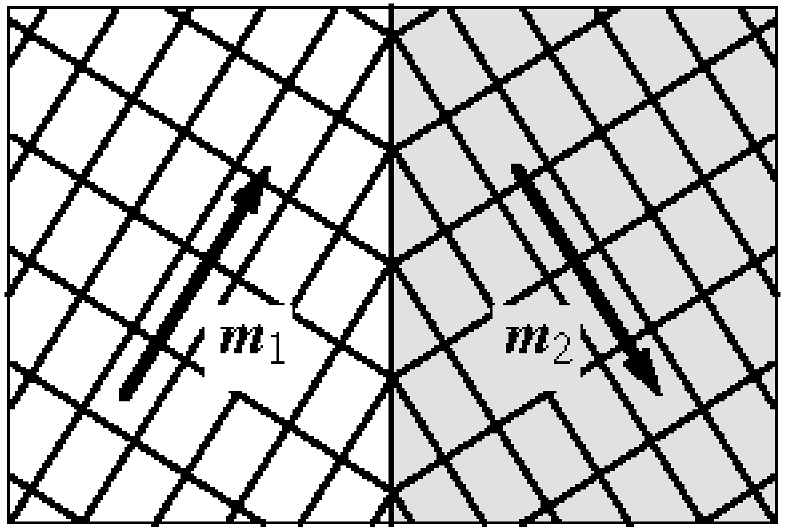

Change of lattice orientation at 90° wall (10–5 radian)

8. X-ray and Neutron topography

8.1 X-ray Topography

X-ray topogram of fir-tree domains on slightly misoriented (100) FeSi crystal (0.1 mm thick)

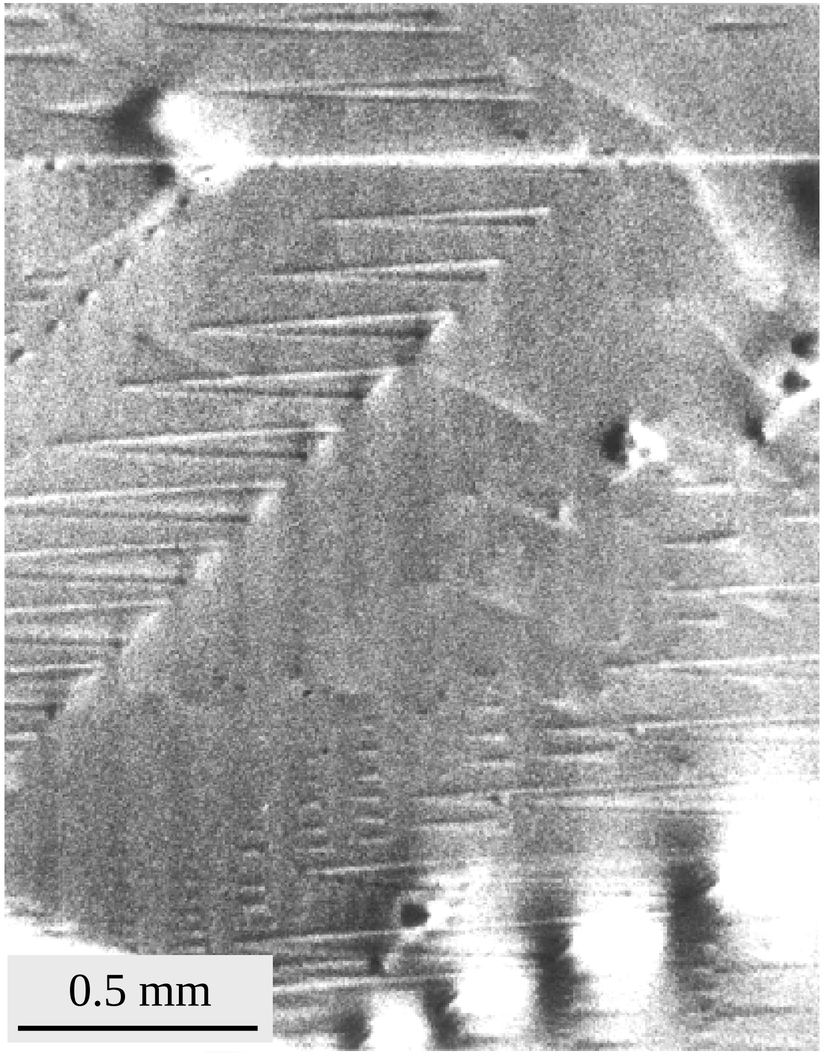

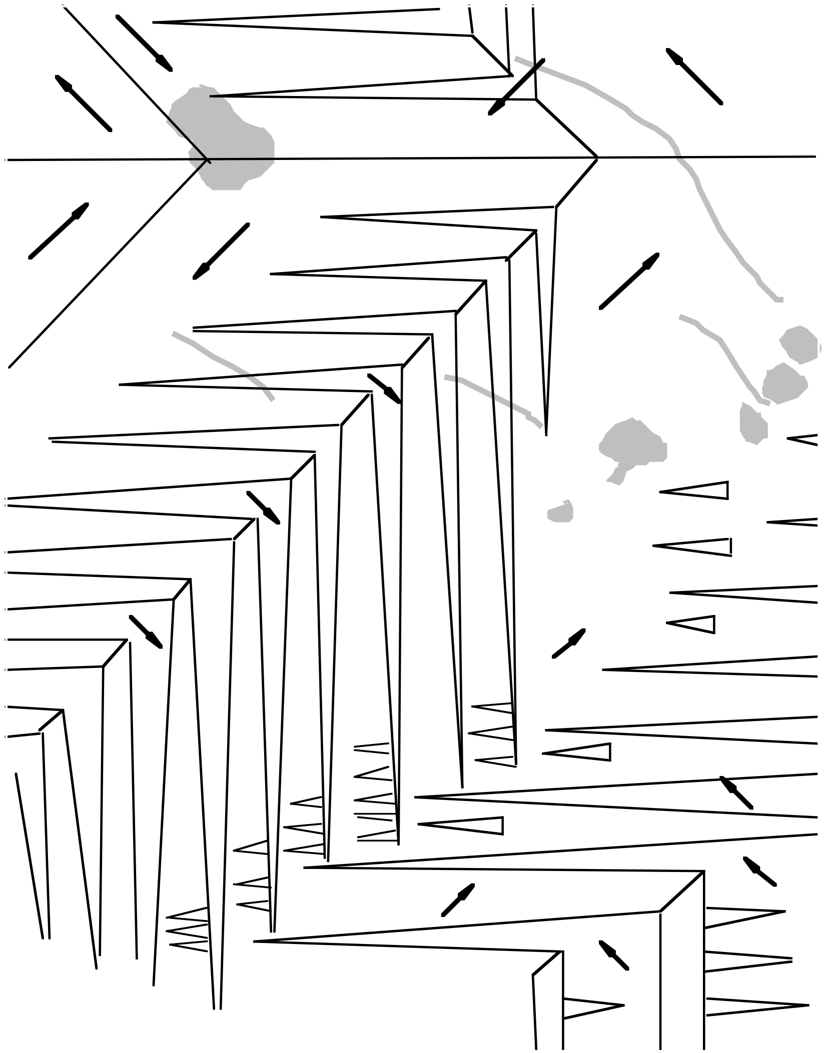

(courtesy J. Miltat)

8. X-ray and Neutron topography

8.2 Neutron Topography

Domains on FeSi crystal

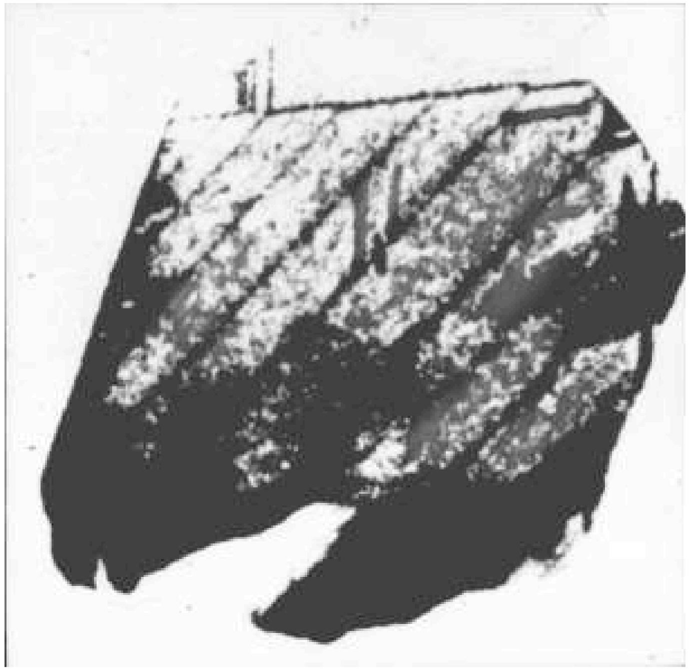

imaged with
unpolarized neutrons

imaged with
polarized neutrons

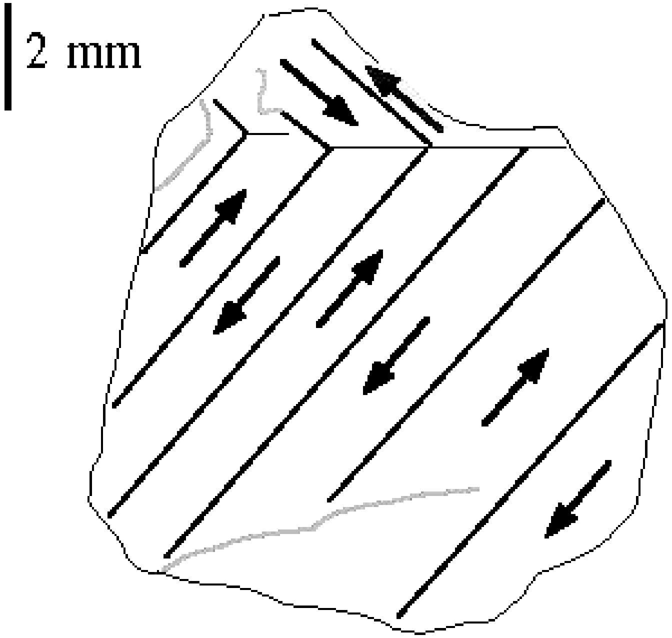

courtesy J. Baruchel

9. Volume domain observation by Libovický method

Bulk domain observation by Libovický-method

S. Libovický: Spatial replica of ferromagnetic domains in iron-silicon alloys.
Phys. Status Solidi A 12 (1972) 539

R. Schäfer, S. Schinnerling: Bulk domain analysis in FeSi-crystals.
J. Magn. Magn. Mat. 215-216 (2000) 140

- Fe 12.8at%Si
- forms submicroscopic precipitates (platelets) at 580°C
- platelets oriented along local magn. direction by elastic interaction
- ⟶ “freezing” domain pattern as precipitation pattern
- domain imaging in polarization microscope after etching due to optical birefringence effect (at room temperature)
- ⟶ “***metallographic***” domain analysis

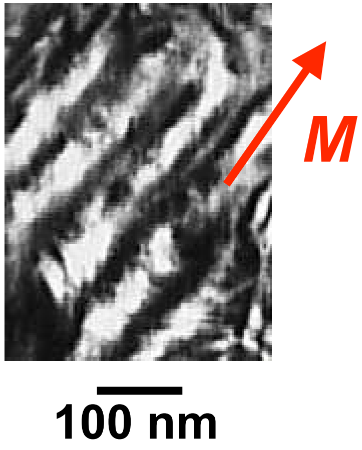

Volume domain observation in FeSi (111) sheet

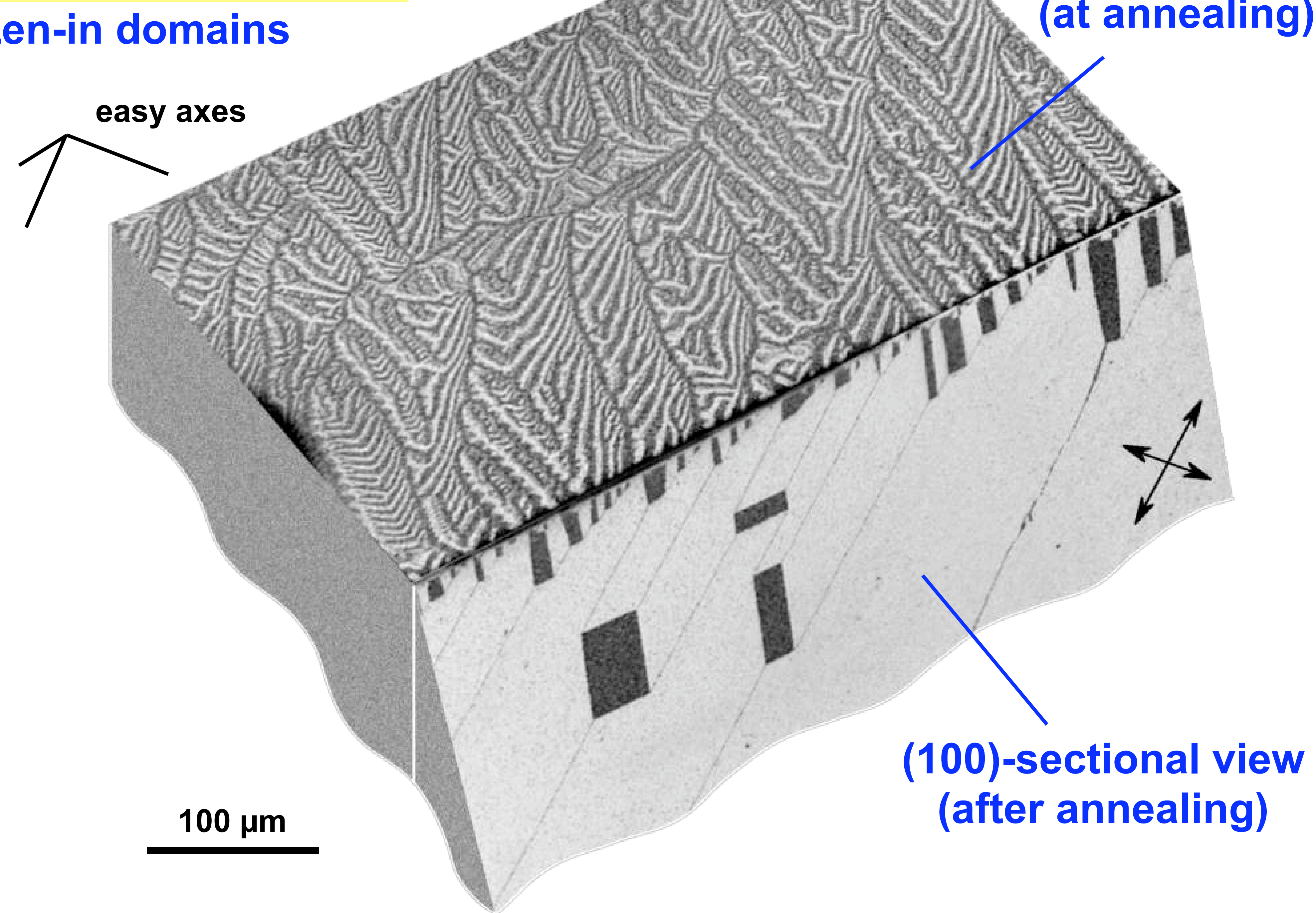

Comparison of
Domain Obervation Techniques

Comparison of Domain Obervation Techniques

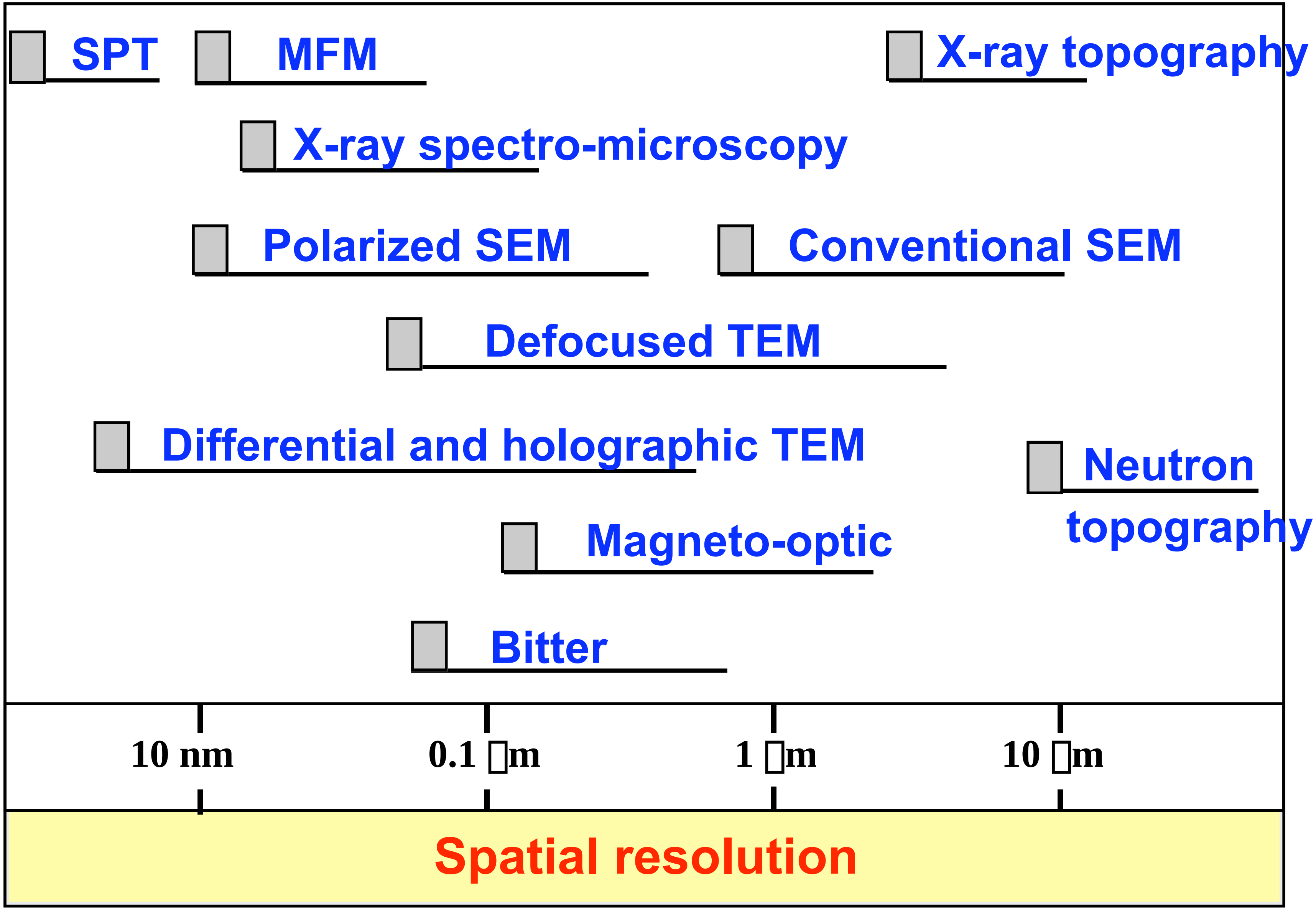

MFM: Magnetic Force Microscopy
SPT: Spin-Polarized Tunneling
MO: Magnetoptic Method
SEM: Scanning (reflection) Electron Microscopy
TEM: Transmission Electron Microscopy

Comparison of Domain Obervation Techniques

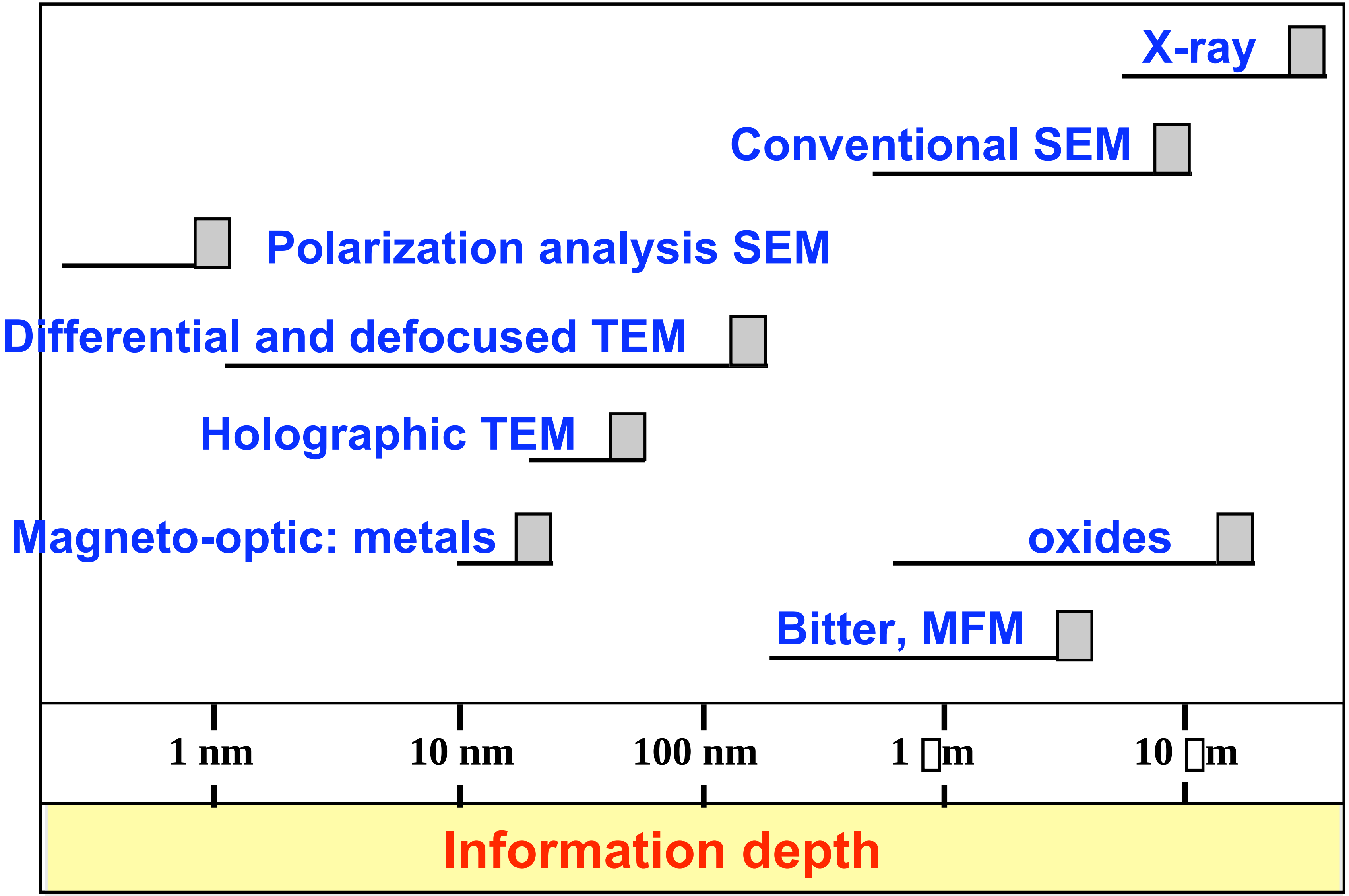

MFM: Magnetic Force Microscopy
SPT: Spin-Polarized Tunneling
MO: Magnetoptic Method
SEM: Scanning (reflection) Electron Microscopy
TEM: Transmission Electron Microscopy

Comparison of Domain Obervation Techniques

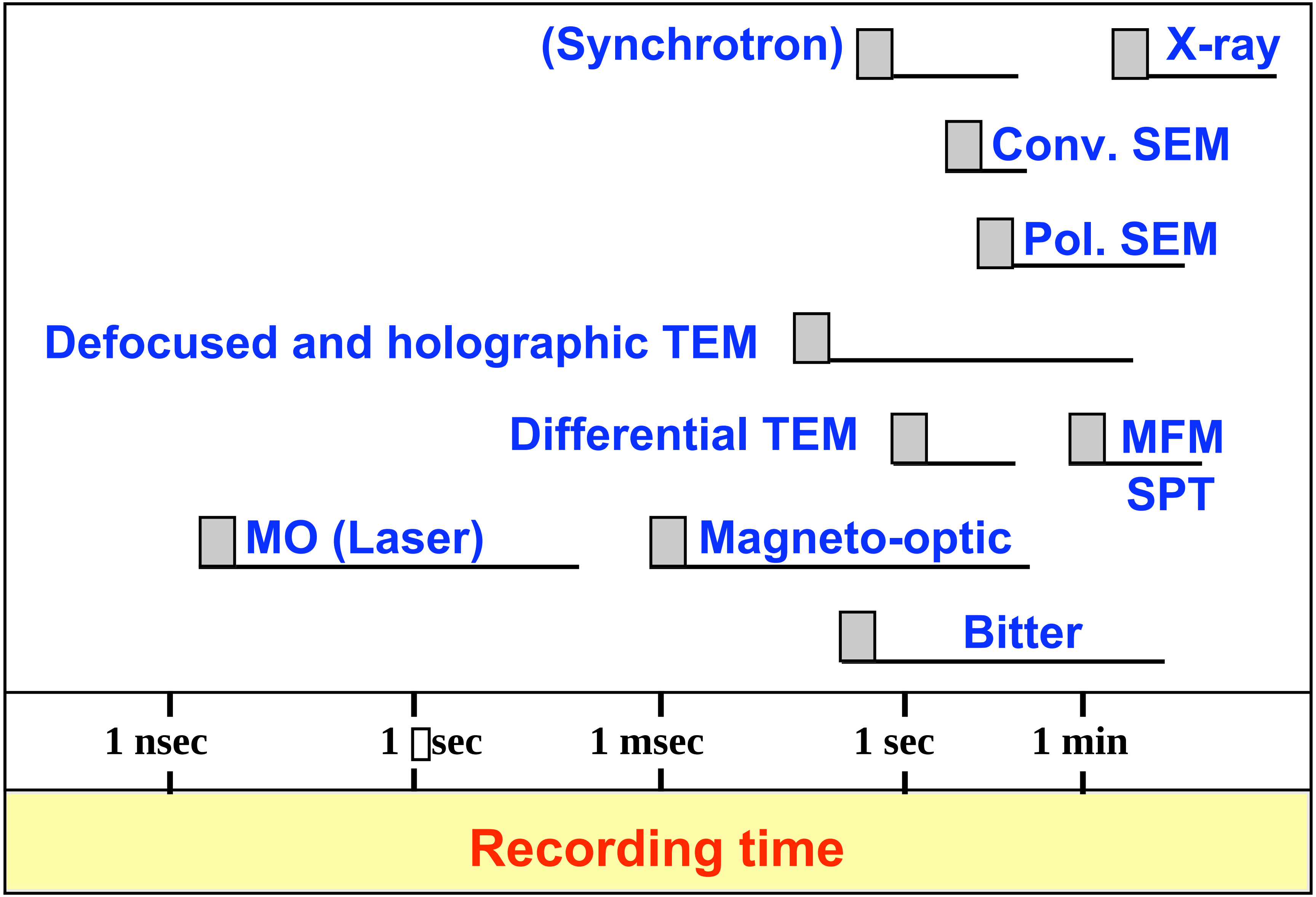

MFM: Magnetic Force Microscopy
SPT: Spin-Polarized Tunneling
MO: Magnetoptic Method
SEM: Scanning (reflection) Electron Microscopy
TEM: Transmission Electron Microscopy

Comparison of Domain Obervation Techniques

Method of domain observation	Sensitivity to small variations in magnetization	Evaluation of the magnetization vector	Allowed magnetic field range	Sample preparation quality requirements	Necessary capital investment
Bitter	very good	indirect	100 A/cm	moderate–low	low
Magneto-optic	fair	direct	any	high	moderate
Digital MO	good	quantitative	any	moderate	high
Defocused TEM	very good	indirect	3000 A/cm	high	high
Differential TEM	good	quantitative	1000 A/cm	high	very high
Holograph. TEM	good	quantitative	100 A/cm	very high	very high
Secondary SEM	poor	indirect	100 A/cm	low	high
Backscatt. SEM	poor	rather direct	300 A/cm	moderate–low	high
Pol. SEM	good	quantitative	100 A/cm	very high	very high
X-Ray topography	poor	indirect	any	moderate	extremely high
Neutron	poor	indirect	any	low	extremely high
MFM	good	indirect	3000 A/cm	low	moderate
SPT	good	direct	3000 A/cm	very high	very high